Delft University of Technology

Faculty of Electrical Engineering, Mathematics and Computer Science

SET3901

# Designing a Solar - Hydrogen system for an industry in the Netherlands

***Author:***
Efstratios Demertzis (5210526)

October 3, 2022

**Thesis committee:**

| | |
|---|---|
| Prof dr. Arno Smets | Professor, supervisor, PVMD Group |
| Dr. Rene van Swaaij | Assistant Professor, PVMD Group |
| Dr. Ir. Marjan Popov | Associate Professor, IEPG Group |
| Dr. Thierry de Vrijer | Post - doc, PVMD Group |

TU Delft Delft University of Technology

# Preface

In this thesis report beyond the whole scientific work done for the ”Design of a solar - hydrogen system for an industry in the Netherlands”, you will also find many other aspects contributed to this final outcome, hidden in there. My passion about sustainable energy technologies. The outcome of the unfinished support from my family and all of my friends being near me all this time either mentally or physically. The hours devoted for this project to be able to present these results and be proud of myself about the work done.

Firstly, I want to thank my supervisor, Arno Smets, at first for shaping this thesis topic following both the academic requirements but also my personal interest. Further than that, for highlighting always the worthiest aspects to focus on and providing me with insights not only in the technical but also in the real world’s developments so I can get a more complete picture of my work.

Furthermore, I also want to thank my supervisor Thierry de Vrijer. Being there to help me overcome the different obstacles that came into my way but also providing me with ideas sourcing from his experience and knowledge to make the outcome of this thesis more complete were a big light in this 9 - months journey.

Finally, I want to conclude my preface with the following phrase that for me represents the true motivation for doing anything in life:

”*If you seek authenticity for authenticity’s shake, you are no longer authentic”* - J.P. Sartre

*Efstratios Demertzis*
*Delft, September 2022*

# Abstract


While the renewable energy sources are rising more and more throughout the years, and the effects of climate change starting to become more visible in our everyday life, some actions need to be taken. Combining different renewable energy sources gives the opportunity to build systems that can help limit these effects and provide energy in different types. The main goal of this project is to model a system that can offer electricity and hydrogen to a steel industry, in this case Tata Steel, and provide an insight for their next steps towards sustainability not only to cover their electricity needs but also investigate alternative steel making routes for their primary processes which are the iron making and further the steel making with hydrogen injection. The models developed for this project aim to answer the following research question:

"*What is the feasibility to cover with a solar - wind - hydrogen system, the loads of the different steel making routes of Tata Steel ?*"

Different models were build through the software TRNSYS for the scenarios investigated that are linked with different combinations of components and loads so more sustainable steel making routes can be followed in the future. The steel making routes refer to the iron making process and the electrification of the industry with green electricity. For the year of 2030 a fuel mix of 70% natural gas and 30% of hydrogen and for the year of 2050, 100% of hydrogen will be used for the iron making process while for both of them 100% of the electricity loads were investigated to be covered by renewable energy sources. The scenarios were divided in a combining structure of local - non local generation and the loads corresponding to the different steel making routes. The local scenario refers to generation in the Netherlands while the non local scenario refers to the generation of hydrogen in the Arabic Peninsula and the generation of the electricity loads of the processes in the Netherlands. The components that were used were wind turbines, solar panels, batteries and electrolyzers. Each system was optimized with the help of GenOpt, an add - on of TRNSYS, to which was set to minimize the levelized cost of electricity, considering also the load coverage both for the hydrogen and electricity loads not to deviate more than 1% from the full coverage. Further than the optimization, a sensitivity analysis with the Sobol method through the programming environment of python and more specifically the SALib library and the parametric analysis of TRNSYS was conducted for all the different scenarios investigated to give an insight how the amount of the different components affects the levelized cost of electricity.

Combining different metrics that were calculated as the Levelised cost of electricity (LCOE), the Self Sufficiency Ratio (SSR), the SSR of hydrogen, the total cost, the avoided emissions per MWh, the area ratio and the avoided emissions per area, a final comparison was done through the different scenarios. The most attractive choices both in a feasibility and economical perspective were the scenarios for local generation of hydrogen and electricity for the projected steel making routes of the years of 2030 and 2050. For the local generation scenario of 2030 an LCOE of 0.383 €/kWh with an electricity coverage of 99.007 % and a hydrogen load coverage of 99.135% were resulted. On the other hand, for the scenario of the local generation of 2050, an LCOE of 0.421 €/kWh, with an electricity load coverage of 99.875% and a hydrogen load

coverage of 99.207% were calculated. The scenario that was the most attractive throughout the different metrics was the one for the local generation of 2050 while the next to come was the one for the local generation of 2030.

Given the aforementioned study and its respectful results, it is a first step to evaluate the impact that such a system can have not only in the emissions reduction of such an intensively emitting industry but also to bring into perspective all the different aspects needed to be considered to realize such a project and evaluate them in more depth in the future.

# Acronyms

**IEA** International Energy Agency

**PERC** Passivated Emitter and Rear Contact

**EAF** Electric arc furnace

**DRI** Direct reduction of iron

**HDR** Hydrogen direct reduction

**HRC** Hot rolled coil

**PSO** Particle Swarm Optimisation

**SOC** State of charge

**BESS** Battery Energy Storage System

**BAU** Business as usual

**LCOE** Levelised cost of electricity

**SSR** Self Sufficiency Ratio

**Nwt** number of wind turbines

**Npv** number of solar panels

**Nbat** number of batteries

**Nely** number of electrolyzers

# List of Figures

# List of Tables

# Contents

# 1| Introduction

## 1.1 Motivation for Tata Steel as the industry to be studied

For this study, the industry that was chosen to be investigated was the steel industry and the focus was on Tata steel's plant in IJmuiden. As reported in [1], the plant is in Velsen-Noord in the Netherlands and became operational in 1918. It currently has a capacity of 7.5 million tons per year which are all produced through the basic oxygen furnace/blast furnace route as described above. Adopted from International Energy Agency (IEA) [2] and Tata Steel's performance [3] data from 2015 to 2020 on average, IJmuiden was responsible for around 8-9% of the total $CO_2$ emissions in the Netherlands. Thus, the initial motivation for conducting this study was to investigate what can be the potential routes for an intensive industry like the steel one so they reduce their carbon footprint and in advance what is the techno-economical feasibility of the routes that Tata Steel is willing to follow in the future to become more sustainable. As it is reported in their sustainability report published in 2020 [4], there are different routes planned to be followed according to the $CO_2$ reduction to be achieved and the availability of renewable energy and hydrogen in the coming years up to 2050. The aforementioned can be seen summarized in the figure 1.1 as well.

In reference to figure 1.1, three different scenarios were established in favor of this study. The first one refers to the business as usual scenario, where a blast furnace and a basic oxygen furnace are used. The second scenario is to investigate what route can bring reduction of emissions by 2030. To achieve such a target, an electric arc furnace will be used as one can see from the figure 1.1 and also direct reduction of iron will take place. It is projected that this technology being based totally on hydrogen will be available in 2050. Thus, for the 2030 scenario, a partial replacement of the natural gas with hydrogen in the shaft for the direct reduction of iron will be considered. Finally, the scenario for 2050, will be to investigate a fully replacement of natural gas with hydrogen in the shaft of the direct reduction of iron. On the other hand, two different scenarios were established for the generation part of the system to be designed. The first one is the installation of solar panels in the Arabic peninsula to power electrolyzers so hydrogen can be produced. Then, it will be transported back to the Netherlands for Tata Steel to use while also offshore wind energy will be considered to provide the electricity loads. The other scenario to be investigated is to install capacity both of solar and offshore wind energy in the Netherlands and also power electrolyzers to produce hydrogen locally. In conclusion, there are three different steelmaking routes that are leading to three different loads and there are two different scenarios for the generation part which in the end lead to six scenarios to be investigated in total, so all the generation - load combinations will be considered. Further than that, a research question will be answered in the end of this study which will be: "*What is the feasibility to cover with a solar - wind - hydrogen system, the loads of the different steel making routes of Tata Steel*".

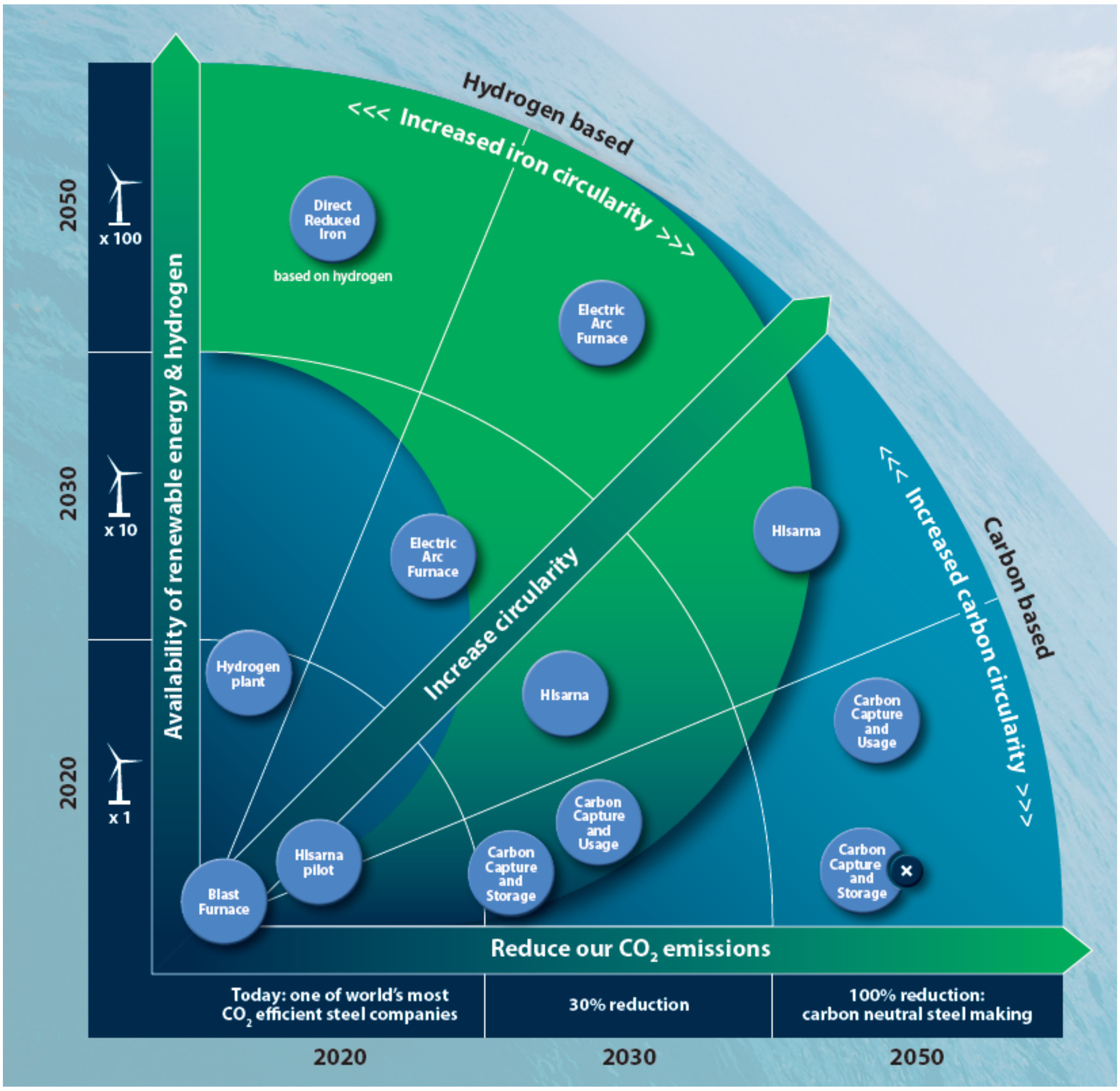


Figure 1.1: Tata Steel sustainability road map that relates the reduction of $CO_2$ emissions with the availability of renewable energy and hydrogen. Adopted from the sustainability report of Tata Steel published in 2020 [4]

## 1.2 Steel making routes

According to [5], there are three main processes that the iron ore has to undergo in order to be produced crude steel. Iron ore or hematite ($Fe_2O_3$), is the raw material one can get directly from the earth and thus the first main process is the preparation of this raw material. This preparation consists of sintering and pelletizing. Sintering is the process in which a solid mass is created under heat and pressure without reaching the melting point of the substance and thus without having liquefaction of it [6]. Pelletizing, is the process of compressing a material to create pellets which are small compressed particles [7]. After preparing the raw material, the next main process is the ironmaking. In this process the main goal is to reduce the hematite by subtracting the oxygen content from the compound and be left with the iron (Fe). There are two different technologies that are used. The first one is the conventional one with a blast furnace that is fueled with either natural gas, oil or coal and oxygen resulting in pig iron. Pig iron, consists of 92% of iron and around 3-4% of carbon [8]. For this technology, is also required to feed the furnace with coke which is produced separately through the coking process by coal. On the other hand, is the direct reduction of iron that is taking place in a shaft furnace, fueled with natural gas which results in a reduced iron product (Fe). Finally, the last process is steel making which happens either in a basic oxygen furnace or in an electric arc furnace. For a basic oxygen furnace, pig iron that is coming from the blast furnace is fed to the basic oxygen furnace with oxygen and recycled steel and resulting in crude steel. However, for the electric arc furnace technology, the direct reduced iron is fed with recycled steel to the furnace and again crude steel is produced. After the aforementioned processes, steel goes through the processes of continuous casting and then hot rolling to finally get hot rolled coils which is the final product of a steel plant.

## 1.3 Thesis Structure

The structure of this thesis report consists of six different chapters. Chapter 1 is the introduction, which includes in section 1.1, the motivation for choosing Tata Steel for this project, while in section 1.2, a brief introduction about the steel making routes is given. In chapter 2, the way the system was simulated in every different aspect is described. At first in section 2.1, further information are provided about the modelling of the system and more specifically, the program that was used, the locations chosen, the separation of the problem in scenarios and case studies to be investigated, the components that will be used, meteorological data and finally an area specification. In the second section 2.2, the loads that will be investigated were analyzed. Loads for a present scenario, a scenario for 2030 and a scenario of 2050 as well as liquefaction and regasification loads for the hydrogen part of the system and the maintenance time considered for such an industry. At chapter 3, there are two sections. In the first one 3.1, the optimization method used is described while in the second section 3.2 the optimization and variables are specified in a more detailed way per scenario and case study investigated. On chapter 4 of this thesis report, the results for each scenario out of the five that were studied are presented with a discussion part for them on each section. A sensitivity analysis was also conducted and the results of it are presented in chapter 5. In the first section 5.1, the theory behind the methodology used is described and the exact approach of this method is further analyzed. In the next five sections 5.2, 5.3, 5.4, 5.5, 5.6, the results of the sensitivity analysis per scenario are presented. In the end of the main report, the chapter 6 consists of the reflection of the results with a comparison between the different scenarios and also the conclusions and ideas for future work. Further than the main report, an appendix chapter A is also included. In appendix A.1, the MATLAB code to add the maintenance time to the loads is added.

# 2| System Simulation

## 2.1 Modelling

In this section is given an initial approach of the system. At first there is an introduction to the software TRNSYS that is used to simulate the system. Then, the locations chosen are discussed and the components that will be used in all scenarios are presented. Finally, the meteorological data are also mentioned with their source and the manipulations made.

### 2.1.1 TRNSYS Software

The simulation tool that was used to perform the analysis of the systems investigated was the TRNSYS Software. A software developed from the University of Wisconsin and is mostly developed for the simulation of energy systems. The version that was used was TRNSYS 18. This software program gives the possibility to design the system per component while it consists of a big library that has preset component models and there is also the possibility for the user to change these models or even create new ones according to their project's needs. The programming language that TRNSYS is setup on, is fortran 90 [9]. TRNSYS is using a black box logic to calculate different variables and simulate the system. This means that each component gets input and extracts output values that are the inputs for a next component until the final values can be printed at the end of the calculations chain. Thus, reaching to the final results in such a continuous way gives the possibility to the user to study a system as a whole.

### 2.1.2 Locations

The chosen regions for this study are the Netherlands and the Arabian Peninsula. The chosen locations for the Netherlands are IJmuiden, the place where Tata Steel plant is and the place where the photovoltaic panels, the batteries and the electrolyzers will be installed according to each scenario and case study. Then it is also chosen the offshore area near IJmuiden where the wind turbines will be installed. The reason for that is the tenders for 2023 - 2025 according to the Dutch government [10] which are referred to a project of 4000 MW offshore wind turbines capacity around 50 km from the shore of IJMuiden 2.1.

As far as the Arabian Peninsula is concerned, five different locations where chosen, according to [11], the study of F. Benetti for the potential of hydrogen in the Arabian Peninsula. More specifically, the places chosen are Saudi Arabia, Oman and Abu Dhabi. They were chosen for the reason that the hydrogen will be liquefied to be transported back to the Netherlands. Referencing to [11] as it can be seen from the figure 2.3, the biggest potential for electrolysis and liquefaction stations is in these three locations. F.Benetti studied three different scenarios, but the one chosen for the locations selection was the export one as the hydrogen will be transported from the Arabian Peninsula to the Netherlands. The series that they are mentioned is also their priority series to install the photovoltaic panels and the electrolyzers following the criterion of distance from the Suez Canal.

A schematic representation of all the different locations chosen for this study can be seen in the next three figures 2.2, 2.3, 2.4.

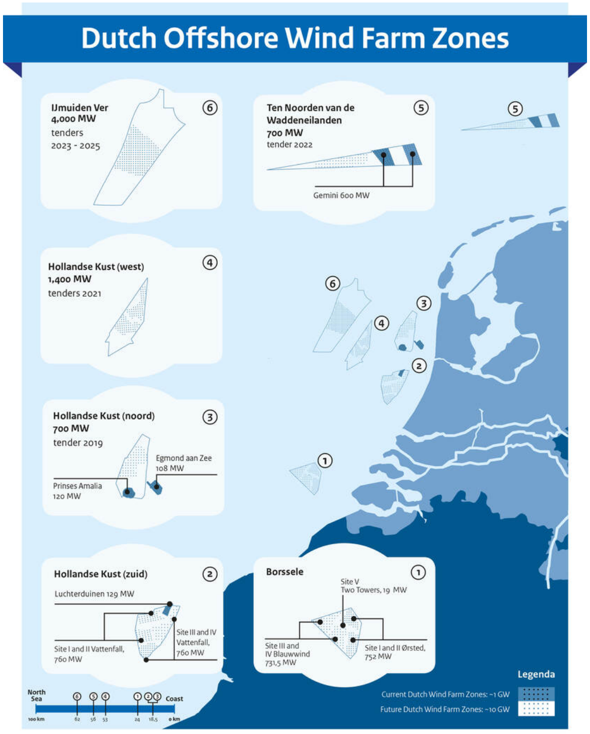


Figure 2.1: Dutch government's plans for the future with respect to the offshore wind farm projects and the respectful tenders

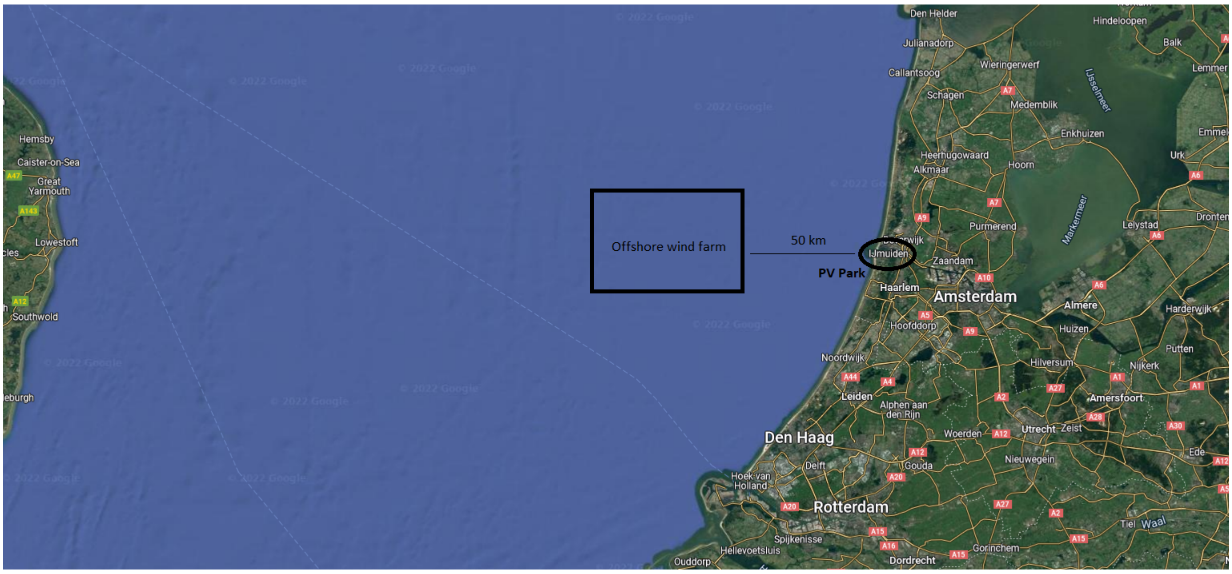


Figure 2.2: The map shows the locations chosen for the system part that will be in the Netherlands displaying both the solar park and the offshore wind farm as well as the distance to the shore

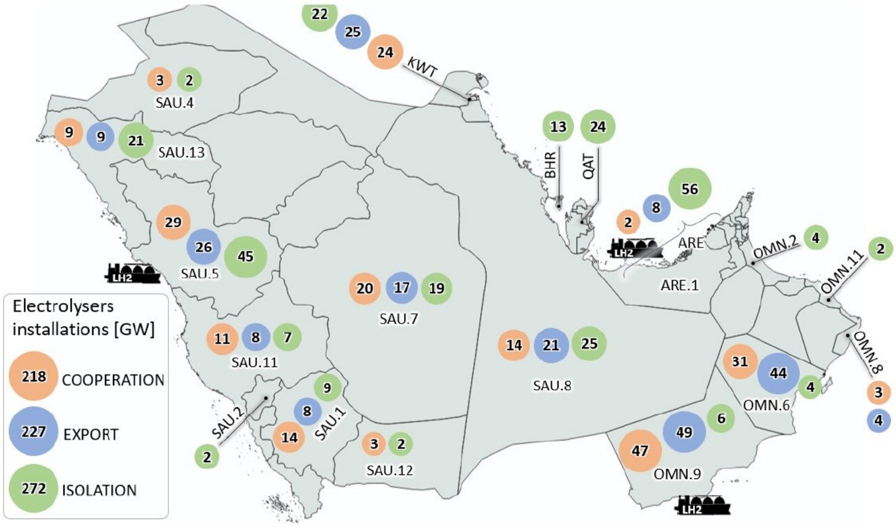


Figure 2.3: The map taken from [11] shows the locations that have the biggest potential for electrolysis. Hydrogen will be transported in liquid state, so the chosen locations are those that show a potential for liquefaction stations as well. The series to be followed in the systems installation depends on the distance to Suez Canal


Figure 2.4: The map shows the locations chosen for the system part that will be in the Arabian Peninsula displaying the areas that the solar park is possible to be installed

### 2.1.3 Scenarios and Case Studies overview

In this section an overview of the different scenarios will be given. At first the scenarios that will be studied can be divided into two bigger categories. The first one is referred to local generation and the second one implicates the Arabian peninsula as a location that the system's hydrogen will be produced. The main structure for the different scenarios will be a combination at first of the local, in IJmuiden, and non local, in the Arabic Peninsula, energy generation. Then according to the energy consumption profile that depending on the evolution of the steel making process to a more sustainable one, the loads will be different for the electricity and the energy carrier, in this case hydrogen, that will be produced. Elaborating further on the scenarios structure, these two categories have each two different scenarios, one for each different steel making route, which gives four in total. Also, a reference scenario will be studied that concerns a business as usual one with the difference that electricity will be produced by a solar - wind hybrid system.

#### Scenario 1: Local Generation

The first case study of this scenario refers to local electricity generation from a hybrid system that consists of offshore wind turbines, photovoltaic panels and batteries. It will be used as a reference case study and the main idea behind the study of it, is to produce the electricity via renewable energy sources instead of the current power plants that Tata Steel is using. This case study will be representing the case of the present as it is showed in figure 2.5 while two more case studies are investigated for the years of 2030 and 2050 with combined hydrogen production in the system.

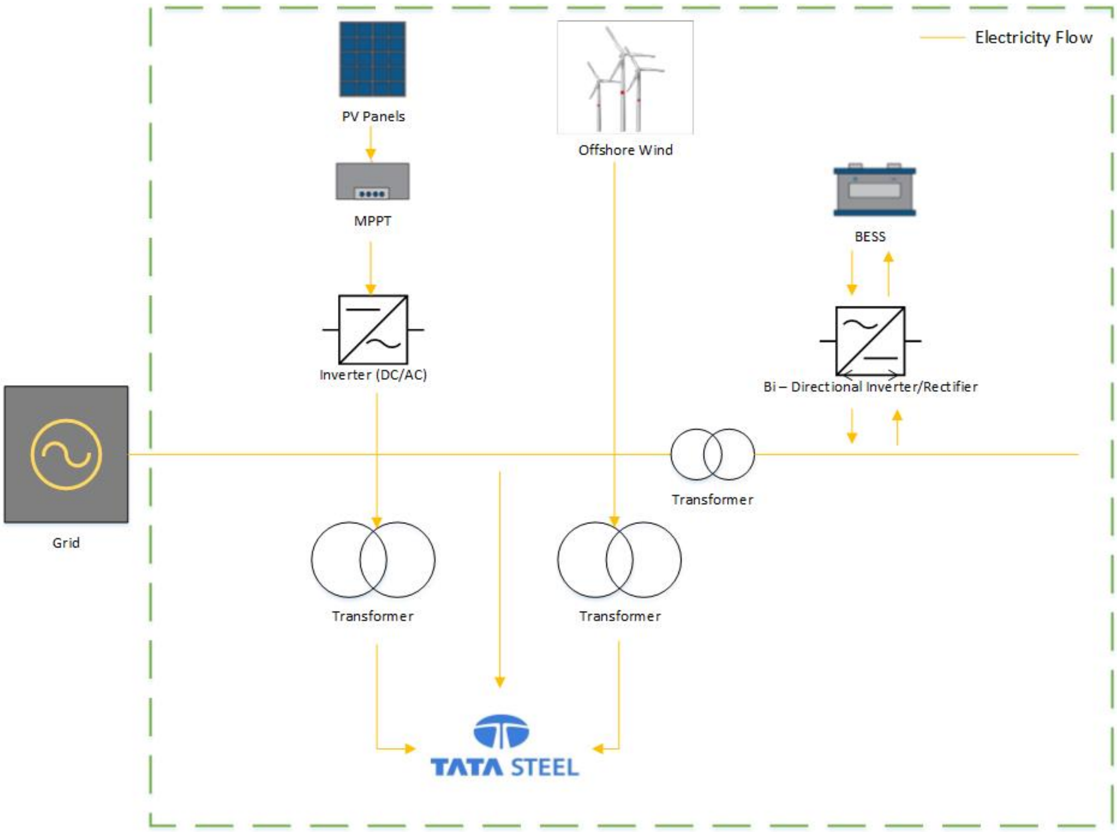


Figure 2.5: The graphic representation of the system for the base scenario case

This scenario will also include the case study that refers to a hybrid system that consists beyond the aforementioned components and an electrolyzer to produce hydrogen. While only the loads are changing for the years of 2030 and 2050 as analyzed in Section 2.2, the components used will remain the same while their size will be adjusted accordingly through the optimization process. In the next figure 2.6 the schematic representation of the different systems simulated are provided.

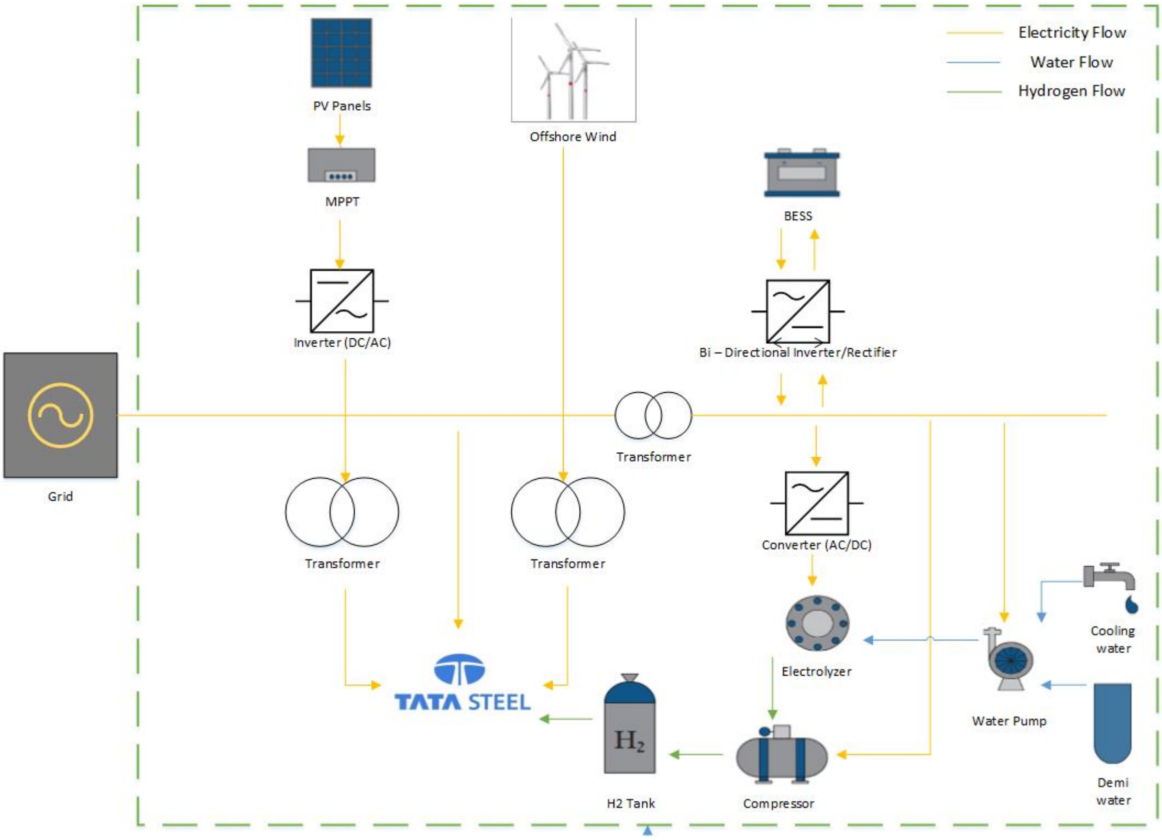


Figure 2.6: The graphic representation of the system for the local generation scenario cases

**Scenario 2: Arabian Peninsula and the Netherlands combined production**

For this scenario there are again two different case studies, in addition to the reference case study, that they refer to the years of 2030 and 2050. These case studies refer to local electricity generation with offshore wind, photovoltaic panels and batteries to confront the intermittency of the renewable energy sources while the hydrogen will be produced in the Arabian Peninsula. The electrolyzers will be powered by photovoltaic panels. The hydrogen will be liquified and then it will be shipped to the Netherlands through the Suez canal. Then it will be regasified back in the Netherlands and it will be used in the processes of Tata Steel. For simplification reasons, the liquefaction and regasification processes for the hydrogen transportation are taken into account in this model by adding their electricity loads to the total loads needed for each case study as analyzed in Section 2.2. The schematic representation of the aforementioned system is given below in figures 2.7 and 2.8. The system can be divided into two separate subsystems since they are not interconnected with each other in any way. The first figure 2.7, show the electricity part of the system in which the regasification load is attempted to be covered as well as the electricity load of Tata Steel. The second figure 2.8, displays the part of the system that is in Arabic Peninsula which is the part of the system producing electricity for liquefying the hydrogen and also the power sent to the electrolyzer. The priority of the power flow is at first to provide to the load, then the electrolyzer and finally the batteries.

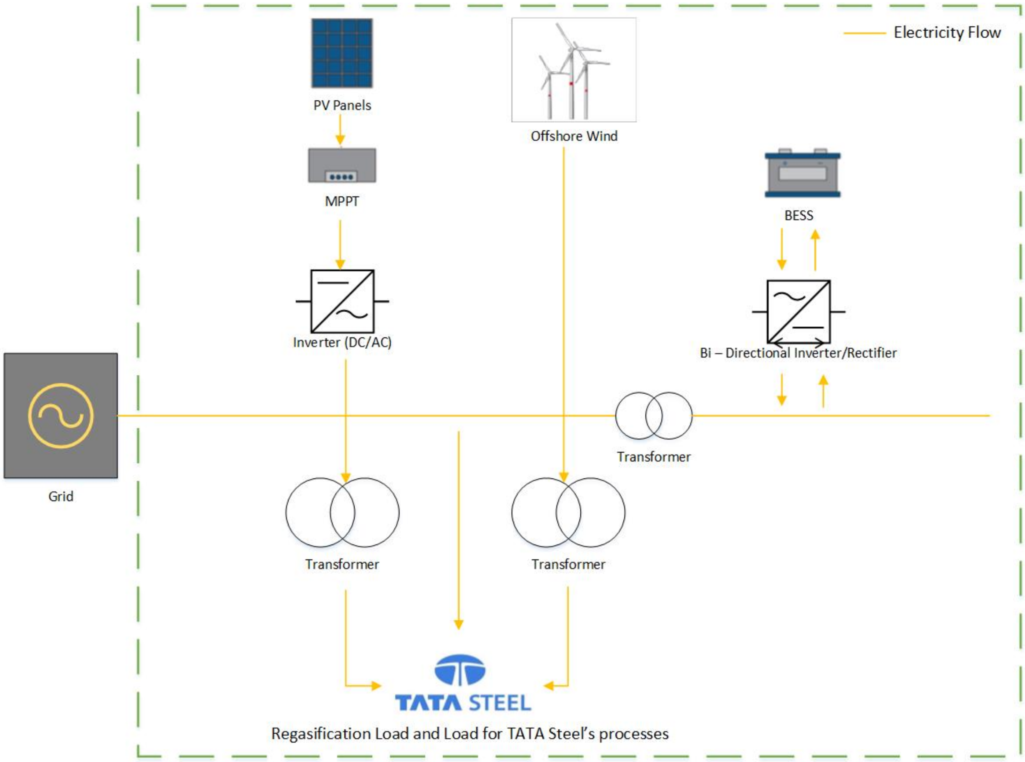


Figure 2.7: The graphic representation of the electricity part of the system for the local generation scenario cases

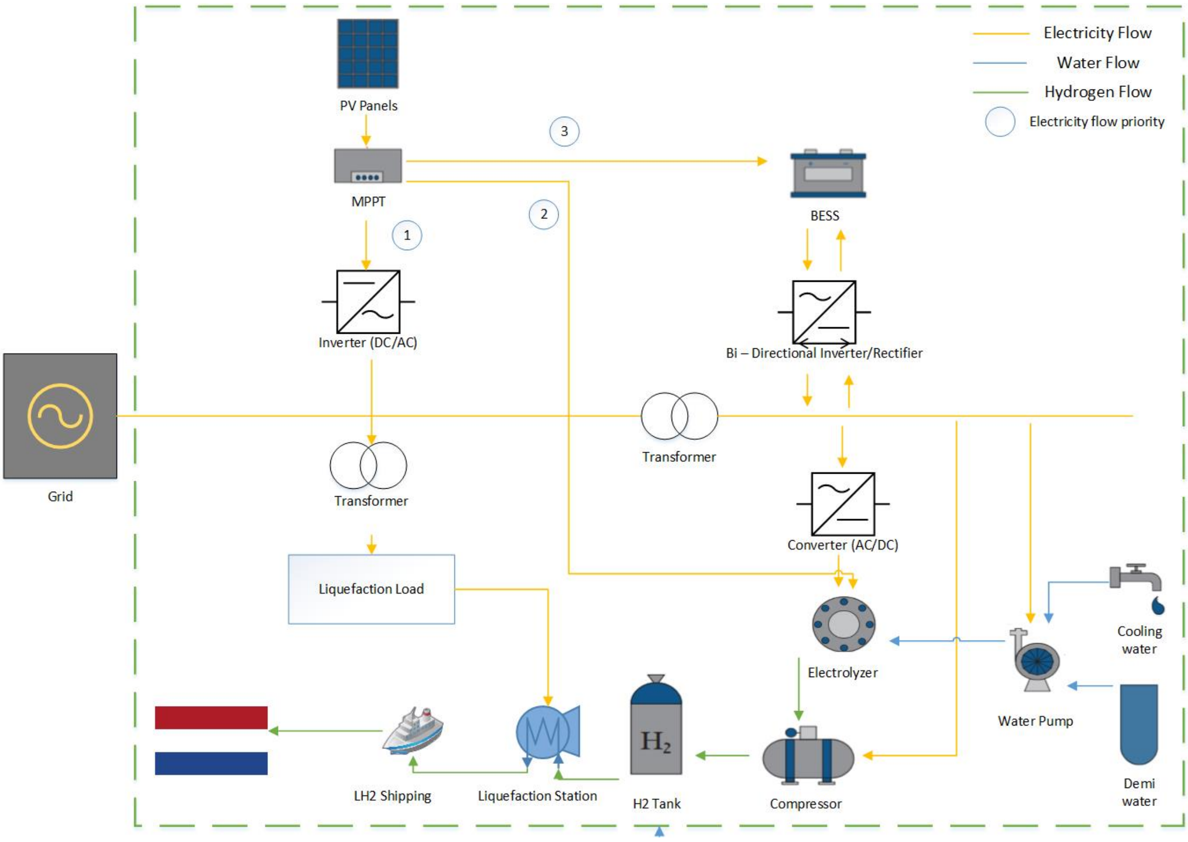


Figure 2.8: The graphic representation of the hydrogen part of the system for the non local generation scenario cases

### 2.1.4 System's components

In this section the different components of the system are analyzed. At first, the motivation for choosing the specific type of component is given and then the role that they have in the system is explained. Finally, an overview with the characteristics of each components is given that are also used as parameters and inputs in the simulation.

#### Wind Turbines

One of the two main sources for the electricity generation and thus the loads coverage are the wind turbines. These will be installed offshore in all scenarios near IJmuiden and with submarine cables in a distance of 50 km according to [12] the electricity will be transferred onshore. Since the loads of Tata Steel are high, many turbines are going to be needed. Also, the spacing between turbines has to follow the rule of 3 to 5 times their rotor diameter when in series and 5 to 9 when in parallel with reference to [13], means that the area with each turbine addition is increasing semantically. The choice came between a 5 MW, a 7 MW and a 10 MW wind turbine type. The final choice made was a 7 MW wind turbine because the 5 MW choice was not power effective and the 10 MW was not costly and area effective. The specific wind turbine that will be used for the wind farm simulation is the SWT - 7.0 - 154 of Siemens [14]. The main characteristics of the wind turbine are given in the table below 2.1.

Table 2.1: The characteristics of the wind turbine model used for the simulation of the offshore wind farm next to IJmuiden for the purpose of this study.

| Variable | Value | Description |
|---|---|---|
| Prated | 7000 kW | The rated power of the wind turbine |
| Blades number | 3 | The number of blades of the wind turbine |
| Rated wind speed | 12 m/s | The rated wind speed of the wind turbine |
| Rotor diameter | 154 m | The diameter of the wind turbine's rotor |
| Lifetime | 25 years | The lifetime of the wind turbine |

#### PV modules

For the solar modules selection the first motivation for their choice was to have a power output suitable for utility scale applications. The second motivation was to choose a technology that will be increasing as a share in the market the next years. Finally, the last motivation was the efficiency of the panels. At first according to the technology roadmap of reglobal published in June of 2022 [15], the Passivated Emitter and Rear Contact (PERC) technology has a market share of 85% that will be increased over the next years.

Further than that, the different panel technologies are the monocrystaline, polycrystaline, PERC and thin film. Between monocrystaline and polycrystaline, the main difference between the two is that even mono-crystalline is more expensive, it is on the same time more efficient (around 25%) than the poly-crystalline type (around 20%) as it is broadly explained in a comparison conducted in [16]. However, according to aurora solar's guide for PV panel types [17], it is explained that PERC technology is the cheapest and most efficient (around 5% more than monocrystaline) out of all the four aforementioned. Thus, the chosen panels that were used for this project with a rated power of 450 Wp are the PERC technology ones of PANASONIC [18] and the parameters can be seen in the table 2.2 below.

For the investment cost of the utility scale solar PV, from [19] it is mentioned that investment cost is divided in soft cost, installation cost and hardware cost. The soft cost includes all the costs for marketing sales, administrative costs and relevant permits. Installation cost includes all the costs for the electrical and mechanical installation of the system and finally hardware cost includes all the materials needed to be bought for the system. For the hardware cost, the cost for PV panels only was considered as the rest of the equipment's cost is calculated separately. All the prices are presented in their respectful scenarios section as they are adjusted for the future years.

Table 2.2: The characteristics of the PV panels used for the simulation of the solar park at IJmuiden for the purpose of this study.

| Variable | Value | Description |
|---|---|---|
| Pmpp | 450 Wp | The rated power of the solar panel |
| Vmpp | 41.4 V | Voltage on the maximum power point |
| Impp | 10.87 A | Current on the maximum power point |
| Voc | 49.2 V | Open circuit voltage of the solar panel |
| Isc | 11.61 A | The short circuit current of the solar panel |
| $\eta_{\text{module}}$ | 20.7 % | Solar panel efficiency |
| NOCT | 44 °C | The normal operating cell temperature |
| $\mu_{\text{power}}$ | -0.36 %/°C | Temperature coefficient relating power change with temperature |
| $\mu_{\text{voltage}}$ | -0.304 %/°C | Temperature coefficient relating voltage change with temperature |
| $\mu_{\text{current}}$ | 0.05 %/°C | Temperature coefficient relating current change with temperature |
| $A_{\text{module}}$ | 2.177 $m^2$ | The area of the PV module with 2.095 m length and 1.039 m width |

**Batteries**

For the scope of this project, a large scale battery bank was needed to be added in the simulation process to suit the utility scale applications that are investigated. The battery bank of CubeEnergy [20] was chosen to be used. The simulation is calculating the number of the different battery strings that are needed to be installed in the final battery bank container with a capacity of 138 kWh each. Each container according to the manufacturer can include up to 20 strings that leads to a battery bank capacity of 2764 kWh that leads to the final calculation for the amount of the different battery banks needed as it can be seen to the final results.

**Converter, Inverter, Rectifier and Cables**

For the scope of this project and since an intermediate level simulation was done, for these four components, the average efficiency values were used. Referencing to [[21], [22], [23]], for the inverter the value used was 0.98 while for the converter and rectifier 0.997. Finally, for the cables a value of 0.995 was used.

**Electrolyzer**

There are two categories of electrolyzers that are commercially available. The one is the alkaline electrolyzer and the other one is the polymer electrolyte membrane or PEM electrolyzer. As PEM electrolyzers are more expensive and their lifetime is lower than the alkaline ones acording to [24] and to [25], the alkaline electrolyzer type was chosen for this project.
The electrolyzer system that was used in this project is the one of hyprovide as specified in [26]. The rated power of the electrolyzer is equal to 250 kW, the maximum current is equal to 1300 A, while the maximum voltage is 250 V. Finally, the temperature operating is between 80 and 150 °C and the pressure 35 - 40 bar.

**Hydrogen Shipping**

For the hydrogen transport method, it was chosen to liquefy it and then transport it through ships from Arabia Peninsula to the Netherlands. When arrives to the Netherlands regasify the hydrogen and store it for further use. This decisions were motivated through the analysis of the different transport methods of hydrogen [27]. It is mentioned that the transport of hydrogen through small distances is chosen to be done by trucks or pipelines while for big distances a hydrogen carrier or hydrogen in liquid state are usually used to transport it through ships.

For the shipping of the hydrogen at first 5 different areas were selected in the countries of Saudi Arabia, Oman and Abu Dhabi. From [28], it was found that the time for the ship to arrive from the Arabian Peninsula to the port of Rotterdam was the smallest for Saudi Arabia equal to 12.9 days with a speed of 15 knots as it is mentioned at [29]. Starting from Abu Dhabi needed 19.8 days while starting from Oman it was needing 18.5 days. Thus, this justifies the decision to select the Saudi Arabia region to install the hydrogen system.

Furthermore, due to the boil - off effect on the gas, some gas is evaporated again due to heat transfer into the tank causing the liquid to boil and the pressure in the tank to rise. Thus, a small percentage of the liquid hydrogen is becoming gas again and to relieve this pressure increase the boil - off gas is released from the tank according to [30]. This percentage referring to the tank's gas volume, was found from [31] in a range from 1 - 5 % per day. Since, the first scenario that is including hydrogen transportation from the Arabian Peninsula to the Netherlands is for the year of 2030, it is assumed that by then the percentage will be low enough equal to 1.5% per day. This is because the technology curve especially on hydrogen components and processes is expected to grow fast as nowadays is the fuel that the most attention was fallen to [32].

### 2.1.5 Meteorological Data

For this study there are two different types of meteorological data that are used. The first one is the incident irradiation on the plane of arrays data for the modelling of the photovoltaic part of the system. The second one refers to the wind turbines part of the system and it includes the wind speeds in the offshore area next to IJmuiden.

The irradiation data are taken from the Meteonorm software [33] and they refer to the IJmuiden area where Tata Steel is. Further than the IJmuiden area, the location of Saudi Arabia was chosen due to the shortest shipping time between the Arabic peninsula and the Netherlands and thus the coordinates of the Madinah area are also given below. More specifically, in the array of data it is included the diffuse radiation ($G_{\text{diffuse}}$), the ground reflected radiation ($G_{\text{ground}}$) and the direct radiation ($G_{\text{direct}}$). Elaborating more on the terminology used from, [34] the sunlight it is partially scattered and attenuates the direct component of the irradiation that is mentioned here as the $G_{\text{direct}}$. A part of the scattered light, will arrive as well at the earth's surface as diffuse sunlight constituting the $G_{\text{diffuse}}$ component. Finally, the last part of the sunlight is reflected from the ground constituting the $G_{\text{ground}}$ component. According to the following equation 2.1.1, the irradiation in the plane of array ($G_{\text{M}}$) can be calculated.

$$G_{\text{M}} = G_{\text{direct}} + G_{\text{diffuse}} + G_{\text{ground}} \tag{2.1.1}$$

Therefore, the location's coordinates can be seen below in 2.4

Table 2.3: The coordinates for the location that the solar data were extracted for. They refer to IJmuiden location and the software used is called Meteonorm.

| **Variable** | **Value** | **Description** |
|---|---|---|
| Latitude | 52.5 | The latitude used for the IJmuiden location |
| Longitude | 4.6 | The longitude used for the IJmuiden location |

Table 2.4: The coordinates for the location that the solar data were extracted for. They refer to Madinah location of Saudi Arabia and the software used is called Meteonorm.

| **Variable** | **Value** | **Description** |
|---|---|---|
| Latitude | 24.53 | The latitude used for the IJmuiden location |
| Longitude | 39.57 | The longitude used for the IJmuiden location |

For the wind data, the wind speeds were extracted from the Meteonorm software for the Amsterdam's data series for a whole year. However, to adjust to the offshore location a further manipulation was needed. The average wind speed for the offshore location next to IJmuiden was 9.41 m/s according to Global Wind Atlas, [35]. The average value was calculated also for the wind data extracted for the Amsterdam's area wind speed, equal to 4.78 m/s. Then the ratio between the two average wind speeds was calculated equal to 1.97. The manipulation of the data was to multiply the Amsterdam's wind speed data series with the ratio number to get a data series that represents the offshore location next to IJmuiden. A graphic representation of the wind speeds after the data manipulation that represent the IJmuiden offshore area, is given in the figure below 2.9.

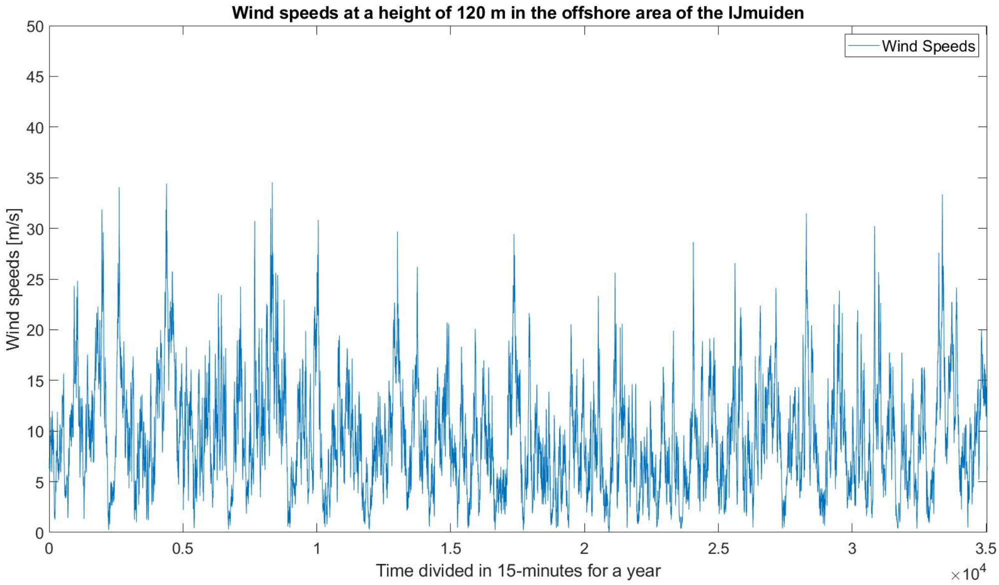


Figure 2.9: The graphic representation of the wind speeds in the offshore area of the IJmuiden

### 2.1.6 Area specification for the resulting optimal system

In this subsection the capacity per required area for the wind farm and the solar park will be calculated by taking into account the spacing between the wind turbines and the solar panels for optimum operation to confront the wake of the wind and the shading issues respectively. Furthermore, the area needed per battery bank and electrolyzer will also be analyzed and calculated accordingly.

#### Wind Turbines

As it has been already mentioned in the section 2.1.2, next to IJmuiden 50 km from the shore, an area is already dedicated for wind farms up to 4000 MW capacity. Following this, the maximum number of wind turbines that the optimization algorithm was able to install was 500 that correspond to 3500 MW capacity. According to [36], the spacing for the direction perpendicular to wind can be 3 to 5 times the diameter of the wind turbine while it can be 5 to 9 times the diameter of the wind turbine for the direction of the wind. This gives an average spacing for a wind turbine of 0.66 km$^2$ as the diameter of the wind turbine's rotor is equal to 156 m. Thus, this leads to 10.61 MW/km$^2$. In the following figure 2.10 the aforementioned are displayed.

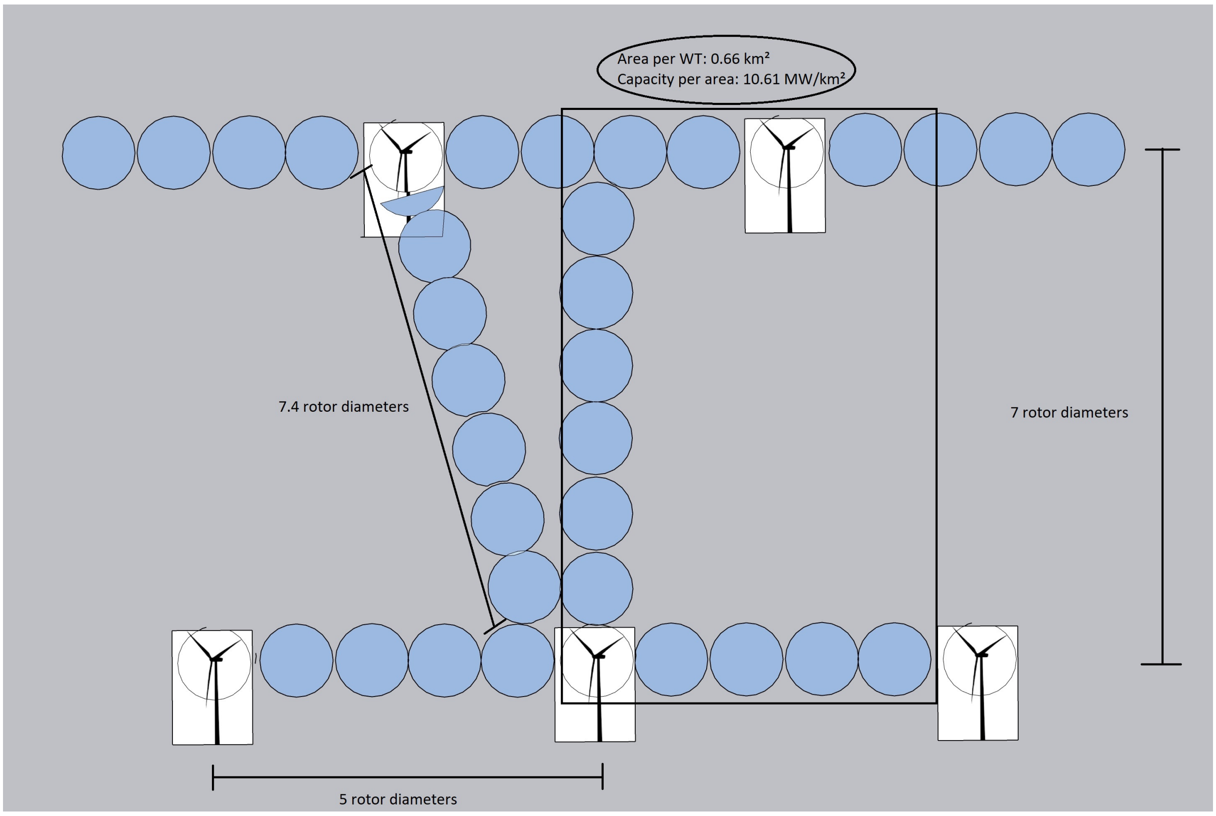


Figure 2.10: The installed capacity of wind turbines per area required in a graphic representation

**Solar Panels**

For the solar panels, according to [34], a distancing between two solar panels to avoid shading effects was used and more specifically the rule of thumb that specifies the distance between two solar panels equal to three times the length of the solar panel. For this calculation it was assumed that the solar panels were installed the one next to the other in the rows direction and with a distance equal to 4 m in the other direction. This calculation is broken down to one term that is equal to three times the length of the panels plus the adjacent side length of the panel, equal to 0.87 m, that is tilted 40 degrees from the ground horizontal. The tilt angle was taken from the global solar atlas online application for the IJmuiden location. [37]. Thus, the capacity per area for one solar panel is equal to 450 W per 8.35 $m^2$ or 53.9 $W/m^2$. For the Saudi Arabia installation of solar panels, according to [38], the optimal tilt angle is equal to 25°. Thus, the capacity per area for one solar panel is equal to 450 W per 8.43 $m^2$ which results in 53.38 $MW/km^2$. The aforementioned analysis can be seen in the figure 2.12 below.

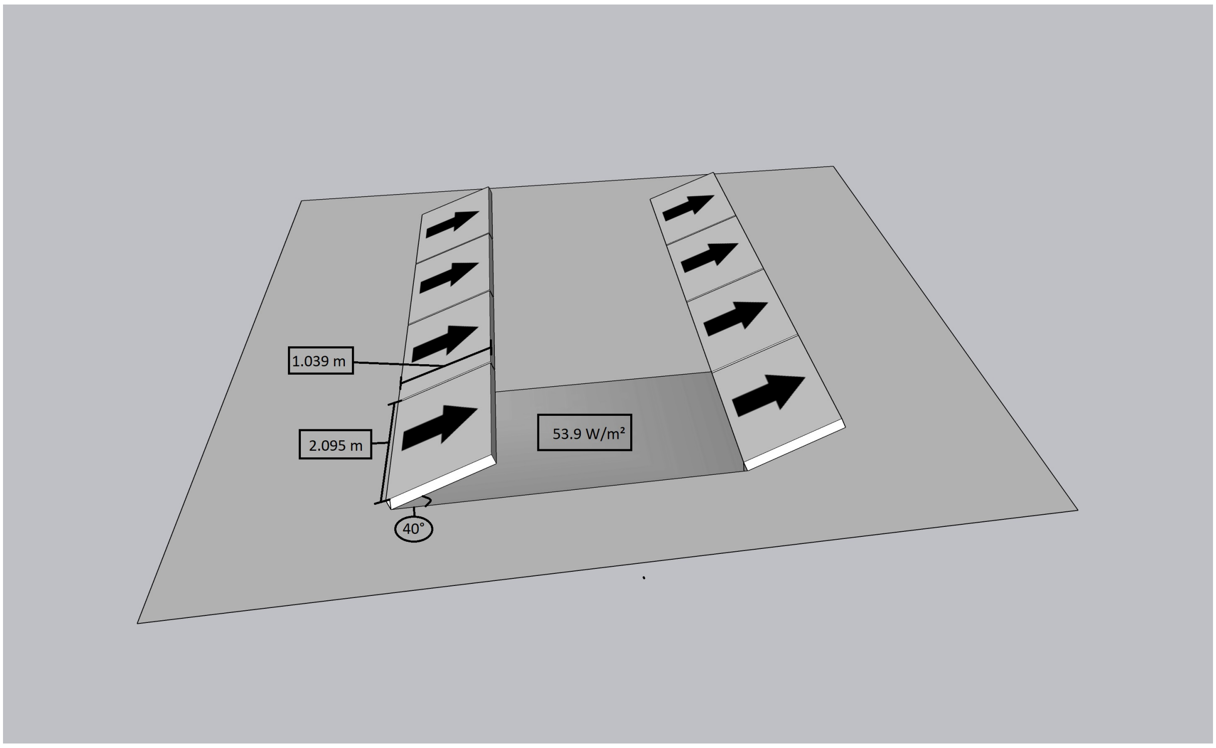


Figure 2.11: The installed capacity of solar panels per area required in a graphic representation for the IJmuiden area

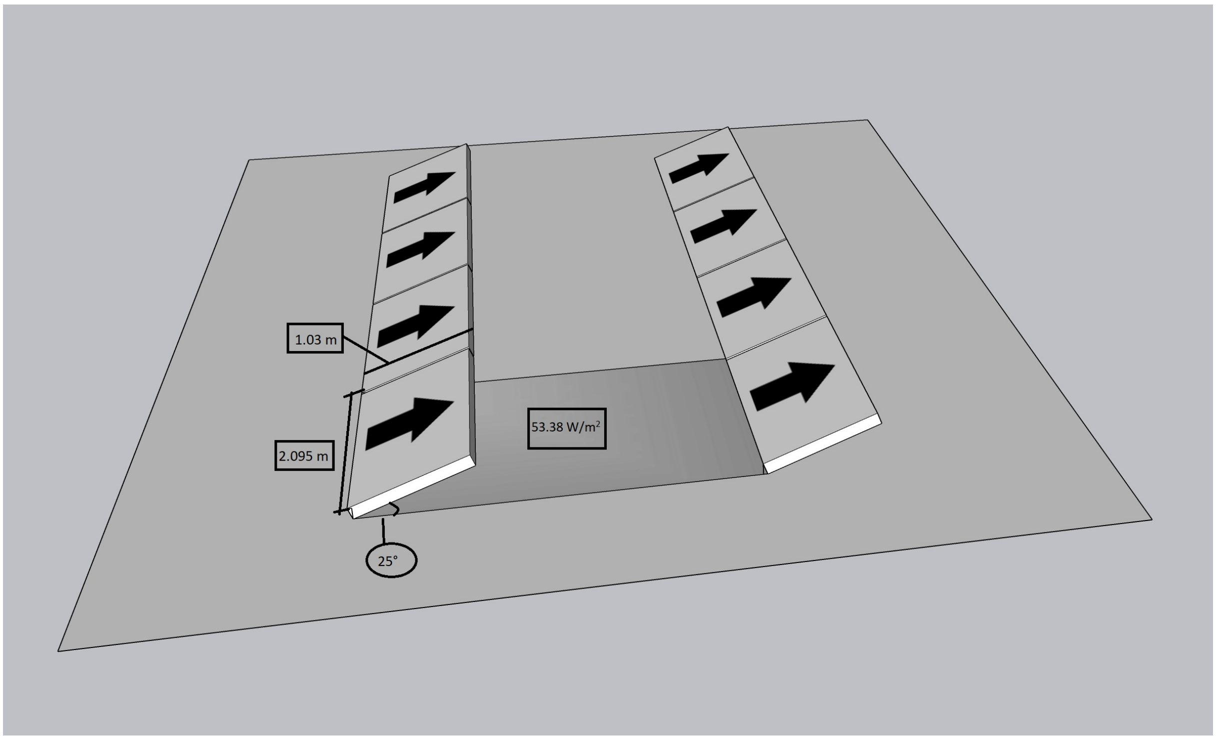


Figure 2.12: The installed capacity of solar panels per area required in a graphic representation for the Al Madinah area

**Battery banks**

According to the battery bank data sheet [20], the area needed per battery bank is equal to 29.72 $m^2$. The dimensions of width and length can be seen in the following figure 2.13.

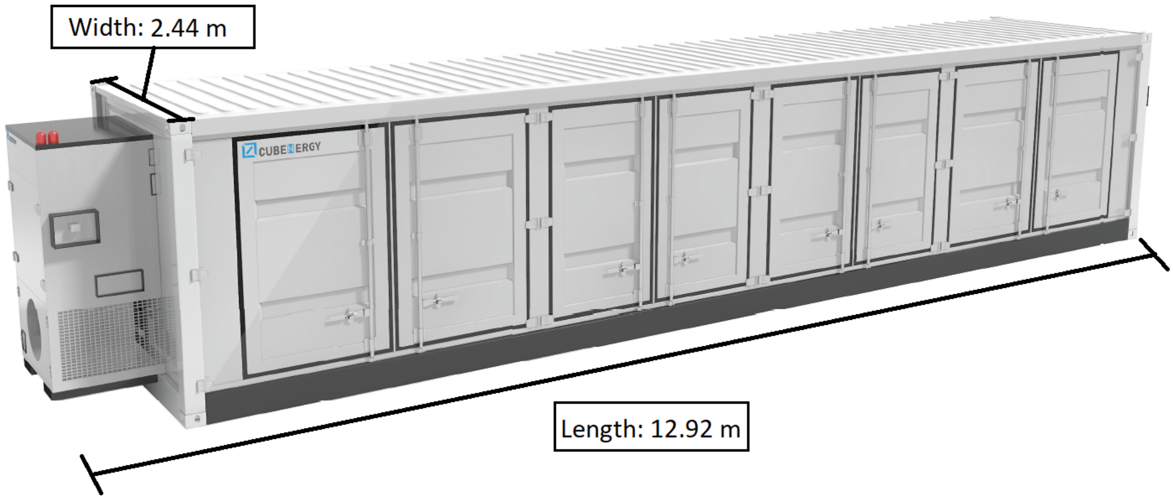


Figure 2.13: The dimensions of the battery bank used in this project in a graphic representation, [20]

**Electrolyzers**

According to [26], the area needed per electrolyzer is equal to 2.53 $m^2$. The dimensions of the length and the width can be seen in the following figure 2.14.

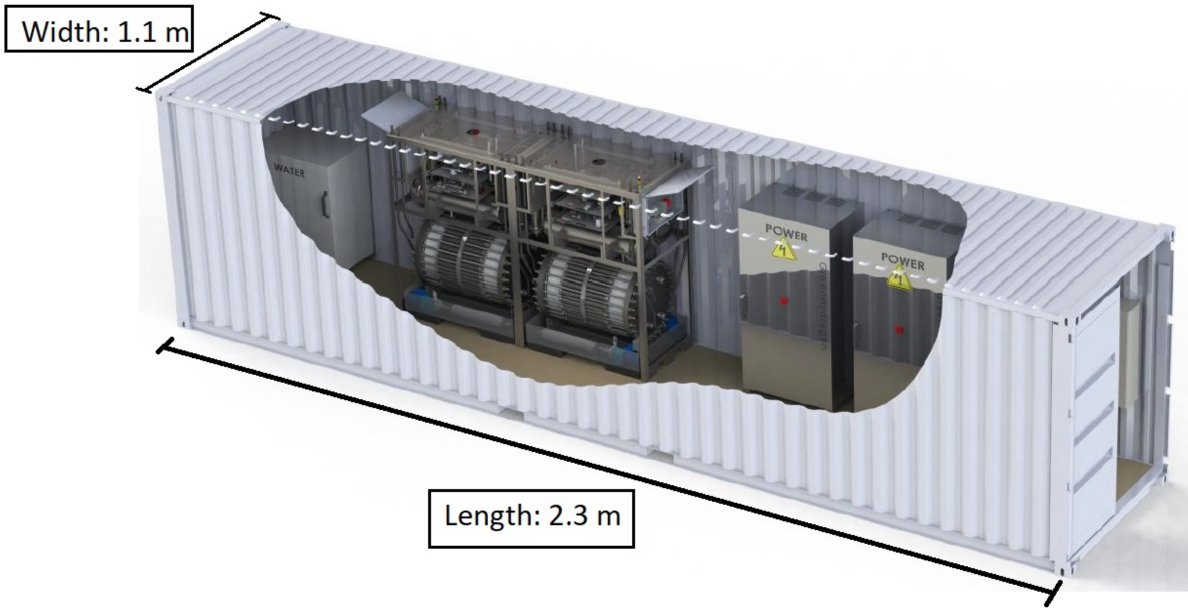


Figure 2.14: The dimensions of the electrolyzer system used in this project in a graphic representation, [26]

## 2.2 Loads Analysis

In this section after introducing the current and projected steel-making processes, the loads for the three different steel-making routes that are studied will be introduced. There is the current route in which a blast furnace is used. Then there is the 2030 potential route in which a direct reduction of iron will be taking place by replacing an amount of the fuel for this process with hydrogen. In this case also the furnace will be electric. Finally, for 2050 the whole reduction process will be potentially happening with hydrogen while again an electric arc furnace will be used.

### 2.2.1 Loads for the blast furnace with basic oxygen furnace route

Starting with the introduction of the current steel making process which can be seen in the figure below 2.15 where the inputs are iron ore and coal to end up with steel.

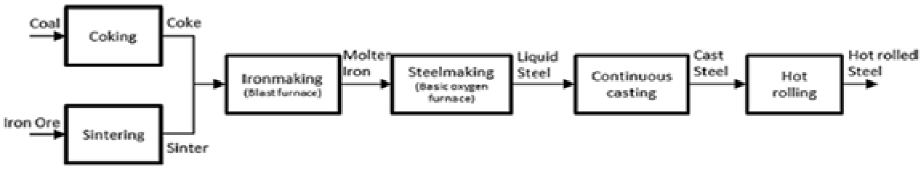


Figure 2.15: The graphic representation of the current steel-making route and the processes involved [39]

At first the sintering of the iron ore and the coking of the coal are taking place, so a powder of iron ore and coke will be produced respectfully. Then, the most intense process is taking place in an emissions sense. This is because two chemical reactions are taking place in the iron making process as presented below and each of them is producing 3 mols of CO2 released to the atmosphere. The first step to improve this process is to replace coal with natural gas which is what Tata Steel is currently doing. This leads to the steel making process which takes place in a basic oxygen furnace. The latter is fed with iron scraps or steel in a percentage of 25%, from the iron making process the liquid iron that consists of around 75% of the feeding stream and finally oxygen and liquid steel is produced [40].

$$2Fe_2O_3 + 3C \rightleftharpoons 4Fe + 3CO_2$$

$$Fe_2O_3 + 3CO \rightleftharpoons 2Fe + 3CO_2$$

After the process explanation, the electricity loads calculation is presented. According to the data from [39], the electrical energy's percentage to the total energy required in a steel industry is 11.42% while the rest is chemical energy. From Tata Steel's annual reports [4] the average annual steel production and the energy intensity data were extracted and thus the electrical loads needed to be provided were calculated including the heating of the fuel to a proper temperature for the reaction. The temperature that the reduction reaction takes place at in the blast furnace is in a range of 800 to 1600 °C. The calculations series that this was done can be seen in the table 2.5 below.

Table 2.5: Electricity loads that will be covered for the Business as usual scenario from Tata Steel's annual reports and McBrien's study of the energy requirements of the steel industry

| Business as usual Elecrricity loads | | |
|---|---|---|
| Annual Production | 6.8 | Million tons |
| Energy Intensity | 19.67 | GJ/ton |
| Electrical Energy | 11.42 | % |
| Chemical Energy | 88.58 | % |
| **Annual Electricity Load** | **15.2** | **PJ** |

### 2.2.2 Loads for the direct reduced iron with electric arc furnace route

Referring to [41], in the iron-making process, the iron ore turns to iron by feeding a shaft furnace with a reducing gas that contains $H_2$, CO, $CH_4$, $H_2O$, $CO_2$ and $N_2$. To produce the reducing gas, a series of reactions are taking place. At first the methane reforming is taking place to produce CO and $H_2$ from $CH_4$. Then, the reduction of iron to turn hematite ($Fe_2O_3$) into iron (Fe) goes through a series of reactions in which is carburized to FeC and finally iron (Fe) is produced. It is currently investigated how the reduction of iron can be done in a more sustainable way.

According to [42], the most popular method is MIDREX technology [43], that uses a shaft reactor for the direct reduction process and replaces a part of natural gas with hydrogen. Thus, this technology is adopted for this study. It is stated at [44], that for up to 30% replacement of natural gas with hydrogen, is acceptable without any change in the process while the respectful temperatures that the reaction takes place is at 700 - 980 °C so the preheating of the fuel is also considered in the loads. The changes with respect to the business as usual steel making route can be seen in the figure 2.16 below.

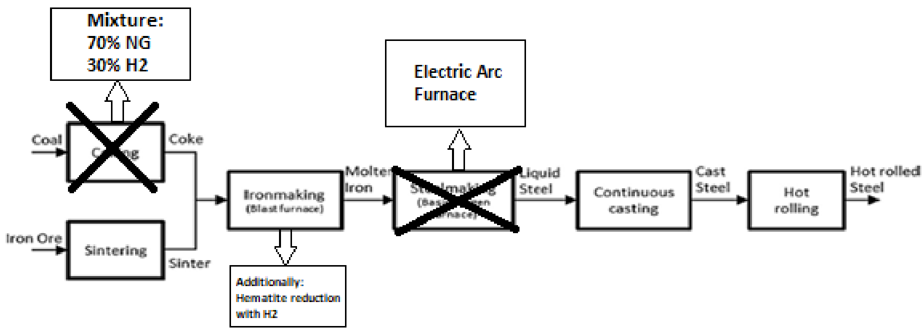


Figure 2.16: The graphic representation of the steel-making route as projected for 2030 and the new processes involved with respect to the business as usual case [39]

Thus, all the calculations performed for a 30% replacement of natural gas with hydrogen. Thus, a new chemical reaction will start taking place, reducing hematite with H2 and producing in the end water in addition to iron as it can be seen below.

$$Fe_2O_3 + 3H2 \rightleftharpoons 2Fe + 3H_2O$$

The electricity demand for the direct reduction of iron and the electric arc furnace are adopted from [45]. For the direct reduction of iron 353 kWh/$t_{HRC}$ or 1.27 GJ/$t_{HRC}$ are needed, where Hot rolled coil (HRC) is the hot rolled coil which is the final product. Tata steel produces on average 6.8 million tons per year [3] and thus the total electricity demand for the electric arc furnace for the period of one year is 8.64 PJ. For the direct reduction of iron, according to [45], 90 kWh/$t_{HRC}$ or 0.32 GJ/$t_{HRC}$ are needed which is translated to 2.2 PJ annually. Further than these two basic processes, electricity is also needed for the continuous casting process and the hot rolling process. According to [45], the amount for both is 2.4 PJ. So, in terms of electricity the amount of 13.25 PJ needs to be covered annually for the basic processes. Other than that, electricity to power the electrolyzer is needed, but it cannot be preset as it is defined through the simulation process.

However, an extra amount of electricity is needed to produce the hydrogen that will be replacing the natural gas. From [44], when operating with 100% of natural gas, 259 $m^3$ of NG per ton of reduced iron are needed. Thus, for a 30% reduction, the amount of natural gas will be 181.3 $m^3$ per ton of reduced iron. For hydrogen, by applying a simple energy balance to equalize the energy needed from the hydrogen and the energy that the replaced amount of natural gas was providing, occurs that 262.24 $m^3$ per ton of reduced iron are needed. To perform the calculations, the higher heating value of hydrogen was taken equal to 3.54 kWh per $m^3$, while for the natural gas, it was adopted the energy content value of 43 MJ/$m^3$ that is also used at [44] or 11.95 kWh/$m^3$. The energy that is offered through green hydrogen is 3.34 GJ/$t_{DRI}$. As it is stated at [39], the ratio between direct reduced iron and the final product of hot rolled coils is equal to 1.04. This is applied to the aforementioned value for the energy provided by the hydrogen and the final amount is equal to 3.47 GJ/$t_{HRC}$. Thus yearly, the hydrogen needed to supplied is equal to 1854.65 million $m^3$. A summary of all the numbers used for this scenario loads analysis are given in table 2.6.

Table 2.6: Total annual electricity consumption breakdown for a 30% replacement of Natural Gas with Hydrogen in the Direct reduction of iron shaft

| Direct reduction - Electric arc furnace Load | | |
|---|---|---|
| Steel Production | 6.8004 | Million $t_{HRC}$ |
| Electric arc furnace (EAF) electricity intensity | 1.27 | GJ/$t_{HRC}$ |
| EAF total electricity consumption | 8.64 | PJ |
| Direct reduction of iron (DRI) electricity intensity | 0.32 | GJ/$t_{HRC}$ |
| DRI total electricity consumption | 2.2 | PJ |
| Continuous casting total electricity consumption | 0.3 | PJ |
| Hot rolling total electricity consumption | 2.1 | PJ |
| H2 production intensity | 1854.65 | Million $m^3$ @ 25 °C |
| Energy offered by green H2 | 3.47 | GJ/$t_{HRC}$ |
| **Total Electricity Consumption** | **13.25** | **PJ** |

### 2.2.3 Loads for a Hydrogen - direct reduction with electric arc furnace route

From the study performed by Holling [46], the route where 100% of hydrogen is investigated in the shaft of the direct reduction of iron. The idea remains the same as described in the previous section but hydrogen will totally replace natural gas. This will lead to a zero emissions steel industry. An electric arc furnace will also be used to replace the basic oxygen furnace and the electricity will be produced in total by renewable energy sources. Breaking down this route, electricity will be needed for the electric arc furnace which is considered to be 8.64 PJ as reported in [45]. Further than that, considering again the average production of 6.8 million tons of Tata Steel, a total consumption of 7.89 PJ for heating and auxiliary sources as they are mentioned in [46] are needed. Without again presetting the load of the electrolyzer as it will be optimized through the simulation process, a total electricity load of 18.95 PJ/year needs to be covered. For the hydrogen load, it is calculated that 660.4 $m^3$/$t_{HRC}$ are needed, including

20% excess of H2. Thus the final amount needed for the whole year is equal to 4491 million $m^3$ at 25 °C. In this case the only reaction that is taking place is the reduction of hematite with hydrogen. Again, for these loads the pre - heating of the fuel has been added to the loads and it refers to a temperature range of 700 - 900 °C.

Table 2.7: Total electricity consumption breakdown for a 100% replacement of Natural Gas with Hydrogen in the Direct reduction of iron

| Hydrogen direct reduction - Electric arc furnace Load | | |
|---|---|---|
| Steel Production | 6.8004 | Million tHRC |
| EAF electricity intensity | 1.27 | GJ/tHRC |
| EAF total electricity consumption | 8.64 | PJ |
| Hydrogen direct reduction (HDR) electricity intensity - Auxiliary and Heating | 1.16 | GJ/tHRC |
| HDR total electricity consumption | 7.89 | PJ |
| Continuous casting total electricity consumption | 0.3 | PJ |
| Hot rolling total electricity consumption | 2.1 | PJ |
| H2 production intensity | 4491 | Million m3 @ 25 °C |
| Energy offered by green H2 | 8.42 | GJ/tHRC |
| **Total Electricity Consumption** | **18.95** | **PJ** |

**Challenges of Hydrogen Direct Reduction process**

While this technology is still not fully commercialized yet, the most important challenges are mentioned. According to [47] and [48], in the product from the direct iron reduction shaft, a carbon content of 1.5 - 3% is needed in the iron. The main problem that occurs is that the reductant without carbon content will be re-oxidized and thus transport and storage difficulties will be occurred. To overcome this problem, a carburization reaction is taking place in the shaft, where carbon content from the fossil fuel of the shaft is provided. This carbon content is needed to metallize the iron and make the electric arc furnace process to happen without any implications and efficiently in the same time. A solution to this problem is to add biomass self reducing pellets in the shaft and thus provide the carbon content needed. Another problem that is challenging as well is the lack of energy sources. While the reduction of iron ore with hydrogen is highly endothermic, extra heat is needed but the temperature needs to be sustained. To solve this problem, more hydrogen has been already added as excess and it is considered that nitrogen is also added because it is an inert gas and acts as a heat carrier.

### 2.2.4 Liquefaction and regasification loads for the non - local generation scenarios

For the analysis of the non local generation scenarios of hydrogen, where it will be produced in the Arabian peninsula and then will be shipped to the Netherlands stored in liquid phase, the loads of liquefaction and regasification were also included. When hydrogen is produced in the Arabian peninsula is directly forwarded to the liquefaction state where it will be converted to liquid hydrogen by store it in a temperature of -253 °C to a well insulated tank. This is the case to avoid temperature increase and thus evaporation of hydrogen that will have to be released from the tank for safety reasons. The amount of gas that is released is also called boil - off gas. The aforementioned as well as the energy intensity for the liquefaction and regasification processes were taken from [30]. The load for the liquefaction process is equal to 2.43 MJ/$m^3$ while for the regasification process the heat exchange is done with seawater in order to evaporate hydrogen. For the regasification process there is an environmental limit stating that seawater after the heat exchange with the $LH_2$, of -253 °C should not be lower than 5 °C. This limit was considered to be the case throughout the whole year for the regasification process. Combining information from [30] and [49], it is feasible to evaporate liquid hydrogen back to its gaseous form by using a SUPER-ORV which is a highly efficient device that can perform this conversion by using seawater. The load that could be consider was the one of the pumps that would transfer the seawater for heat exchange with the $LH_2$. Each tank that performs such a heat exchange with seawater can be 6 to 8 meters high. Thus the only load that needed to be calculated and generated, under the aforementioned assumptions, was the one of the pump. A pump's power requirement is calculated as the hydraulic power needed, which is also the theoretical energy to perform such a work. Depending on the efficiency of the pump then, which is considered equal to 0.75, the final shaft power is calculated as described in the following equations 2.2.1, 2.2.2 which is also the load considered for the regasification process. In the table 2.8 below, the liquefaction and regasification loads for the non - local generation scenarios are presented.

$$P_{\text{hydraulic}} = \frac{Q * d * g * h}{3.6 * 10^6} \tag{2.2.1}$$

Where,

$P_{\text{hydraulic}}$ = Theoretical power needed to pump the fluid up to a specific height [kW]

Q: the volumetric flow [$m^3/h$]

d: the density of the fluid [$kg/m^3$]

g: gravity acceleration equal to 9.81 [$m/s^2$]

h: the height difference to pump the fluid [m]

$$P_{\text{shaft}} = \frac{P_{\text{hydraulic}}}{Eff_{\text{pump}}} \tag{2.2.2}$$

Where,

$P_{\text{shaft}}$ = The power required from the motor [kW]

$\text{Eff}_{\text{pump}}$: Pump's efficiency [-]

Table 2.8: Load for liquefying and regasifying hydrogen for the non - local generation scenarios for the years of 2030 and 2050

| ***Non local generation scenario*** | | |
|---|---|---|
| **Case/Process** | **2030** | **2050** |
| Regasification | 0.215 PJ | 0.522 PJ |
| Liquefaction | 4.496 PJ | 10.913 PJ |

### 2.2.5 Operation and maintenance time

For an industry like the steel one, the load is assumed to be constant throughout the year. Thus, the operation time is taken equal to 7908 out of the 8760 hours per year and thus the total electricity amounts are divided into 15 - minutes steps for these 7908 hours. The rest are considered to be maintenance time, which is equal to 852 hours or 35.5 days. To reach to these numbers, the ratio between the average production of the IJmuiden plant and the total capacity was considered. The average production is equal to 6.8 million tons per year while the total capacity is equal to 7.5 million tons per year. By applying this ratio of 0.903 to the 8760 hours of a year, the operational time occurred equal to 7908 hours which leaves us with a maintenance time of 852 hours. According to literature [50], the amount of days under maintenance were reported for the years of 2015, 2016 and 2017 and an average downtime of 39.3 days occurred by manipulation of the data. Thus, by following the aforementioned approach the relative difference between the calculated number and the reported one is 11% and is considered to be solid enough for the purpose of this study. The downtime, is basically divided into planned and unplanned downtime. By planned downtime, the reference is done to the regular maintenance of a plant, and according to [50] is equal to around one month per year which is divided into two weeks periods throughout the year. Since it is a planned activity, for the optimization of the results it is forced to happen when the availability of the energy source depending on the scenario studied is the least. It was found that the planned maintenance will be happening during the fifteen days period between the 22$^{nd}$ of January and 6$^{th}$ of February and at the end of the year during the 26$^{th}$ of November and the 11$^{th}$ of December. For the unplanned maintenance, a random input to the load data series of these 5.5 days took place throughout the year to approach as much as possible the reality. The loads data manipulation were done through a MATLAB code that can be found in A.1

# 3| System Optimization

In this chapter, the optimization method used to find the optimal system design is described. At first in section 3.1, the optimization algorithms used are briefly discussed and the variables used for the optimization objective function are presented. Then in section 3.2, the optimization process used per scenario is described. Finally in section 3.3, the values for the prices to evaluate the financial part of the system are presented.

## 3.1 Optimization Method

To perform the optimization of the system the TRNOPT component from the TRNSYS library was used. This component is allowing the direct link of the Generic Optimisation Program (GenOpt), created by Lawrence Berkeley National Laboratory, with the TRNSYS program. According to [51] GenOpt, includes a lot of different optimisation algorithms that can be used but the chosen one for this project was the hybrid method that is using the Particle Swarm Optimisation (Particle Swarm Optimisation (PSO)) and the Hooke - Jeeves algorithms in series. At first, the PSO algorithm is investigating the objective function's results by trying many different starting points that prevent the algorithm to be trapped in a local minimum solution. Then, the Hooke - Jeeves algorithm is using the minimum found by the PSO algorithm and by carrying out a pattern movement around the different points search for a global minimum solution.

### 3.1.1 Particle Swarm Optimisation

The PSO algorithm, created by Kennedy, Eberhart and Shi to optimize continuous and non - linear functions. As described in [52], the main idea of this algorithm is to correlate the values of the different control variables that are about to be optimized with a swarm of birds. Each different combination of the control variable values constitutes a particle and this particle is directly linked with the idea of a bird in a swarm. The birds in a swarm share information with each other about their distance and location with their goal to reach altogether in their final destination. This is the idea of the PSO algorithm as well. From each set of different values of the control variables, these information are shared to create a new set of control variable values, a particle. Each generation of particles is making the algorithm more accurate as the information from the previous generation is shared and a new generation is created until the specified number of different generation to be investigated is reached. The lowest optimal solution can then be found and this point is the initial point for the next algorithm used in this project named as Hooke - Jeeves.

### 3.1.2 Hooke - Jeeves algorithm

The Hooke - Jeeves algorithm is a combination of two different actions. According to [53], these actions are in series an exploratory and a pattern move. Starting from the point found in the PSO algorithm an exploratory move is done by increasing and decreasing, with respect to the preset step size, the value of a control variable at a time to determine if this yields a better result of the objective function. For the pattern move to be activated it needs to happen that neither the increase or decrease of the control variable gave a better result for the objective function. Then the pattern move is launched by using the best result control variable values of the exploratory move and moves to this direction. This leads to the creation of a new base point from which then is again followed the same approach with an exploratory move. When the pattern move cannot offer an improvement anymore to the result of the objective function, then the step size is reduced to make the final solution more accurate and the same approach with an exploratory move is followed. After investigating also a better solution with the reduced step size and no improvement is occurring, then the global optimum has been found.

### 3.1.3 System performance and cost variables

To optimize the system using the aforementioned hybrid algorithm, an objective function has to be built each time by combining system performance and cost variables in order to minimize them. The variables that were used to construct the objective function each time are specified in the following sections. In this section the equations and the definitions of each variable will be given.

**Levelised cost of electricity**

The levelised cost of electricity is defined as the ratio between the total cost of a system throughout its lifetime divided by the generated energy that was delivered to the load. The equation 3.1.1 that gives the LCOE calculation is given below. Furthermore, a net LCOE value is also calculated through the following equation 3.1.2, that includes the monetary gain by selling the excess of power to the grid as well as including this energy utilization in the total energy calculation of the LCOE equation.

$$LCOE = \frac{\sum_{y=1}^{y=25} \frac{I_{\mathrm{Cy}}+M_{\mathrm{Cy}}+R_{\mathrm{Cy}}+F_{\mathrm{Cy}}}{(1+r)^{\mathrm{y}}}}{\sum_{y=1}^{y=25} \frac{EnergytoLoad}{(1+r)^{\mathrm{y}}}} \tag{3.1.1}$$

Where,

$\mathrm{I_{Cy}}$: The investment cost of the system in year, y

$\mathrm{M_{Cy}}$: The maintenance cost of the system in year, y

$\mathrm{R_{Cy}}$: The replacements cost of the system in year, y

$\mathrm{F_{Cy}}$: The fuel cost for the system in year, y

EnergytoLoad: The generated and bought energy delivered to the load

r: The discount rate that was taken equal to 5%

$$LCOE_{\mathrm{NET}} = \frac{\sum_{y=1}^{y=25} \frac{I_{\mathrm{Cy}}+M_{\mathrm{Cy}}+R_{\mathrm{Cy}}+F_{\mathrm{Cy}}+Revenues_{\mathrm{y}}}{(1+r)^{\mathrm{y}}}}{\sum_{y=1}^{y=25} \frac{EnergytoLoad+EnergytoGrid}{(1+r)^{\mathrm{y}}}} \tag{3.1.2}$$

Where,

$\mathrm{I_{Cy}}$: The investment cost of the system in year, y

$\mathrm{M_{Cy}}$: The maintenance cost of the system in year, y

$\mathrm{R_{Cy}}$: The replacements cost of the system in year, y

$F_{Cy}$: The fuel cost for the system in year, y

$Revenues_y$: The revenues for selling the electricity to the grid

EnergytoLoad: The generated and bought energy delivered to the load

EnergytoGrid: The energy that is sold to the grid

r: The discount rate that was taken equal to 5%

**Self Sufficiency Ratio**

Another variable that was used for the construction of the objective function was the Self Sufficiency Ratio (SSR). This variable is defined as the ratio between the power that was provided by the grid to the total power demanded. Thus, the self sufficiency ratio represents the percentage of the power that the system was not able to provide to the load and instead was purchased by the grid. For the calculation of this variable, the following equation 3.1.3 was used.

$$SSR = \frac{\sum_{i=1}^{i} Pfromgrid_{\mathrm{i}}}{\sum_{i=1}^{i} Pload_{\mathrm{i}}} \tag{3.1.3}$$

Where,

i: the time step

$Pfromgrid_i$: the power purchased from the grid at time step i

$Pload_i$: the power to the load at time step i

In the same way the SSR for the hydrogen is also defined. The ratio this time is the $H_2$ purchased from the grid to the load of the $H_2$. The equation 3.1.4 is given below.

$$SSR_{\mathrm{H_2}} = \frac{\sum_{i=1}^{i} H_2fromgrid_{\mathrm{i}}}{\sum_{i=1}^{i} H_2load_{\mathrm{i}}} \tag{3.1.4}$$

Where,

i: the time step

$H_2fromgrid_i$: the power purchased from the grid at time step i

$H_2load_i$: the power to the load at time step i

## 3.2 Scenarios and Case Studies

In this section the different scenarios that will be studied are broadly explained. After the overview given in Section 2.1.3, the optimization variables and the ranges that will be investigated as well as the penalty functions will be presented for each scenario. Finally, the respectful objective function that needs to be minimized is also presented.

### 3.2.1 Business as usual scenario with a hybrid solar - wind electricity system

This case study will be the base case scenario for this study. It will be used as a reference case for the rest of them to make comparisons and reach to conclusions. The main components that are used in this case study are PV panels, offshore wind turbines and battery energy storage systems (BESS). Through optimization, the number of PV panels and their orientation, the number of wind turbines and the number of BESS will be determined. To achieve the aforementioned, the LCOE, the SSR and the difference between the initial state of charge and the final state of charge of the BESS will be calculated. The sum of all four functions will be used as the objective function to be minimized so the system will be optimized.

SSR: Self Sufficiency Ratio

$$p_{\mathrm{SSR}}(x) = SSR(x) \tag{3.2.1}$$

pSOC: The difference between the initial and the final state of charge of the battery bank

$$p_{\mathrm{SOC}}(x) = ABS(SOC_{\mathrm{initial}} - SOC_{\mathrm{final}}) \tag{3.2.2}$$

LCOE: The levelized cost of electricity

$$f(x) = LCOE(x) \tag{3.2.3}$$

LoadCoverage: The percentage of the load that is not covered

$$LoadCoverage(x) = ABS(1 - \frac{TotalEnergyToTheSystem}{TotalLoad}) \tag{3.2.4}$$

So, the objective function that will be minimized for the optimization of this system is:

$$ObjectiveFunction = \min_{x}[LCOE(x) + p_{\mathrm{SSR}}(x) + p_{\mathrm{SOC}}(x) + LoadCoverage(x)] \tag{3.2.5}$$

To achieve such an optimization, the main variables that are linked to the aforementioned functions are displayed in the table below 3.1

Table 3.1: Optimization variables and settings used to optimize the Business as usual scenario - 1 for its LCOE, SSR, load coverage and SOC of the BESS.

| **Variable** | **Range** | **Stepsize** | **Description** |
|---|---|---|---|
| $N_{\mathrm{WT}}$ | 0 - 500 | 1 | Number of offshore wind turbines to be installed |
| $N_{\mathrm{bat}}$ | 0 - 22.5*$10^7$ | 100 | Number of battery strings to be installed |
| $N_{\mathrm{S}}$ | 0 - Inf | 100 | Number of PV panels that will be oriented South |
| $N_{\mathrm{E}}$ | 0 - Inf | 100 | Number of PV panels that will be oriented East |
| $N_{\mathrm{W}}$ | 0 - Inf | 100 | Number of PV panels that will be oriented West |

**Scenario BAU - Economics**

For every component there are three different types of costs, the sum of which gives the total cost. At first, is the investment cost, then is the replacement cost if the lifetime of the component is smaller than the project's lifetime and finally the maintenance costs.

Table 3.2: Investment, Maintenance and Replacement costs of the components used in the BAU scenario and their lifetime.

| **Component** | **Investment Cost** | **Maintenance Cost** | **Replacement Cost** | **Lifetime** |
|---|---|---|---|---|
| PV Panels | 0.607 €/Wp | - | - | 25 |
| Wind Turbines | 1850 €/kW | 3% | - | 25 |
| Batteries | 0.13 €/Wh | - | 100% | 15 |
| Converter | 0.75 €/W | 3% | 100% | 10 |
| Inverter | 0.065 €/W | 3% | 100% | 10 |
| Rectifier | 0.22 €/W | 1% | - | 25 |

For the PV panels as explained in 2.1.4, the price used as the hardware cost is 0.213 €/Wp from averaging the prices reported in [54] while for investment cost the price is equal to 0.394 €/Wp giving a total investment cost of 0.607 €/Wp. For the PV maintenance cost a value of 3% of the investment cost was used [55].

For the wind turbines according to [56] the investment cost used is 1850 €/kW while for the maintenance cost a 3% of the investment cost was used.

For the batteries, according to [55] the investment cost used is 0.13 €/Wh and since the lifetime of the Li - ion batteries was taken as 15 years, the replacement cost is equal to the whole investment cost, discounted for the $15^{\text{th}}$ year. Maintenance cost was not considered under the assumption that the batteries will be replaced directly after 15 years working in a proper level.

For the inverter and converter the investment costs used were equal to 0.065 €/W and 0.75 €/W respectively. Both inverter's and converter's lifetime used is 10 years and thus the investment cost discounted after 10 and 20 years was used as the replacement cost. Finally, maintenance cost used was 3% of the investment cost [55].

For the rectifier, the investment cost was equal to 0.22 €/W while for the maintenance cost a value of 1% of the investment cost was used. [55].

Finally, for the buying and selling prices of the electricity from and to the grid, the prices assumed equal to 0.5 €/kWh for buying and 0.05 €/kWh for selling electricity. It was chosen an expensive buying price for pushing the system to generate the electricity needed on its own and also a low selling price for not linking the decrease of the levelized cost of electricity to over-generation during the optimization.

The prices that were used for the components are presented in the following table 3.2 per component.

### 3.2.2 Local Generation - Direct iron reduction and Electric arc furnace

For the second scenario the technology of an electric arc furnace will be used for the steel making process and the direct reduction of iron will be done with the addition of hydrogen to the fuel mix. Two different cases will be studied for the local generation scenario for both the processes presented, for the years of 2030 and 2050 and their respectful loads, in subsections 2.2.2 and 2.2.3. The system for both cases is the same and only the loads for the hydrogen and electricity production are changing. The system is comprised of PV panels, offshore wind turbines, batteries energy storage, electrolyzers and its auxiliary components. The latter are storage hydrogen tanks, compressors and pumps so it is possible to compress and store the hydrogen as well as also to let the water flow to the electrolyzer via the pumps. The functions that were added to the objective function were the electricity self sufficiency ratio, the self sufficiency ratio for the hydorgen, the LCOE, the hydrogen load coverage, the electricity load coverage and also the difference between the initial and final state of charge of the batteries. The sum of all these five was minimized to optimize the system.

SSR: Self Sufficiency Ratio

$$p_{\mathrm{SSR}}(x) = SSR(x) \tag{3.2.6}$$

pSOC: The difference between the initial and the final state of charge of the battery bank

$$p_{\mathrm{SOC}}(x) = ABS(SOC_{\mathrm{initial}} - SOC_{\mathrm{final}}) \tag{3.2.7}$$

LCOE: The levelized cost of electricity

$$f(x) = LCOE(x) \tag{3.2.8}$$

LoadCoverage: The percentage of the load that is not covered

$$LoadCoverage(x) = ABS(1 - \frac{TotalEnergytothesystem}{TotalLoad}) \tag{3.2.9}$$

$\mathrm{SSR}_{\mathrm{H2}}$: Self Sufficiency Ratio for the Hydrogen production

$$p_{\mathrm{SSR}_{\mathrm{H2}}}(x) = SSR_{\mathrm{H2}}(x) \tag{3.2.10}$$

$\mathrm{H2}_{\mathrm{Load}}$Coverage: The percentage of the load that is not covered

$$H2_{\mathrm{Load}}Coverage(x) = ABS(1 - \frac{TotalH2produced}{TotalH2Load}) \tag{3.2.11}$$

So, the objective function that will be minimized for the optimization of this system is:

$$ObjectiveFunction = \min_{x}[LCOE(x) + p_{\mathrm{SSR}}(x) + p_{\mathrm{SOC}}(x) + LoadCoverage(x) + p_{\mathrm{SSR}_{\mathrm{H2}}}(x) + H2_{\mathrm{Load}}Coverage] \tag{3.2.12}$$

To achieve such an optimization, the main variables that are linked to the aforementioned functions are displayed in the table below 3.1

Table 3.3: Optimization variables and settings used to optimize the Local Generation Scenarios - 2,3 for its LCOE, SSR, load coverage, H2 load coverage, hydrogen SSR and SOC of the BESS.

| **Variable** | **Range** | **Stepsize** | **Description** |
|---|---|---|---|
| $N_{WT}$ | 0 - 500 | 1 | Number of offshore wind turbines to be installed |
| $N_{bat}$ | 0 - 22.5*$10^7$ | 100 | Number of battery strings to be installed |
| $N_S$ | 0 - Inf | 100 | Number of PV panels that will be oriented South |
| $N_E$ | 0 - Inf | 100 | Number of PV panels that will be oriented East |
| $N_W$ | 0 - Inf | 100 | Number of PV panels that will be oriented West |
| $N_{ely}$ | 1 - Inf | 100 | Number of electrolyzers |

For these scenarios an optimization of the tank size was also done. The goal of the optimization was to find the best size of the tank to dump the less hydrogen, while trying to match the initial and final state of charge of the tank in the lowest cost. This problem was stated through the following objective function which consists of the variables of LCOE, hydrogen dump quantity over a year and the function that specifies the difference between the initial and final state of charge of the tank.

The function that specifies the difference between the initial and the final state of charge is given below

Where,

$$p_{\mathrm{SOC}_{\mathrm{H_2\ tank}}}(x) = ABS(SOC_{\mathrm{initial}} - SOC_{\mathrm{final}}) \tag{3.2.13}$$

$\mathrm{pSOC}_{\mathrm{H_2\ tank}}$: The difference between the initial and the final state of charge of the hydrogen storage tank

Thus, the objective function used to be minimized for finding the optimum size of the hydrogen storage tank is given below.

$$ObjectiveFunction = p_{\mathrm{SOC}_{\mathrm{H_2\ tank}}}(x) + H_2TotalDumping + LCOE(x) \tag{3.2.14}$$

The variables and the range that the aforementioned objective function was minimized for are given below.

Table 3.4: Optimization variables and settings used to optimize the Local Generation Scenarios - 2,3 for the volume of the hydrogen storage tank.

| **Variable** | **Range** | **Stepsize** | **Description** |
|---|---|---|---|
| Tank volume | 0 - 1.86*$10^9$ | 100 | Total volume of the hydrogen tanks |
| Initial tank's state of charge | 0.2 - 0.8 | 0.05 | Initial state of charge of the hydrogen tank |

### 3.2.3 Non Local Generation - Hydrogen Direct Iron reduction and Electric arc furnace

For this scenario, including the reduction of iron with 100% hydrogen in the fuel mix and an electric arc furnace two cases were studied. The one is for the loads calculated for the year of 2030 and the other one for the year of 2050. To study this scenario, the system can be divided into two subsystems. The one will be the hydrogen part of the system where the hydrogen will be produced in the Arabic Peninsula and will include the load to liquefy the hydrogen to be shipped back to the Netherlands. The second part of the system will be the local generation of electricity to cover the load for the regasification of the liquefied hydrogen and also the electricity loads of Tata Steel. The final variables that are referring to the optimal sizing of the system were calculated for both the two subsystems but also were calculated for the total system of each case.

**Electricity part of the system**

For this part of the system the optimization method followed is the same one described in the subsection 3.2.1. The variables to be minimized are the Self Sufficiency Ratio (SSR), the load coverage, the penalty function for the state of charge of the batteries and finaly the LCOE.

**Hydrogen part of the system**

For the second part of the system the optimization method that was followed was the same as the one analyzed in the subsection 3.2.1. The variables to be minimized for the optimized size of the system were the Self Sufficiency Ratio of the hydrogen, the load coverage for both the electricity and hydrogen loads, the state of charge of the battery and the LCOE.

## 3.3 Economics for the scenarios of Local and non Local generation

In this section the economic data that were used for the simulation of the system are analyzed. Both for the cases of 2030 and 2050 the prices were found in the literature regarding the projections of the prices for each component used on the systems simulated.

### 3.3.1 Scenario Local and non Local Generation 2030 - Economics

Following the approach already described in 3.2.1, the cost for each component will be briefly discussed in this subsection and also the sources that the values were taken from will be referenced.

For the PV panels, the value of 0.493 €/Wp as the total investment cost was used. This value can be broken down to the hardware cost of 0.213 €/Wp which is assumed to remain the same while for the investment cost from [57], the value of 0.28 €/Wp was chosen. The maintenance cost was kept the same with the BAU scenario at 3% of the investment cost.

For the wind turbines, the cost projection for 2030 from IRENA - Future of Wind report [58] was used equal to 1670 €/kW, while for the maintenance cost a value of 3% of the total investment cost was used.

Finally, for the batteries, inverters, converters, rectifiers, electrolyzers and its auxiliary components the prices were taken from [55], and are presented in the summary table below 3.5. Furthermore, in the next table 3.6, the prices for purchasing hydrogen when the demand is higher than the production for the year of 2030 was extracted from [59] and taken equal to 0.44 €/m$^3$. Also, the utility prices for demi and cooling water are given [55].

Table 3.5: Investment, Maintenance and Replacement costs of the components used in the Local generation scenario for 2030 and their respective lifetime.

| **Component** | **Investment Cost** | **Maintenance Cost** | **Replacement Cost** | **Lifetime** |
|---|---|---|---|---|
| PV Panels | 0.493 €/Wp | - | - | 25 yr |
| Wind Turbines | 1670 €/kW | 3% | - | 25 yr |
| Batteries | 0.075 €/Wh | - | 100% | 15 yr |
| Converter | 0.75 €/W | 3% | 100% | 10 yr |
| Inverter | 0.048 €/W | 3% | 100% | 10 yr |
| Rectifier | 0.22 €/W | 1% | - | 25 yr |
| Alkaline Electrolyzer | 0.21 €/W | 2.5% | 15% | 60000 hr |
| Storage tank | 85.39 €/$m^3$ | 1% | - | 60000 hr |
| Compressor | 130000 € | 6% | - | 60000 hr |
| Pumps | 0.09 €/$m^3$ | 5% | 100% | 15 yr |

Table 3.6: Utilities prices

| **Utilities** | **Costs** |
|---|---|
| Demi water | 30 €/$m^3$ |
| Cooling Water | 0.93 €/$^3$ |
| H2 price | 0.44 €/$m^3$ |

### 3.3.2 Scenario Local and non Local Generation 2050 - Economics

For the PV panels, the value of 0.383 €/Wp as the total investment cost was used. This value can be broken down again to the hardware cost of 0.213 €/Wp, while for the investment cost from [57], the value of 0.17 €/Wp was chosen. The maintenance cost was kept the same with the BAU scenario at 3% of the investment cost.

For the wind turbines, the cost projection for 2030 from IRENA - Future of Wind report [58] was used equal to 1375 €/kW, while for the maintenance cost a value of 3% of the total investment cost was used.

Finally, again for the batteries, inverters, converters, rectifiers, electrolyzers and its auxiliary components the prices were taken from [55], and are presented in the summary table below 3.7. Furthermore, in the next table 3.8, the prices for purchasing hydrogen when the demand is higher than the production for the year of 2030 was extracted from [59] and taken equal to 0.388 €/m$^3$. Also, the utility prices for demi and cooling water are given [55].

Table 3.7: Investment, Maintenance and Replacement costs of the components used in the Local generation scenario for 2030 and their respective lifetime.

| **Component** | **Investment Cost** | **Maintenance Cost** | **Replacement Cost** | **Lifetime** |
|---|---|---|---|---|
| PV Panels | 0.383 €/Wp | - | - | 25 yr |
| Wind Turbines | 1375 €/kW | 3% | - | 25 yr |
| Batteries | 0.035 €/Wh | - | 100% | 15 yr |
| Converter | 0.75 €/W | 3% | 100% | 10 yr |
| Inverter | 0.022 €/W | 3% | 100% | 10 yr |
| Rectifier | 0.22 €/W | 1% | - | 25 yr |
| Alkaline Electrolyzer | 0.095 €/W | 2.5% | 15% | 60000 hr |
| Storage tank | 85.39 €/m$^3$ | 1% | - | 60000 hr |
| Compressor | 130000 € | 6% | - | 60000 hr |
| Pumps | 0.09 €/m$^3$ | 5% | 100% | 15 yr |

Table 3.8: Utilities prices

| **Utilities** | **Costs** |
|---|---|
| Demi water | 30 €/m$^3$ |
| Cooling Water | 0.93 €/$^3$ |
| H2 price | 0.388 €/m$^3$ |

# 4| Results and Discussion

In this chapter, the final results of the optimized systems, a discussion and a reflection to the results per scenario are presented. To answer the research question "*What is the feasibility to cover with a solar - wind - hydrogen system, the loads of the different steel making routes of Tata Steel*", 5 different scenarios has been constructed. In section 4.1, the business as usual scenario optimized system is presented. It refers to a system that will cover the current electricity loads of Tata Steel with a hybrid system of wind turbines, solar panels and batteries. In the next section 4.2, the first scenario that refers to the local generation of both electricity and hydrogen, from a hybrid system of wind turbines, solar panels, batteries and electrolyzers is presented. It refers to the route of a fuel mix consisting of 30% of hydrogen and 70% of natural gas on the year of 2030. Then, in section 4.3, the scenario for the year of 2050 for the steel making route of 100% hydrogen usage in the reduction process is studied and hydrogen and electricity will be produced locally by a hybrid system of wind turbines, solar panels, batteries and electrolyzers. In section 4.4, the system is divided into two parts. The steel making route for the year of 2030 is studied again but the loads are attempted to be covered by two different systems into two different locations. The one will be in IJmuiden covering the electricity loads of the primary processes and the regasification loads for hydrogen, with a hybrid system of wind turbines, solar panels and batteries while the other part will be in the Arabic Peninsula including solar panels, batteries and electrolyzers and will be producing hydrogen and the electricity needed for liquefying the hydrogen for transport. The last scenario is presented in section 4.5, and it is structured as the one of section 4.4 but the electricity loads and the hydrogen demand are according to the steel making route for the year of 2050. Finally, a summary section 4.6 has been included that gives the total view of the final results in all the different aspects that have been studied throughout the scenarios.

## 4.1 Business as usual scenario

Following the optimization method described for this scenario in 3.2.1, the results that occurred for the principle parameters are an LCOE of 0.245 €/kWh with an SSR of 0.44 % and a Load Coverage of 99.56%. Also, the net $LCOE_{NET}$ was calculated that is also including the power sold to the grid and is equal to 0.065 €/kWh. Furthermore, the final values of the variables characterizing the system are presented and the performance of the system is discussed.

### 4.1.1 Results - BAU Scenario

The system consists of 350 Wind Turbines corresponding to a capacity of 2.45 GW. For the solar panels, the south oriented are 15000000 while none are installed in the east and the west orientation. The installed capacity for the south orientation is 6.75 GW. The amount of battery strings is 100100 and since each battery bank includes 20 strings, this gives a final number of 5005 battery banks with a total energy capacity of 13.81 GWh. The load to be covered is equal to 4701.34 GWh, while the system covered 4680.8 GWh. From these 4680.8 GWh, the 3999.63 GWh were offered directly from the hybrid system of the solar panels and the wind turbines while the rest 681.16 GWh were offered by the batteries due to the intermittency of the renewable energy sources. A total cost of the system of 16.22 billion € was calculated while the energy offered was equal to 4680.8 GWh and thus this leads to an LCOE of 0.245 €/kWh. The $LCOE_{NET}$ which also includes the energy that is sold to the grid is calculated equal to 0.065 €/kWh The energy bought from the grid to cover the load was equal to 20.55 GWh while the load investigated had a value of 4701.35 TWh and this led to an SSR of 0.44 %. The following summary tables are giving all the results of the optimization for this scenario. In table 4.1 the amount for each component needed is displayed, in table 4.2 the energy balance of the system and finally in table 4.3 the system performance variables.

Table 4.1: The amount of the different components of the system and their respectful installed capacity - BAU scenario

| **Variables** | **Value** | **Installed Capacity** |
|---|---|---|
| Number of wind turbines | 350 | 2.45 GW |
| Number of panels oriented south | 15000000 | 6.75 GW |
| Number of panels oriented east | - | - |
| Number of panels oriented west | - | - |
| Number of battery banks | 5005 | 13.81 GWh |

Table 4.2: The energy balance of the system which proves that the load equals the sum of the energy provided by the system, the batteries and the grid - BAU scenario

| **Variables** | **Value** | **Units** |
|---|---|---|
| Load | 4701.34 | GWh |
| System to the load | 3999.63 | GWh |
| Batteries to the load | 681.16 | GWh |
| Grid to the load | 20.55 | GWh |

Table 4.3: The system performance variables that were optimized through the objective function chosen as described in 3.2.1 - BAU scenario

| **Variables** | **Value** | **Units** |
|---|---|---|
| LCOE | 0.245 | €/kWh |
| $LCOE_{NET}$ | 0.065 | €/kWh |
| SSR | 0.44 | % |
| Load Coverage | 99.56 | % |

### 4.1.2 Discussion - BAU Scenario

The only constraint that could not be fulfilled by the optimization was the equality between initial and final state of charge of the battery. To overcome this problem, a different start time of the project was chosen for which the state of charge was equal to the final one. To fulfil the constraint given for the equality of the initial and final state of charge of the battery, the optimization algorithm was trying to install huge amounts of battery banks that would never charge during the year in a noticeable percentage. This was done because the initial SOC for the battery was chosen as 0.2 but in the end of the year was fully charged. As a result the constraint of the battery was investigated on another way. It was assumed that the batteries were charged when the project started at a SOC of 0.78 and that way the initial and final value matched. The aforementioned can be seen from the following figure 4.1 displaying the state of charge throughout the year the initial and final value of the state of charge match.

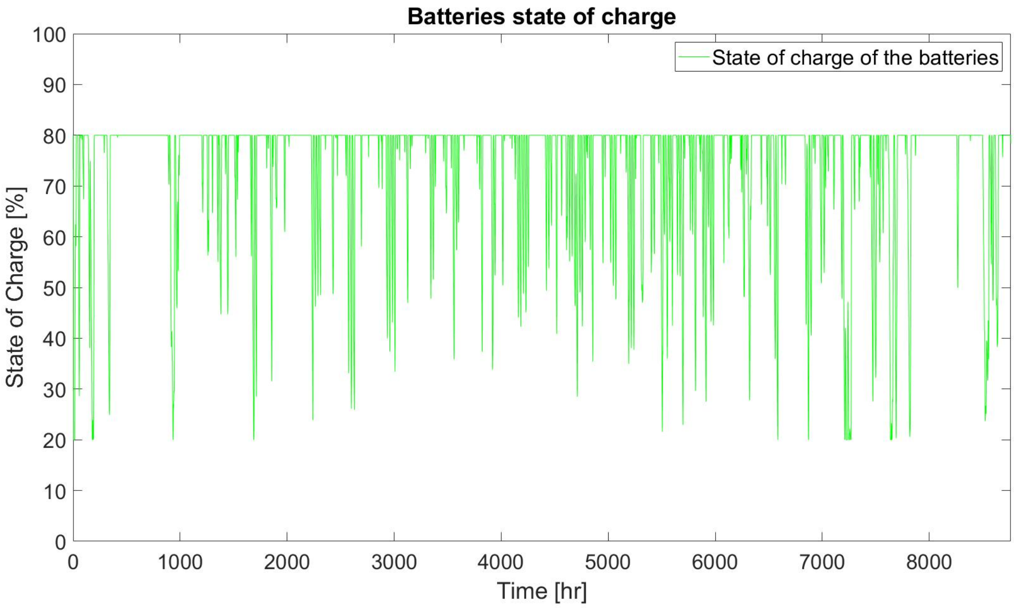


Figure 4.1: The graphic representation of the state of charge. The initial and the final state of charge for the one year simulation presented here is equal to 0.78 and they match with each other - BAU scenario

For the wind and the solar energy the power output from both the sources for the aforementioned system can be seen in the next two figures 4.2 and 4.3. More specifically, it is a fact that the rated capacity of the wind farm has the value of 2.377 GW which is 3% less than the installed wind capacity of 2.45 GW. This is because a 3% power loss has been assumed for the wind farm according to [60].
For the solar panels power output, it can be observed that with respect to the installed capacity the power generated is lower except of three times over a year. In these three times irradiation is higher than the standard test conditions one (I = 1000 W/m$^2$) and thus the power produced is also a bit higher than the cumulative rated capacity of the PV system.

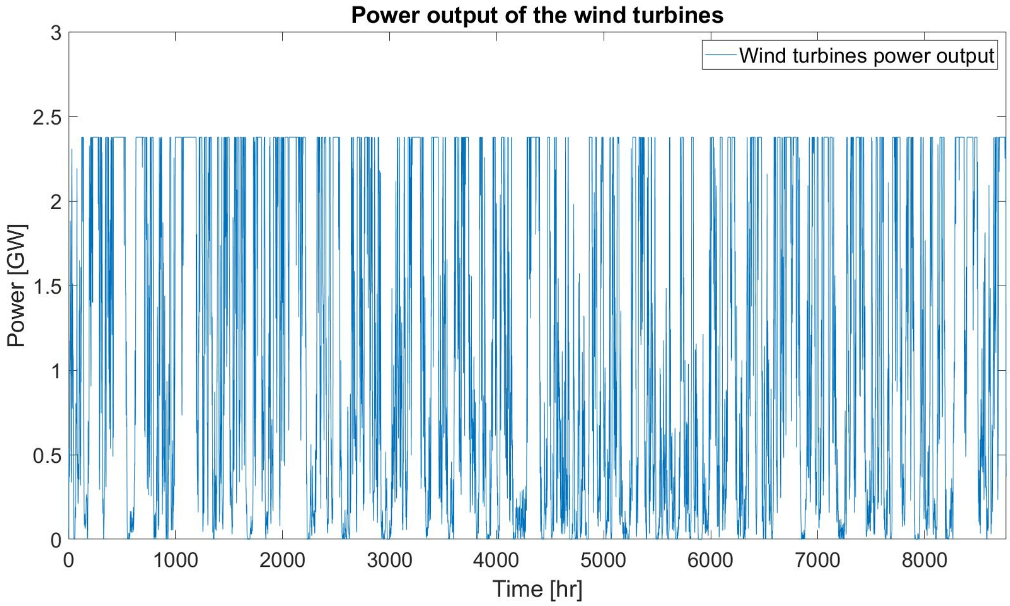


Figure 4.2: The graphic representation of the wind power output - BAU scenario

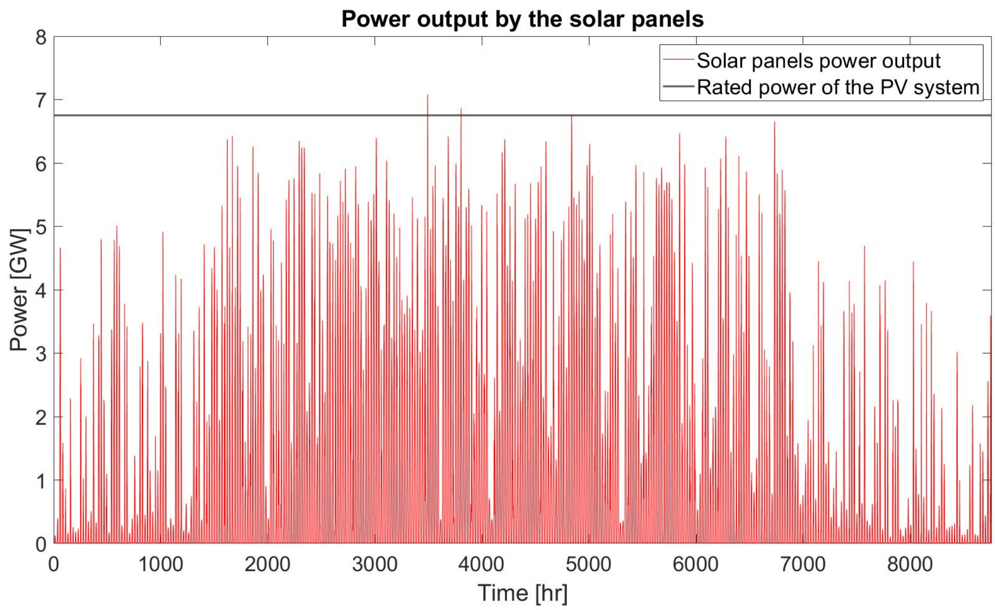


Figure 4.3: The graphic representation of the solar power output - BAU scenario

In the following figures 4.4.a and 4.4.b the coverage of the load, equal to 99.6 %, from the battery and the hybrid system with respect to the load is showed. The aforementioned percentage refers to the energy that the batteries and the hybrid system provide for the load while the rest 0.4% missing is the energy bought from the grid equal to 18.75 GWh as it is displayed in figure 4.4.c. As it is shown, the most of the energy is provided directly from the system while the rest is provided by the battery and the small percentage missing is bought from the grid.

Finally, the power sold to the grid is presented with the state of charge. In the following figure 4.5, it can be seen that the system is generating more power than needed. This power can be considered as sold power to the grid. The $LCOE_{NET}$ was calculated to show the effect of selling power to the grid with the LCOE change. This result cannot be considered accurate as

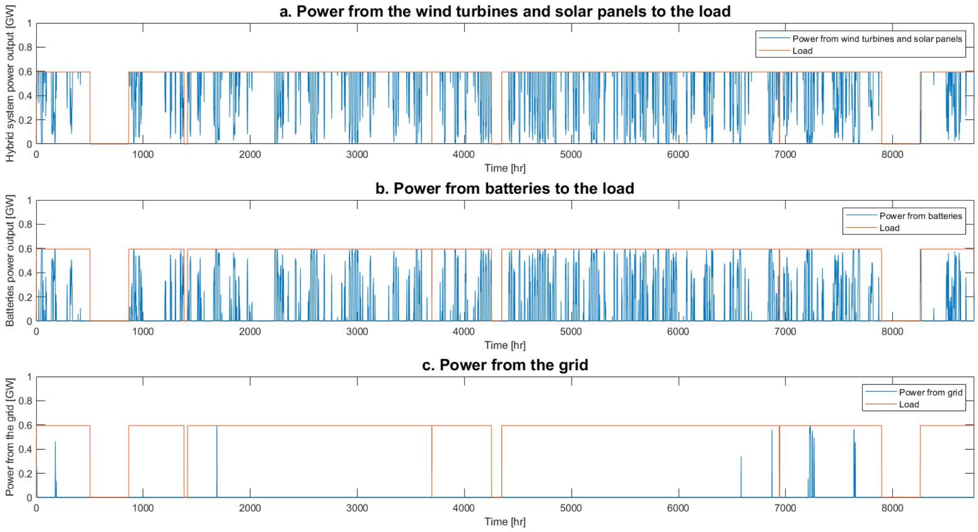


Figure 4.4: (a). The graphic representation of power provided by the hybrid system of the solar panels and the wind turbines to the load, (b). The graphic representation of the power provided from the batteries to the load, (c). The graphic representation of the power bought from the grid compared with the load - BAU scenario

the value to sell to the grid is not defined accurately as it depends on many factors and especially to the agreement one have with the grid operating company. Thus, a value of 0.05 €/kWh was chosen to represent the low price one can constantly sell to the grid and the energy that was sold to the grid annualy was equal to 13 TWh. The amount of energy sold to the grid is quite large, however the storage is sized in a proper way to confront the intermittency of the solar and wind power and thus the rest of the energy is not worth it according to the optimization of the system to be stored on a battery as the load is already covered and that would lead to over-sizing of the battery storage. It is visible from the following graph that there are some dense areas in which the over - generation occurs when the corresponding state of charge of the battery is equal to 0.8 meaning that there is no charge possibility at these points. On the other hand, the other times that areas are quite sparse are matching with the discharging periods of the batteries when state of charge is decreasing.

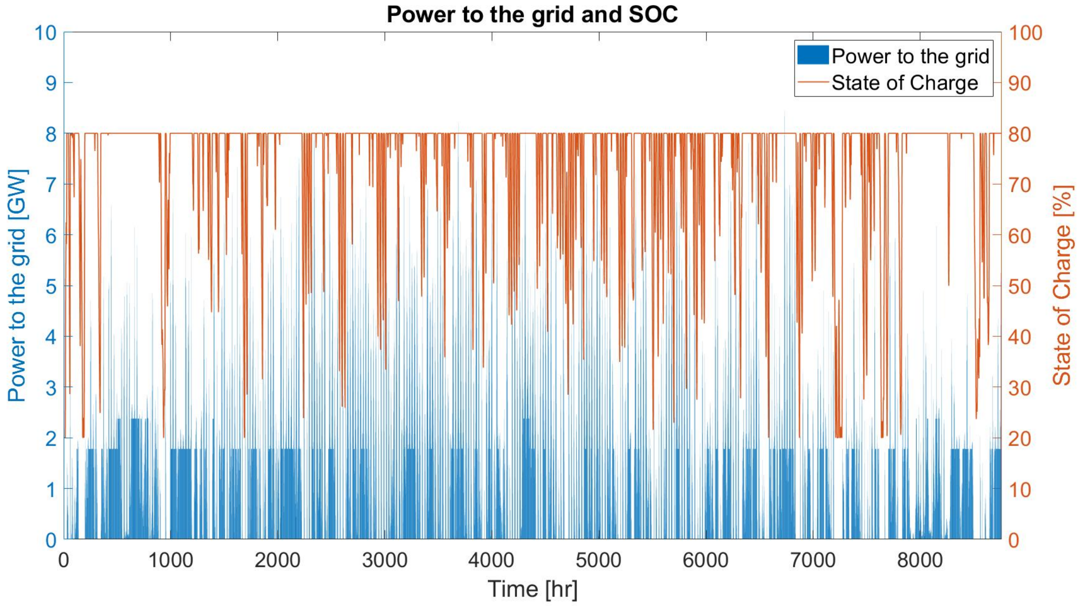


Figure 4.5: The over-generation of the system annually with the respective SOC - BAU scenario

**Results reflection**

Starting with the difference between the LCOE calculated without considering the selling to grid energy equal to 0.245 €/kWh is four times larger from the one calculated while considering the grid selling equal to 0.065 €/kWh. The price set for selling electricity to the grid was firstly chosen with the motivation to be cheap so the optimization algorithm will not follow a direction for over generation for a cheaper system instead of covering the load in the most optimum way which was the main target. To avoid that, the optimization was realized by not including in the total costs the revenue of selling the electricity to the grid. The results then were extracted by using a selling to the grid price of 0.05 €/kWh which can really fluctuate depending on the deal with the company selling the electricity and the grid provider. Thus, the result of the 0.065 €/kWh represents an approximation of the final LCOE that is really sensitive and keen to change in reality. On the other hand, the LCOE that assumes no selling power to the grid can represent more accurately the system cost of electricity as it is only considered the load coverage during the optimization process.

In terms of area, the total area for the wind farm the battery banks and the solar park were calculated including also the spacing between them as described in 2.1.6. For the wind farm 2.45 GW need to be installed and thus with 10.61 MW/km$^2$ power per area ratio the final area needed is equal to 230.91 km$^2$. For the solar park, 6.75 GW need to be installed with a power per area ratio of 53.9 MW/km$^2$ leads to an area of 125.23 km$^2$. For the wind farm, since the tender from the Dutch government specifies an area near IJmuiden for a wind farm with a maximum capacity of 4000 MW, and the installed capacity for the load coverage of Tata Steel is equal to 2450 MW, means that is needed more than half of the aforementioned wind farm for the Tata Steel's loads. This is tackling the feasibility of such a scenario. Finally, for the battery banks a space of 0.149 km$^2$ is calculated that is needed which is considered to be a reasonable area to be found near IJmuiden for installing the BESS plant. Furthermore, to bring the aforementioned areas to a perspective, a comparison with the area of the Netherlands that is equal to 41543 km$^2$ [61] is done. To realize such a system, 0.3% of the whole country's area to be covered by solar panels and install also the BESS system is needed. It is important to be mentioned that no area optimization or research was done in this project and the area calculations are indicative for the numbers magnitude realisation. While the area requirements seems to be high, the output of the project was considered with the reduction of emissions of Tata Steel as it was responsible for the 9% of the whole Netherlands emissions. According to [62], the amount of $CO_2$ emissions that is avoided because of greener electricity generation instead of fossil fuels is equal to 3.67 million tons of $CO_2$. As a disclaimer for this scenario the loads that were studied refer to the 11.42% of the total loads of Tata Steel as that much are the electricity ones. Thus, a fair comparison is impossible to be done with the total emissions of Tata Steel as the fuel mix from which these emissions occur is unknown.

In terms of matching the generation with the load, it is concluded that it is feasible as with a reasonable LCOE outcome of 0.265 €/kWh, the electricity loads of Tata Steel can be covered in their 99.6%. This leads to the conclusion that with a cheap system the loads can be almost completely covered. In terms of costs, the value of 0.065 €/kWh is a price that is highly attractive for such an investment if power is able to be sold to the grid. According to [63], the operating cost of a lignite plant is equal to 0.04 €/kWh, which is a magnitude comparable with the LCOE of the system studied in this scenario. The impact of operating a lignite plant in the atmosphere is high enough to disregard such a difference between the occurring LCOE of this system and the lignite plant's operating cost and making it really attractive as an investment both in economic and environmental terms.

## 4.2 Local Generation Scenario - 2030

The optimization method was followed as described in section 3.2.1 and the following results were extracted. The LCOE value calculated for the system is 0.383 €/kWh with an SSR of 0.993% and a load coverage value of 99.007 %. For the hydrogen part of the system the $SSR_{H_2}$ was equal to 0.865% while the hydrogen load coverage was equal to 99.135 %. Finally, the $LCOE_{NET}$ was calculated equal to 0.066 €/kWh when selling to the grid is considered as well. The values of the variables characterizing the system are presented and the performance of the system is further discussed.

### 4.2.1 Results - Local Generation Scenario - 2030

The aforementioned values resulted from a system that consists of 415 wind turbines with a capacity of 2.905 GW. For the solar panels the optimization algorithm concluded only for the south direction at the number of 17516004 solar panels that corresponds to an installed capacity of 7.882 GW. The amount of the batteries that are needed to balance the intermittency of the renewable energy sources for the electricity provided to the load and the electrolyzer are equal to 99900 strings that corresponds to 4995 battery banks with a total energy capacity of 13.786 GWh. The load was covered by 3268.33 GWh from the system of the wind turbines and the photovoltaics, while the batteries offered to the load 377.52 GWh. The total load is equal to 3682.42 GWh, thus the rest of the energy that was bought from the grid was equal to 36.57 GWh. The total cost of the system was equal to 21.16 billion € and the LCOE calculated was equal to 0.384 €/kWh. The $LCOE_{NET}$ was also calculated when the selling of electricity to the grid was allowed equal to 0.067 €/kWh. Due to optimization complexity, the best tank volume was found through MATLAB and the LCOE and $LCOE_{NET}$ were recalculated. The adjusted values were 0.383 €/kWh and 0.066 €/kWh. Since the energy bought from the grid was equal to 36.57 GWh and the total load 3682.42 GWh, the SSR value is equal to 0.993 %. For the hydrogen part of the system, 1140 electrolyzers of 0.298 GW capacity were installed and hydrogen tanks of a total volume equal to 172000 $m^3$ before and 148570 $m^3$ after the adjustment of the tank. The hydrogen load was equal to 1.855 billion $m^3$ and the production of hydrogen from the electrolyzers was equal to 1.849 billion $m^3$. This leads to an amount of 6 million $m^3$ of hydrogen being purchased and thus the SSR value is equal to 0.865%. In the following summary tables the results of the main variables from the optimization can be found. In table 4.4, the amount for each component and the installed capacity are given while in table 4.5 the energy balance of the whole system. Finally, in table 4.6 are presented the system performance variables.

Table 4.4: The amount of the different components of the system and their respectful installed capacity - Local Generation 2030 scenario

| **Variables** | **Value** | **Installed Capacity** |
|---|---|---|
| Number of wind turbines | 415 | 2.905 GW |
| Number of panels oriented south | 17516004 | 7.882 GW |
| Number of panels oriented east | - | - |
| Number of panels oriented west | - | - |
| Number of battery banks | 4995 | 13.786 GWh |
| Number of electrolyzer | 1190 | 0.298 GW |
| Volume of hydrogen storage tank | - | 172000 $m^3$ |
| Volume of hydrogen storage tank after adjustment | - | 148570 $m^3$ |

Table 4.5: The energy balance of the system which proves that the load equals the sum of the energy provided by the system, the batteries and the grid as well as the mass balance of hydrogen which proves that the load is equal to the sum of the hydrogen produced and purchased - Local Generation 2030 scenario

| **Variables** | **Value** | **Units** |
|---|---|---|
| Electricity Load | 3682.42 | GWh |
| System to the electricity load | 3268.33 | GWh |
| Batteries to the electricity load | 377.52 | GWh |
| Grid to the electricity load | 36.57 | GWh |
| Hydrogen load | 1.855 | billion $m^3$ |
| System to the hydrogen load | 1.849 | billion $m^3$ |
| Purchased hydrogen amount | 6 | million $m^3$ |

Table 4.6: The system performance variables that were optimized through the objective function chosen as described in 3.2.1 - Local Generation 2030 scenario

| **Variables** | **Value** | **Units** |
|---|---|---|
| LCOE | 0.383 | €/kWh |
| $LCOE_{NET}$ | 0.066 | €/kWh |
| SSR | 0.993 | % |
| Electricity Load Coverage | 99.007 | % |
| $SSR_{H_2}$ | 0.865 | % |
| Hydrogen Load Coverage | 99.135 | % |

### 4.2.2 Discussion - Local Generation 2030 Scenario

**Electricity generation part of the system**

In this scenario as well the same approach was followed as in the BAU one, to fulfill the constraint of the batteries so the state of charge will be identical in the beginning and the end of the year. The following figure 4.6 displays the state of charge of the battery and the matching between the initial and final values can be also observed and they are equal to 0.79. It is also visible that the maximum state of charge is 0.8 while the minimum one is equal to 0.2.

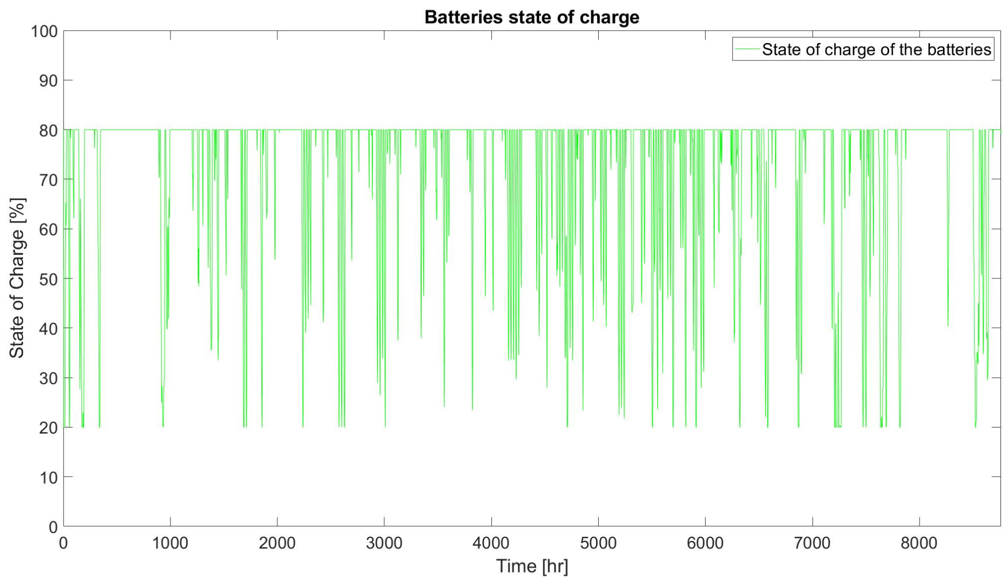


Figure 4.6: The graphic representation of the state of charge. The initial and the final state of charge for the one year simulation presented here is equal to 0.79 and they match with each other - Local Generation 2030 scenario

For the wind and solar energy the power generation can be observed in the following figures 4.7, 4.8. For the wind power the installed capacity is equal to 2.905 GW, while the maximum power produced, as observed in 4.7, is equal to 2.818 GW which includes the 3% power losses set as mentioned in [60].
The solar panels power output is displayed in figure 4.8 and it is observed that with respect to the rated power equal to 7.882 GW, the irradiation is higher than the standard test conditions one (I = 1000 W/m$^2$) for three times per year while for the rest of the year the power output is lower than cumulative rated capacity of the PV system.

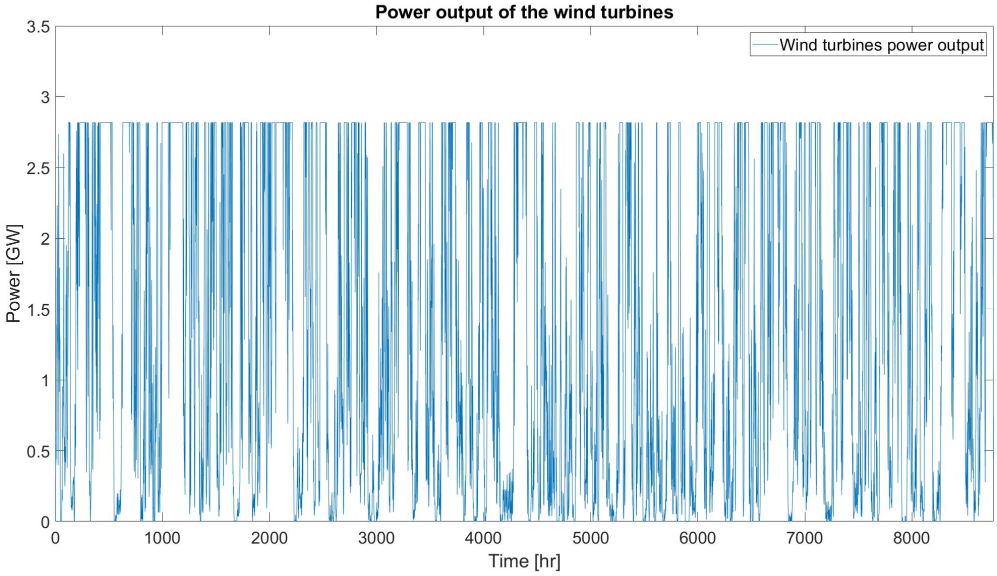


Figure 4.7: The graphic representation of the wind power output - Local Generation 2030 scenario

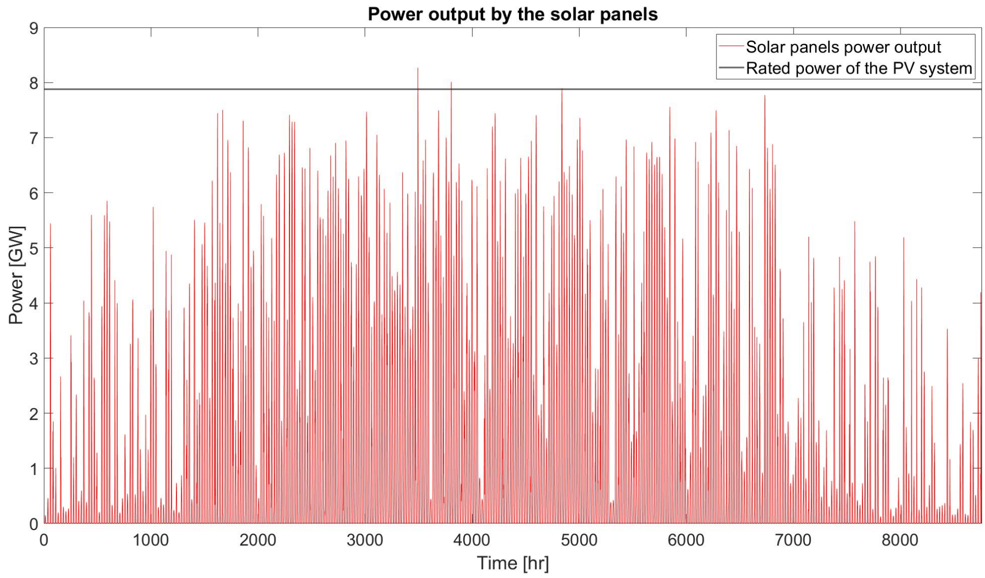


Figure 4.8: The graphic representation of the solar power output - Local Generation 2030 scenario

In the following figures 4.9.a and 4.9.b, it is displayed the power given from the wind turbines - solar panels system to the load and from the batteries to the load respectively. In figure 4.9.c, the power bought from the grid with respect to the load is presented. It is visible that a value of 0.993% for the value of SSR is calculated from the low density of the graph showing the power purchased from the grid. Also, the load coverage of 99.007 % is also indicated from the high density of the two first graphs of figure 4.9.

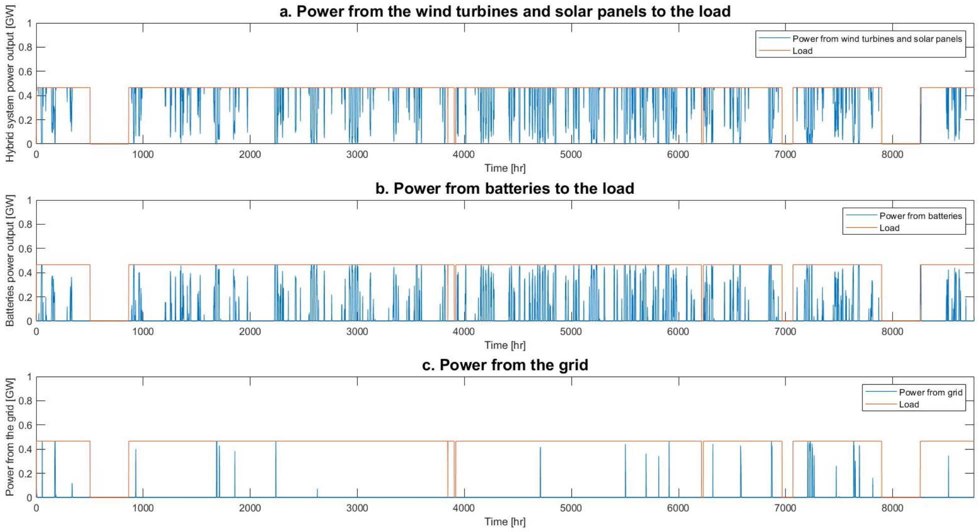


Figure 4.9: (a). The graphic representation of power provided by the hybrid system of the solar panels and the wind turbines to the load, (b). The graphic representation of the power provided from the batteries to the load, (c). The graphic representation of the power bought from the grid compared with the load - Local Generation 2030 scenario

Finally, for the electricity part of the system, the figure 4.10 below, shows the power sold to the grid and the state of charge of the batteries. It is visible from the dense areas of the power sold to the grid graph, that when the battery is on the upper limit of the state of charge equal to 0.8, the energy is directly sent to the grid to be sold.

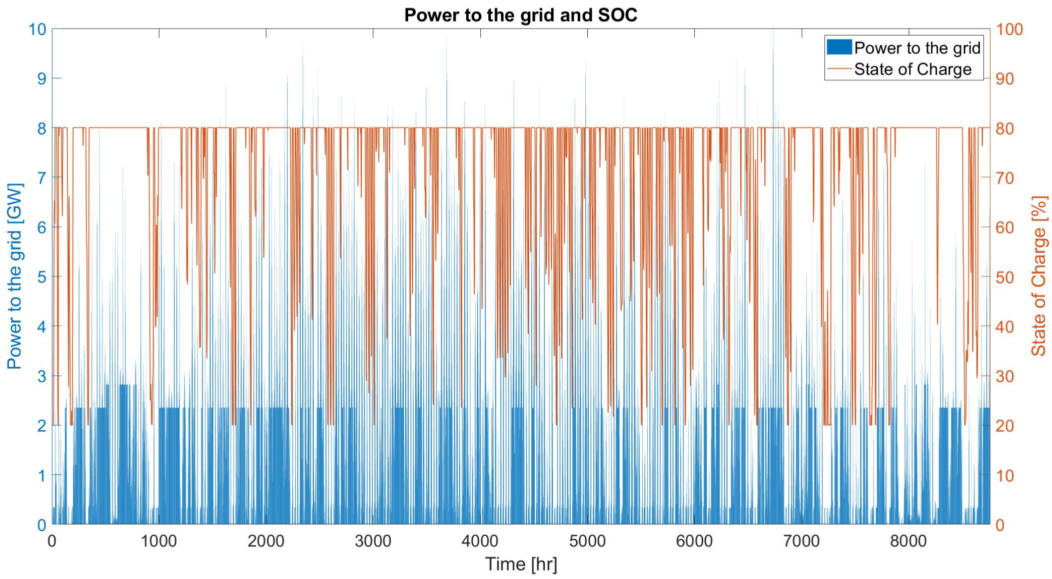


Figure 4.10: The over-generation of the system annually with the respective SOC - Local Generation 2030 scenario

**Hydrogen production part of the system**

In the following figure 4.11, the flow rate of the electrolyzers system and the amount from the hydrogen tank with respect to the load can be seen in 4.11.a, while in 4.11.b it is shown

the amount of hydrogen purchased with respect to the load. The system was optimized with following the constraint of producing 90% of the load at the same time, while the rest of the quantity to meet the load was taken from the tank directly as it was charging especially on the moments of maintenance. Thus, the amount missing is always given by the tank that is charging during maintenance times, as it can be also seen from the next graph showing the state of charge of the tank 4.12. The number of 10% was chosen because the maintenance time during a year of 35.5 days is almost 10% of a whole year. Under the assumption that the quantity stored can cover almost 10% of the load as the electrolyzer was almost working in rated power conditions producing the maximum amount possible. To conclude, this amount during maintenance times was stored in the tank increasing the state of charge and that way the excess stored could be also used.
The state of charge of the tank should also follow the constraint of matching the initial and final state of charge. The minimum difference achieved between the initial and final state of charge was 5.74% after every difference optimization trial. Thus, an assumption to secure continuity that this 5.74% is pressure relieving of the tank. This amount is 5.74% of the actual volume of the tank meaning a volume of 8528 $m^3$ that are added to the total costs an amount of 3752 € and the and the final SSR and LCOE values include this additional cost.

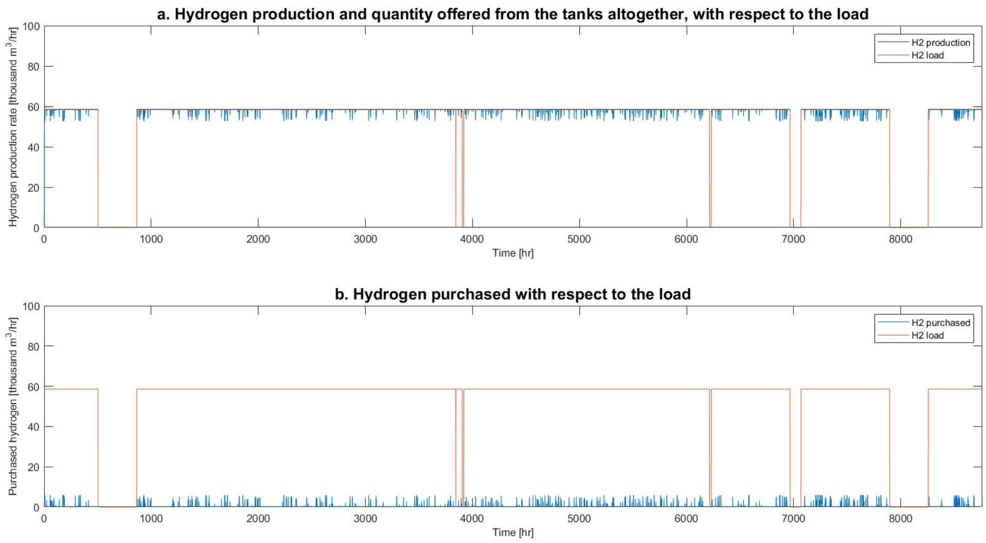


Figure 4.11: (a).Hydrogen production and amount offered from the tanks altogether with respect to the load, (b).Hydrogen amount being purchased with respect to the load - Local Generation 2030 scenario

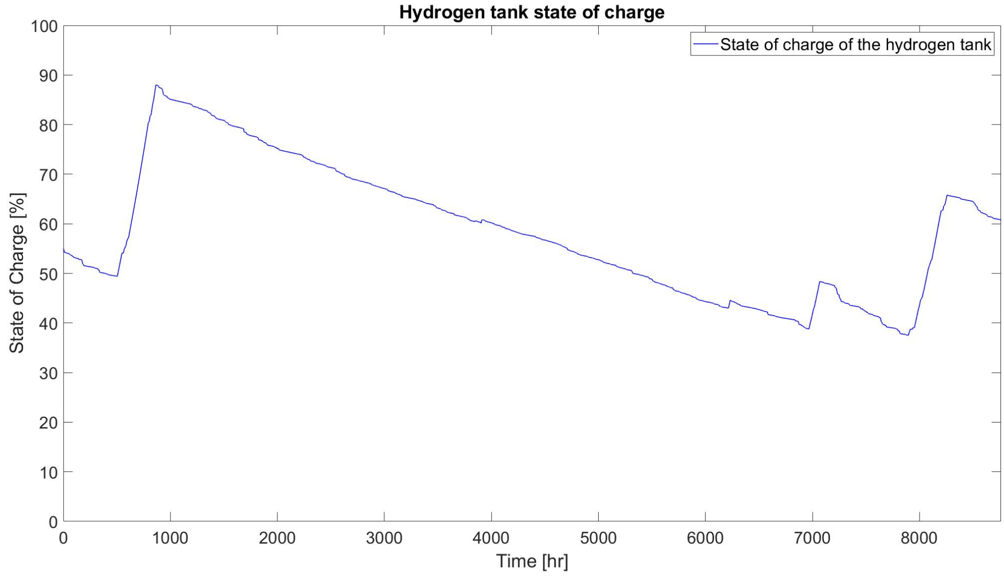


Figure 4.12: State of charge of the hydrogen tank - Local Generation 2030 scenario

The optimization process was quite complex as many different variables had to be adjusted and the final outcome was a really large tank for which the state of charge was ranging between 0.42 and 0.62. Thus, an adjustment on the size was done so the volume of the tank will be 5% more than the maximum level of the tank. This 5% choice was made to avoid dumping if it occurs at some point higher hydrogen production throughout the 25 years of the project's lifetime. That way, the cost was reduced and the full tank volume was used. The new adjusted volume was equal to 284600 m$^3$. Furthermore, the 2% additional amount of hydrogen that was assumed it escapes from the tank as described above was subtracted and the final graph shows a better solution the state of charge and the volume of the tank as it is displayed in figure 4.13 below.

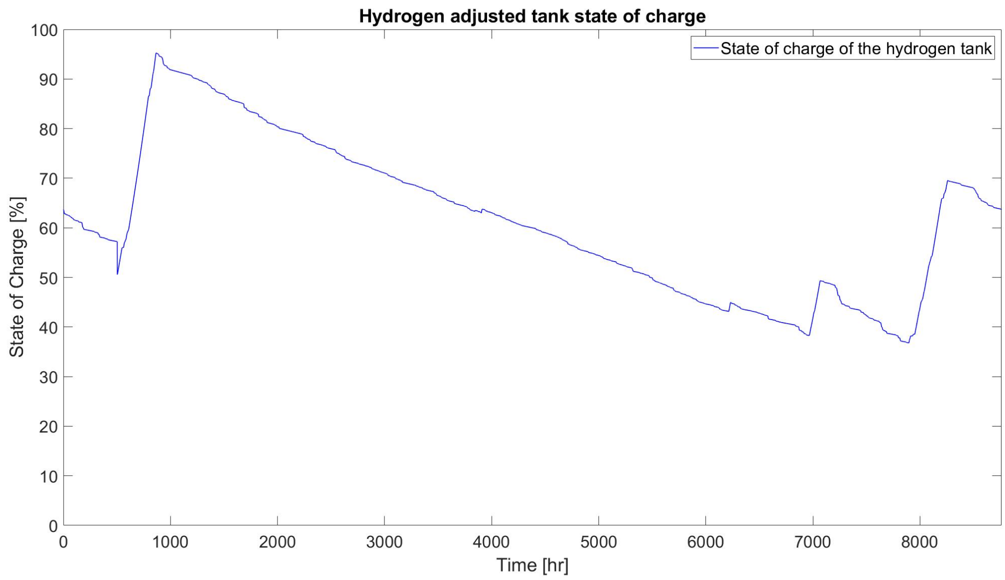


Figure 4.13: State of charge of the adjusted hydrogen tank - Local Generation 2030 scenario

Finally, in the following graph 4.14, the overall efficiency of the electrolyzer is presented. It can be seen that it is operating on rated power almost all the time. This is increasing the possibility to meet the demand for hydrogen however it is also more possible to need an electrolyzer replacement after completing more than 60000 operation hours which is its lifetime. The times that the electrolyzers need to be replaced are three during the whole project lifetime.

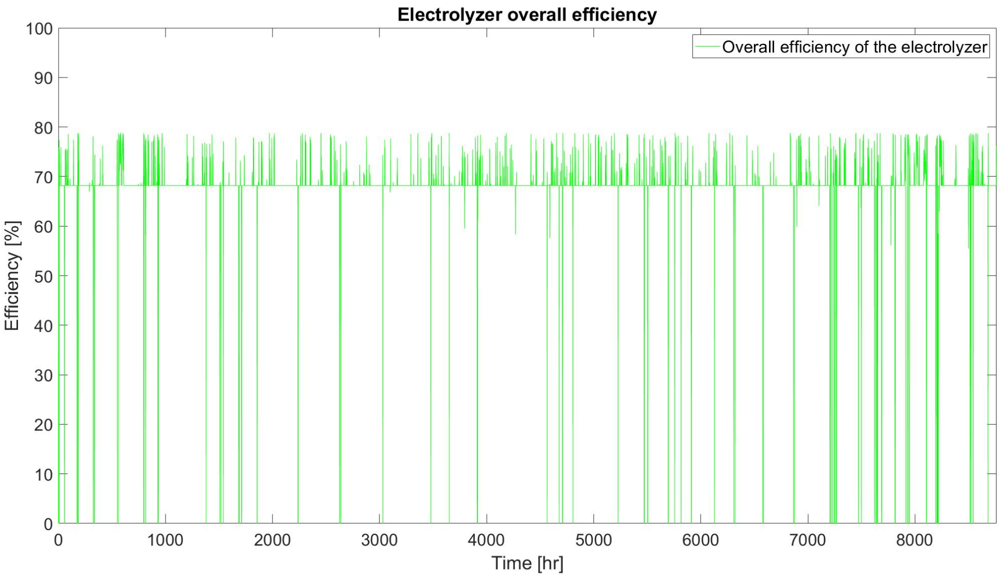


Figure 4.14: Efficiency of the electrolyzers - Local Generation 2030 scenario

### Results Reflection

The LCOE values calculated as a closed system equal to 0.383 €/kWh and the net one equal to 0.066 €/kWh when selling power to the grid have a difference between them that is not highly considerable. Comparing with the business as usual scenario where the LCOE values have considerable difference it can be concluded that the power that is over - generated in this scenario is sent to the electrolyzers system and thus hydrogen is produced through it. This leads to the conclusion that the power sent back to the grid to be sold is considerably lower than the one of the business as usual scenario.

Regarding the area specification of the system, the area needed for the battery banks, the solar park, the wind farm and the electrolyzers plant are calculated. Starting with the wind farm, 2.905 GW of power were installed. According to the section's 2.1.6 analysis, the power per area is equal to 10.61 MW/km$^2$. Thus, the area needed for the wind farm is equal to 273.8 km$^2$. For the solar park the installed capacity is equal to 7.882 GW. Referring to section 2.1.6, the power per area is equal to 53.9 MW/km$^2$, which leads to a total area requirement of 146.23 km$^2$. For the battery banks part of the system, 4995 battery banks are needed that each one of them consumes 29.72 m$^2$. Thus, the area needed for the BESS is equal to 0.148 km$^2$. Finally, for the electrolyzers part of the system, 1190 electrolyzers are needed and each one of them according to section 2.1.6 consumes 2.53 m$^2$. Thus, a total area of 3010.7 m$^2$ is needed. To bring the areas calculated into perspective, the area of the Netherlands is equal to 41543 km$^2$ according to [61]. Thus, the area needed for the electrolyzers, BESS and solar panels is about the 0.35% of the total area of the Netherlands. To reflect on the total areas calculated further, as an area requirement can be considered really high. However, comparing it with the outcome of this study that will be the emissions reduction of an industry that emits 9-10 % of the total country's emissions is considered to be reasonable enough. With such a system the emissions avoided with the electricity generation via renewable energy sources instead of fossil fuels that Tata Steel is currently using was found according to [62], equal to 2.85 million tons of CO2. Furthermore, according to [57], for the primary route's emission with the current technology used by Tata Steel of a direct reduction with an electric arc furnace, the range of emissions per ton of steel is on average equal to 0.95 ton $CO_2$/ton of steel. This leads to a total amount of 6.46 million tons for the primary process. Since 30% of natural gas in this case is replaced with emissions free, green hydrogen, then another 30% of these emissions are avoided leading to an amount of 1.94 million tons. Thus, in total the $CO_2$ emissions avoided with the implementation of renewable energy sources and green hydrogen to the steel production processes, after realizing this project are equal to 4.79 million tons.

Finally, in terms of matching the generation with the load, the system was optimized in a proper way to cover not only the hydrogen but also the electricity loads with a coverage of 99.135 % and 99.007 % accordingly. The LCOE value to achieve such a coverage is equal to 0.383 €/kWh which is considered to be reasonable value but not comparable yet with the electricity price from the grid. According to [63], the operating cost of a closed cycle gas turbines plant will be in 2030 around 0.08 to 0.12 €/kWh. Not only the cost will be higher than the current prices of 0.06 €/kWh but also year by year the impact of $CO_2$ released to the atmosphere will be higher for the environment and the planet. Considering all above, a price of 0.383 €/kWh is 3 times higher than operating a closed cycle gas turbine plant, but the impact of the emissions avoided equal to 4.79 million tons, is making the system quite attractive as an investment in environmental terms. If a system for which the selling of electricity to the grid is enabled then it can be really comparable with the operational costs of the closed cycle gas turbine plants. However, since no analysis was conducted for the deal between the grid operator and the system holder, there is no solid results for how the business case would be realized and no further reflection will be added on this part of the results.

## 4.3 Local Generation Scenario - 2050

The values occurred after the optimization of the system for this scenario were an LCOE of 0.421 €/kWh while the net value of it with selling power to the grid was equal to 0.042 €/kWh. An SSR value of 0.125 % and a load coverage of 99.875 % while for the hydrogen the $SSR_{H_2}$ value was equal to 0.793 % while the hydrogen load coverage was equal to 99.207 %. In the following section the results of the optimization are presented and further discussed.

### 4.3.1 Results - Local Generation Scenario - 2050

The system that occurred from the optimization for this scenario consists of 424 wind turbines with a capacity of 3.038 GW. The solar panels for this scenario are 75135760 panels oriented south with an installed capacity of 33.81 GW, while another 140500 oriented east with an installed capacity of 0.063 GW and 139000 oriented west with a capacity of 0.0626 GW. In total the installed capacity needed for the solar panels was equal to 33.94 GW. The amount of batteries that will help to tackle the renewable energy sources intermittency were 16905 battery banks with an energy capacity of 46.66 GWh. Regarding the energy balance of the system, the total load was equal to 5262.5 GWh that was covered from the system by 4624.73 GWh and from the batteries by 631.21 GWh. The rest of the energy was bought from the grid equal to 6.56 GWh. The total system's cost was equal to 62.55 billion € and thus the LCOE calculated was equal to 0.422 €/kWh. Due to the complexity of the optimization program the hydrogen tank size was not optimal and thus through MATLAB the tank size was adjusted leading to an LCOE value of 0.421 €/kWh. Furthermore, the $LCOE_{NET}$ value was calculated referring to the situation were power is also sold to the grid. The value of the $LCOE_{NET}$ was equal to 0.06 €/kWh while after the adjustment of the hydrogen tank occurred to be equal to 0.042 €/kWh. For the hydrogen part of the system, 2920 electrolyzers of 0.73 GW needed to be installed and a hydrogen tank of 264500 $m^3$ before and 252270 $m^3$ after the adjustment of the tank. A hydrogen load of 4.4906 billion $m^3$ was covered as 4.455 billion $m_3$ produced and the rest 35.6 million $m^3$ were purchased. The SSR value of hydrogen occurred to be equal to 0.793 %. In the tables 4.7, 4.8 and 4.9, the results of the optimization, the energy balance of the system are presented and the system performance values.

Table 4.7: The amount of the different components of the system and their respectful installed capacity - Local Generation 2050 scenario

| **Variables** | **Value** | **Installed Capacity** |
|---|---|---|
| Number of wind turbines | 434 | 3.038 GW |
| Number of panels oriented south | 75135760 | 33.81 GW |
| Number of panels oriented east | 140500 | 0.063 GW |
| Number of panels oriented west | 139000 | 0.0626 GW |
| Number of battery banks | 16905 | 46.66 GWh |
| Number of electrolyzer | 2920 | 0.73 GW |
| Volume of hydrogen storage tank | - | 264500 $m^3$ |
| Volume of hydrogen storage tank after adjustment | - | 252270 $m^3$ |

Table 4.8: The energy balance of the system which proves that the load equals the sum of the energy provided by the system, the batteries and the grid as well as the mass balance of hydrogen which proves that the load is equal to the sum of the hydrogen produced and purchased - Local Generation 2050 scenario

| **Variables** | **Value** | **Units** |
|---|---|---|
| Electricity Load | 5262.5 | GWh |
| System to the electricity load | 4624.73 | GWh |
| Batteries to the electricity load | 631.21 | GWh |
| Grid to the electricity load | 6.56 | GWh |
| Hydrogen load | 4.4907 | billion $m^3$ |
| System to the hydrogen load | 4.455 | billion $m^3$ |
| Purchased hydrogen amount | 35.6 | million $m^3$ |

Table 4.9: The system performance variables that were optimized through the objective function chosen as described in 3.2.1 - Local Generation 2050 scenario

| **Variables** | **Value** | **Units** |
|---|---|---|
| LCOE | 0.421 | €/kWh |
| $LCOE_{NET}$ | 0.042 | €/kWh |
| SSR | 0.125 | % |
| Electricity Load Coverage | 99.875 | % |
| $SSR_{H_2}$ | 0.793 | % |
| Hydrogen Load Coverage | 99.207 | % |

### 4.3.2 Discussion - Local Generation 2050 Scenario

#### Electricity generation part of the system

The first constraint needed to be fulfilled for the battery banks part was to have a matching between the initial and final state of charge for the one year simulation time. The following figure 4.15, presents that this was succeed having an initial and final state of charge equal to 0.77 which is also near the maximum state of charge of 0.8. Furthermore, the maximum depth of discharge of the battery banks is 0.2 which is also visible in the figure below.

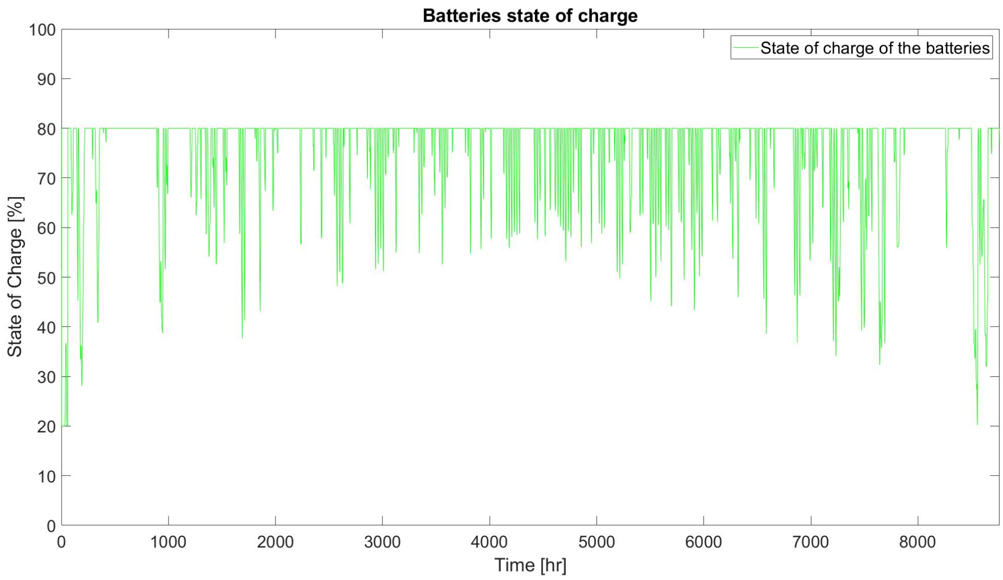


Figure 4.15: The graphic representation of the state of charge. The initial and the final state of charge for the one year simulation presented here is equal to 0.77 and they match with each other - Local Generation 2050 scenario

In the following figures, 4.16 and 4.17 the wind and solar power generation can be observed. For the wind energy the installed capacity is equal to 3.038 GW and the maximum power generated is equal to 2.947 GW as a 3% of power losses is included during the simulation according to [60]. The solar panels power output can be seen in figure 4.17 where the cumulative rated capacity of the PV system is equal to 33.94 GW as the solid black line displays and the power generated exceeding this value only three times per year where the irradiation is more than the standard test conditions one (I = 1000 W/m$^2$).

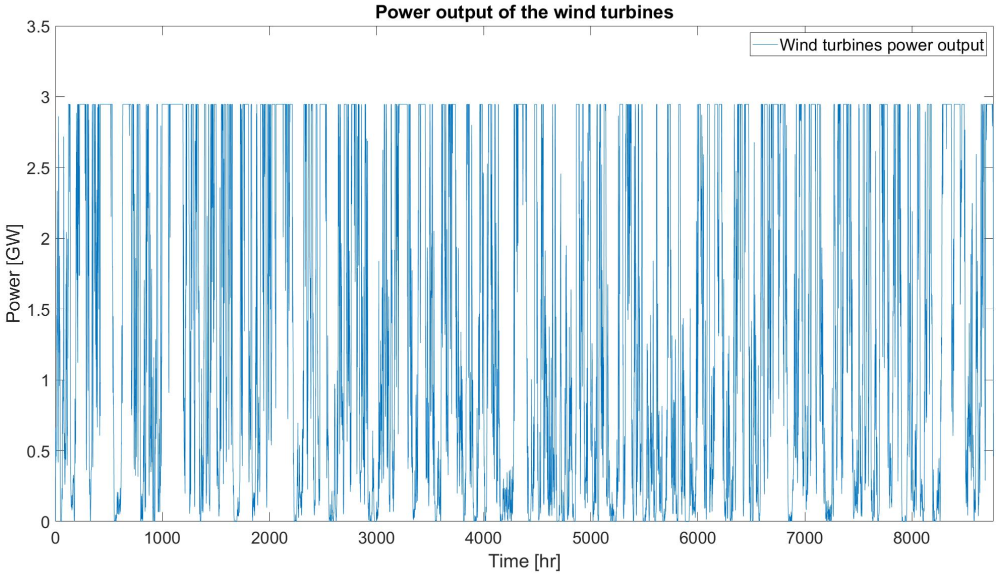


Figure 4.16: The graphic representation of the wind power output - Local Generation 2050 scenario

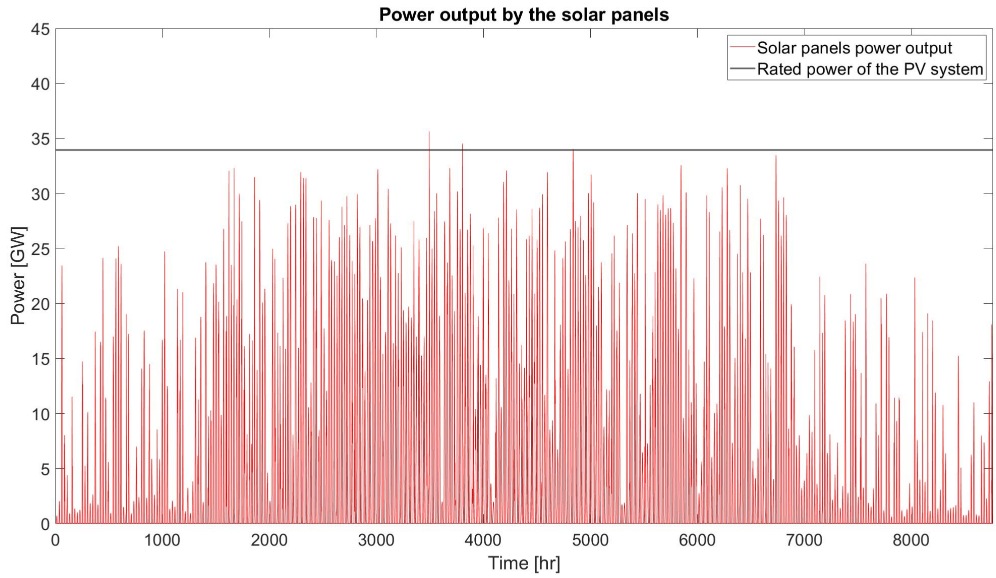


Figure 4.17: The graphic representation of the solar power output - Local Generation 2050 scenario

In the following figures 4.18.a and 4.18.b, the power given from the system of the wind turbines and solar panels to the load as well as the power given from the batteries are presented. Furthermore, the power that is offered from the grid with respect to the load is also displayed in figure 4.18.c. It can be observed from the really sparse graph that displays the power purchased from the grid that the load is covered from the batteries and the wind turbines - solar panels system which also matches with the 99.875 % of load coverage calculated.

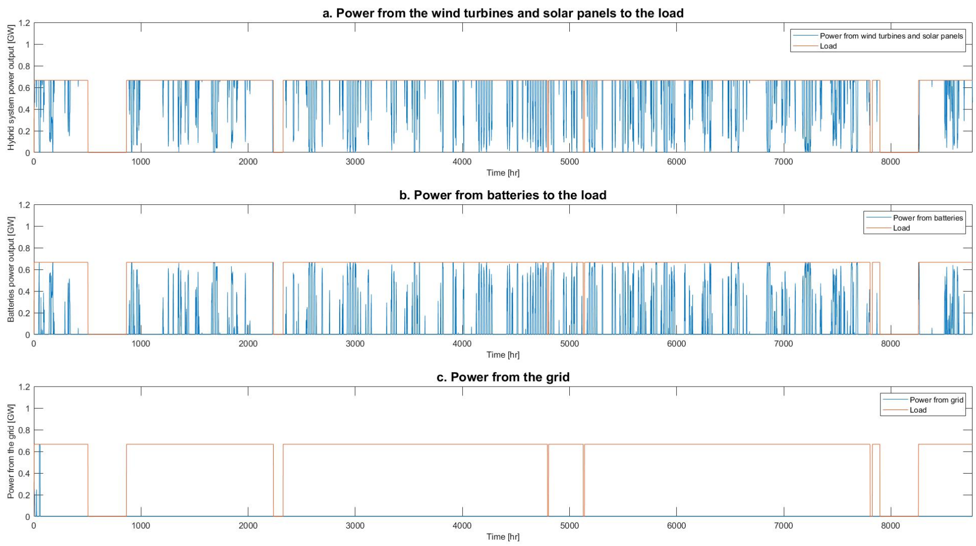


Figure 4.18: (a). The graphic representation of power provided by the hybrid system of the solar panels and the wind turbines to the load, (b). The graphic representation of the power provided from the batteries to the load, (c). The graphic representation of the power bought from the grid compared with the load - Local Generation 2050 scenario

Finally, for the electricity part of the system, the power sold to the grid is displayed to the following graph 4.19, combined with the state of charge of the batteries. It can be seen that the dense areas of the power graph are shaped when the state of charge of the batteries is already at a maximum and thus the power is directed to the grid.

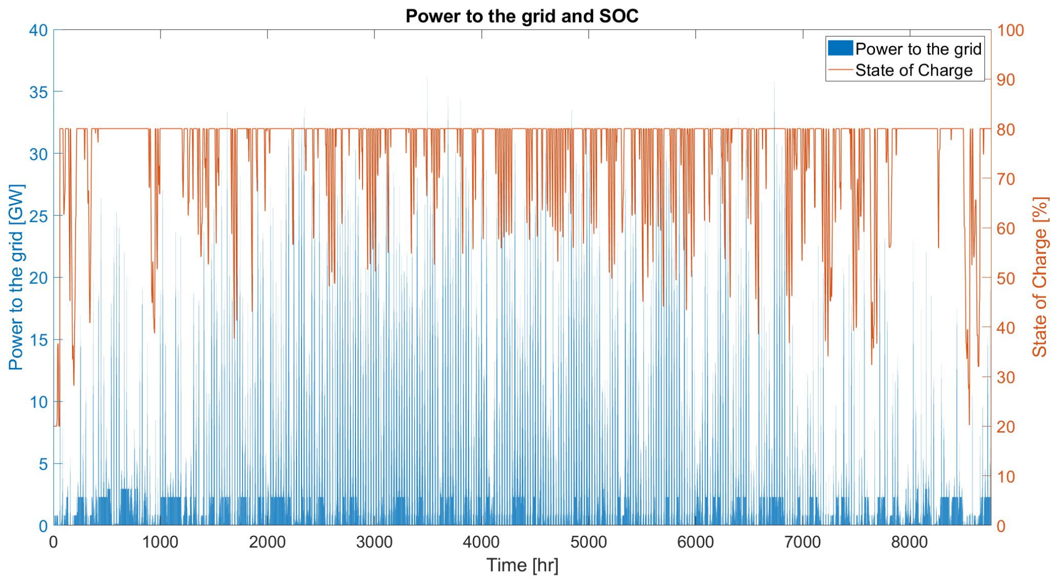


Figure 4.19: The over-generation of the system annually with the respective SOC - Local Generation 2050 scenario

**Hydrogen production part of the system**

In this subsection the figures representing the results for the hydrogen part of the system are analyzed. Firstly, the figure 4.20 below, displays the hydrogen produced and the hydrogen purchased so the load will be met.

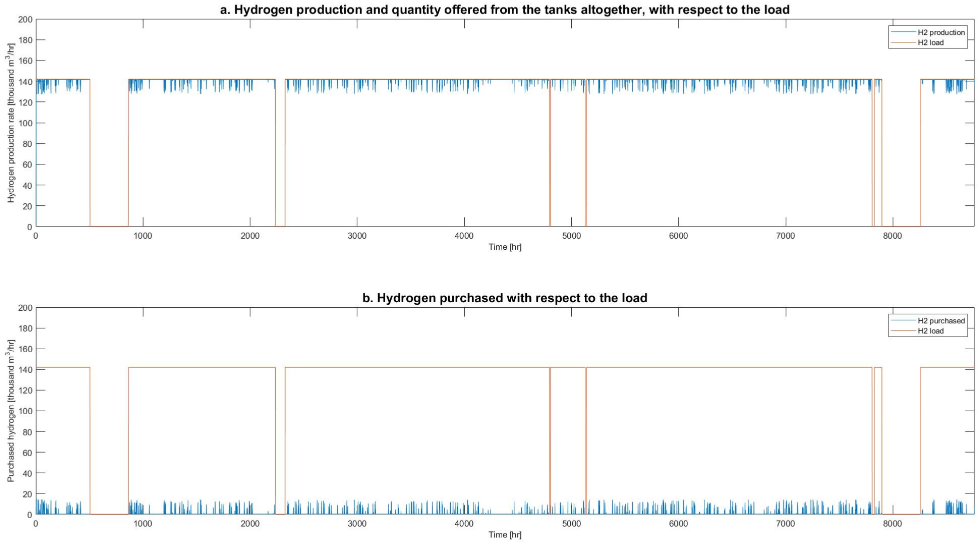


Figure 4.20: (a).Hydrogen production and amount offered from the tanks altogether with respect to the load, (b).Hydrogen amount being purchased with respect to the load - Local Generation 2050 scenario

The system was optimized the same way as done for the scenario of local generation in 2030 4.2.2. The final difference between the initial and the final state of charge of the hydrogen tank was equal to 9.13%. Thus, the new assumption made for this scenario was the the released gas for safety reasons was equal to this amount spread throughout the year. Thus, the first optimized tank volume gave the following figure 4.21 which was optimized further through MATLAB to be using the most of the tank's capacity for the hydrogen storage purpose. Both graphs with the state of charge for the initial tank volume and the optimized one are presented below 4.21 and 4.22. The adjusted volume of the tank is equal to 252270 and the initial state of charge is equal to 52.42% which also matches with the final one. This amount of the hydrogen lost is assumed that is purchased and the effect of it has already been added to the LCOE and SSR parameters while the additional cost is equal to 8936.5 €.

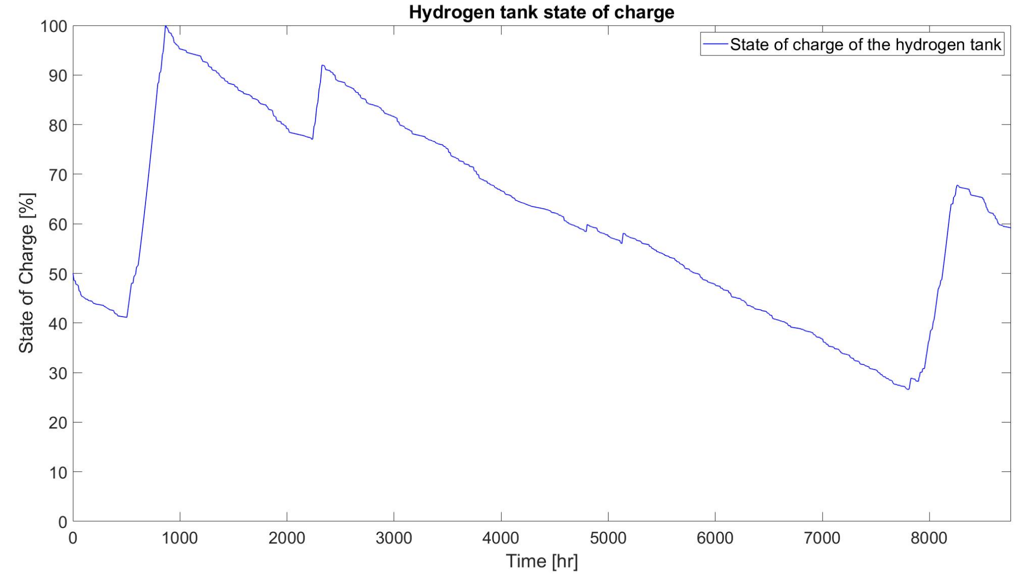


Figure 4.21: State of charge of the hydrogen tank from the initial optimization - Local Generation 2050 scenario

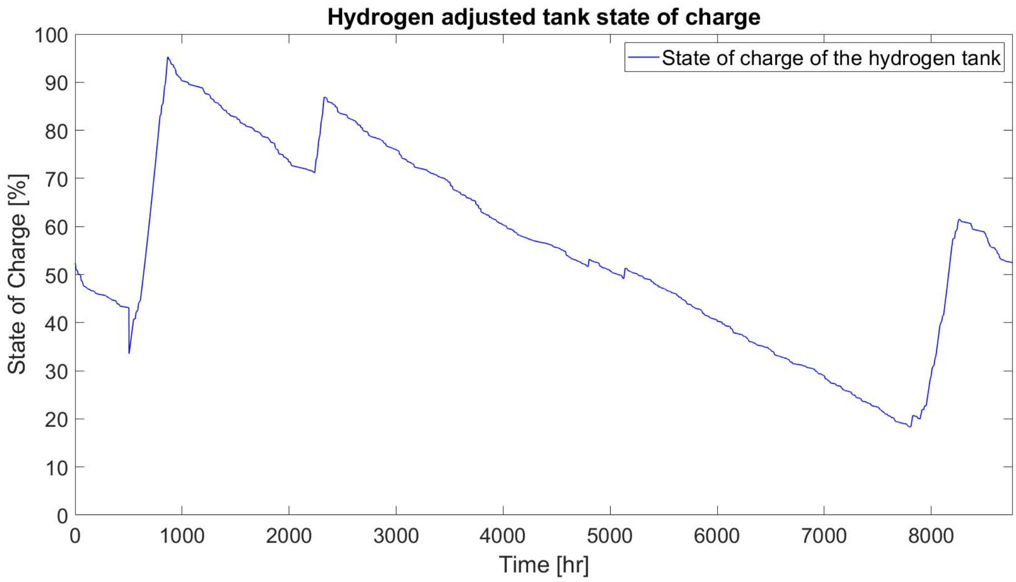


Figure 4.22: State of charge of the adjusted hydrogen tank after optimizing further the tank's size - Local Generation 2050 scenario

Finally, for the hydrogen part of the system, in the following figure 4.23 the electrolyzer's efficiency is presented. It can be seen that is operating almost every time in rated power or near it. This is the reason why after the 60000 operation hours, which is the lifetime of the electrolyzer it is replaced for 3 times during the lifetime of the project.

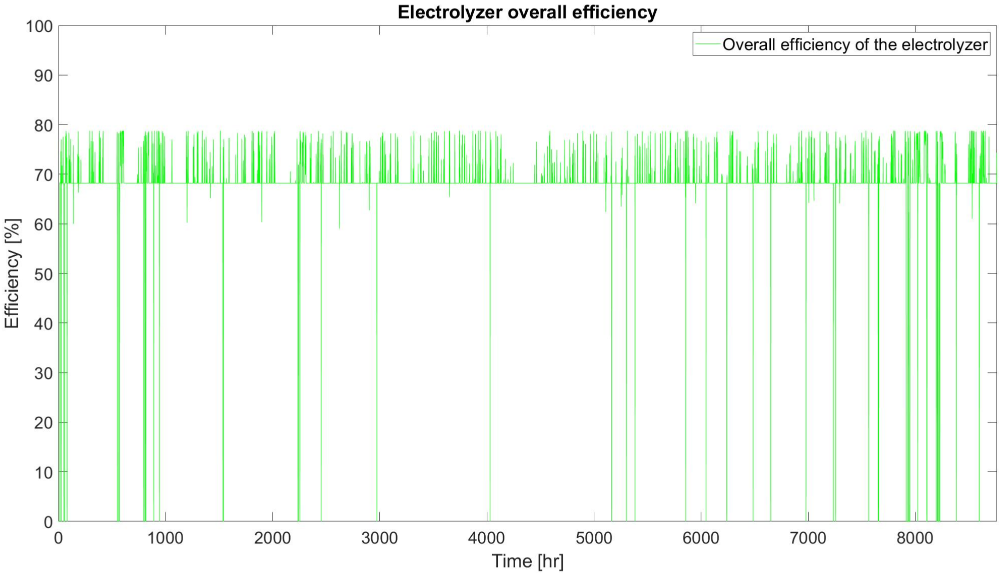


Figure 4.23: Efficiency of the electrolyzers - Local Generation 2050 scenario

**Results Reflection**

From the economic point of view, this scenario output an LCOE of 0.421 €/kWh when no selling of power to the grid is enabled while the LCOE after enabling it was equal to 0.042 €/kWh. This difference is because of the additional revenues that are decreasing the total cost. Furthermore, the difference between the two is that big because the additional energy that is generated by the renewable energy sources is also used in this scenario for the hydrogen production if a comparison is done with the BAU scenario where the over - generated energy was directly fed to the grid. However, it is a fact that due to the higher load as a big amount of hydrogen is demanded to be produced, the installed capacity of all the energy sources is sensibly higher.

The second aspect is the reflection in the area specification of such a system. At first there are 424 wind turbines in the wind farm. This corresponds to 3.038 GW and according to 2.1.6 the ratio per installed capacity and area for the wind turbines was calculated equal to 10.61 $MW/km^2$. Thus, the area requirement for the wind farm is equal to 286.33 $km^2$. For the solar park the installation becomes more complicated in the sense that for this scenario, solar panels needed to be installed in the east and west orientation. This is because the loads are really high in comparison with the business as usual and the scenario with the steel making route for the year of 2030 and thus a trade - off had to be balanced between the cost of the system and the load coverage. The optimization concluded to a specific size for the battery banks that were not full at sometimes in need and thus to correct this, east and west oriented solar panels that were more efficient after a specific time of the day could still charge the batteries to be ready and offer to the continuous and constant load. The total capacity of the solar park is equal to 33.94 GW and according to section 2.1.6, the capacity per area ratio is equal to 53.9 $MW/km^2$. Thus, the total area needed is equal to 629.68 $km^2$. Further than that the optimization output was to also install solar panels on the east and west direction. Since no area specification is studied for this project, no conclusions about the further space requirement were extracted. A possible scenario can be to add solar trackers in some of the solar panels so to avoid the different orientation installations. Since the optimization conducted has concluded that an important amount of solar panels need to be installed in the other two orientations, is certain that financially is the most feasible solution. The presented results can be considered enough to provide an answer to the research question set for this project with the current optimized system. To continue, the battery banks amount is 16905 for this scenario and per battery bank an area of 29.72 $m^2$

is needed. This leads to an area requirement of 0.502 $km^2$. Finally, for the electrolyzers, 2920 needs to be installed and each one consumes a space of 2.53 $m^2$, which leads to a total space of 7387.6 $m^2$. To bring the areas calculated into perspective, the area of the Netherlands is equal to 41543 $km^2$ according to [61]. At first to bring into perspective the calculated areas, the space needed refers to the 1.5% of the total area of the Netherlands. To reflect on the total area calculated in a reasonable metric, a comparison with the emissions avoided with this project has been conducted. It is a fact that Tata Steel is responsible for the 9-10% of the total emissions of the Netherlands. With the realization of this project only from electricity generation, 4.104 million tons of $CO_2$ were avoided instead of producing them with coal as the aforementioned number has been extracted for. Further than that, according to [64], from the primary route of the steel production on average the emissions ratio per ton of steel is equal to 0.95 ton $CO_2$/ton of steel. Since on average Tata Steel produces 6.8 million tons, an amount of 6.46 million tons of $CO_2$ will be avoided as the reactions will be realized with the addition of green hydrogen assuming that also the quantity purchased will also be produced with green electricity. This leads to a total amount of avoided emissions equal to 10.564 million tons of $CO_2$.

To conclude the results reflection, the system was optimized in a way that the load can be covered only by the system of the batteries, wind turbines and solar panels in a percentage of 99.875%. On the hydrogen part of the system, the optimization of the system led to a coverage of 99.207% of the load with the minimum cost. The LCOE value of the closed system, meaning that no selling to the grid was enabled, was found equal to 0.421 €/kWh that is also reasonable but not comparable with the electricity price from the grid. According to [63], the operating cost of a closed cycle gas turbines plant will be in a range of 0.09 to 0.15 €/kWh. Including also the high impact that the imposed carbon taxes will potentially have on the year of 2050, leads to the conclusion that probably the LCOE extracted for this project might not be the ideal case but will have a competitive attraction for investment especially for the environmental point of view. Financially, since it is not predictable what will be the carbon taxes to adjust the operational cost of the closed cycle gas turbine plants no safe conclusion can be extracted from the data existing so far for the year of 2050. If a system for which the selling of electricity to the grid is enabled then it can be really comparable with the operational costs of the closed cycle gas turbine plants. However, since no analysis was conducted for the deal between the grid operator and the system holder, there is no solid results for how the business case would be realized and no further reflection will be added on this part of the results.

## 4.4 Non - Local Generation Scenario - 2030

The results for this scenario will be presented into two parts. The system is divided in the electricity part which produces electricity to cover the electricity loads of the Tata Steel's processes as well as the energy requirement production for regasifying the $LH_2$. The index that represents the whole system is the LCOE value and with a system total cost of 52.2 billion €, it was found equal to 0.765 €/kWh before adjusting the volume of the hydrogen tank of the system while after the adjustment the final LCOE value was equal to 0.764 €/kWh. For the $LCOE_{NET}$ value, it was calculated equal to 0.0279 €/kWh before the adjustment while after the adjustment it was found equal to 0.0218 €/kWh. The SSR for the electricity part of the system was equal to 0.051 % which leads to a load coverage of 99.949 %. For the hydrogen part of the system, the SSR value was calculated equal to 0.089 % which leads to a load coverage of 99.911 % while the SSR for the hydrogen load was found equal to 0.467%, leading to a load coverage of 99.534%. In the two following subsection each part of the system will be analyzed separately. In the following table 4.10, the variables for the whole system of both the electricity and hydrogen side are presented.

Table 4.10: The system performance variables that were optimized through the objective function chosen as described in 3.2.1 for the combined system of the electricity and hydrogen parts - non Local Generation 2030 scenario

| Variables | Value | Units |
|---|---|---|
| LCOE | 0.764 | €/kWh |
| $LCOE_{NET}$ | 0.0279 | €/kWh |
| SSR | 0.042 | % |
| Electricity Load Coverage | 99.941 | % |
| $SSR_{H_2}$ | 0.456 | % |
| Hydrogen Load Coverage | 99.534 | % |

### 4.4.1 Electricity part of the system - Non local generation scenario for 2030

The system that resulted after the optimization method as described in 3.2.3, consists of 414 wind turbines with a capacity of 2.898 GW. The solar panels for this scenario were 14990000 that are oriented south and then another 9000 east and 12005 west. The capacity for each orientation is 6.745 GW, 4.05 MW and 5.4 MW respectively. The total capacity is equal to 6.754 GW. For the battery banks part of the system a total of 98200 battery strings will be needed, which leads to an amount of 4910 battery banks. The total energy capacity of the batteries is equal to 13.511 GWh. For the energy balance of the system, the energy generated and provided by the system and the batteries plus the energy from the grid should match the load. This was the case for this scenario as well with the following numbers. At first, the load for this case was equal to 3756.15 GWh which was covered by 3330.09 GWh from the system of wind turbines and solar panels and by 424.16 GWh from the batteries. The rest was purchased from the grid and it was equal to 1.9 GWh. This part of the system had a total cost of 16.2 billion € and the LCOE values for this specific part of the system were equal to 0.348 €/kWh and for the net one 0.064 €/kWh. Finally the SSR value is equal to 0.051 % and this leads to a load coverage of 99.949 %. The results occurred from this optimization are summarized in the following tables 4.11, 4.12 and 4.13 that show respectively the components amount, the energy balance of the system and the optimization variables values.

Table 4.11: The amount of the different components of the system and their respectful installed capacity - non Local Generation 2030 scenario

| Variables | Value | Installed Capacity |
|---|---|---|
| Number of wind turbines | 414 | 2.898 GW |
| Number of panels oriented south | 14990000 | 6.745 GW |
| Number of panels oriented east | 9000 | 4.05 MW |
| Number of panels oriented west | 12005 | 5.4 MW |
| Number of battery banks | 4910 | 13.511 GWh |

Table 4.12: The energy balance of the system which proves that the load equals the sum of the energy provided by the system, the batteries and the grid - non Local Generation 2030 scenario

| Variables | Value | Units |
|---|---|---|
| Electricity Load | 3756.15 | GWh |
| System to the electricity load | 3330.09 | GWh |
| Batteries to the electricity load | 424.16 | GWh |
| Grid to the electricity load | 1.9 | GWh |

Table 4.13: The system performance variables that were optimized through the objective function chosen as described in 3.2.1 - non Local Generation 2030 scenario

| **Variables** | **Value** | **Units** |
|---|---|---|
| LCOE | 0.348 | €/kWh |
| $LCOE_{NET}$ | 0.064 | €/kWh |
| SSR | 0.051 | % |
| Electricity Load Coverage | 99.949 | % |

### 4.4.2 Hydrogen part of the system - Non local generation scenario for 2030

The hydrogen part of the system consists of solar panels, battery banks and the electrolyzer and the hydrogen tank. At first, the capacity resulted from the optimization as well as the amount of solar panels to be installed are as follows. In the south orientation, 125033504 solar panels will be installed with a capacity of 56.26 GW. On the east and west orientations, 65000 and 56000 solar panels were needed to be installed with a capacity of 0.029 GW and 0.025 GW respectively leading to a total capacity of 56.314 GW. For the battery banks part of the system, it was calculated that 82500 strings were needed, which leads to 4125 battery banks with an energy capacity of 11.385 GWh. For the electrolyzers, it was found that 1400 were needed with a capacity of 0.35 GW while the hydrogen tank at the initial optimization was equal to 132350 $m^3$ and after the adjustment it was found equal to 105380 $m^3$. For the energy balance of the system the total load was equal to 1092.11 GWh and from the solar panels it was provided 547.36 GWh, while from the batteries the rest of 542.75 GWh, while from the grid 2 GWh were purchased. For the hydrogen mass balance, a total load of 2.187 billion $m^3$ was covered, which is the 1.855 billion $m^3$ plus the amount that will be released as boil - off gas so the proper amount will reach IJmuiden after shipping the hydrogen. The production of hydrogen was equal to 2.177 billion $m^3$ while the quantity purchased was equal to 10 million $m^3$. The LCOE for this part of the system was found equal to 2.59 €/kWh while the $LCOE_{NET}$ equal to 0.0216 €/kWh. The SSR for the electricity was found equal to 0.089 % , with a load coverage of 99.911%, while the SSR of the hydrogen was equal to 0.467% with a load coverage of 99.534%. The results from the optimization of this part of the system are displayed in the following summary tables 4.14, 4.15 and 4.16 where the components amount, the energy balance of the system and the optimization variables are presented respectively.

Table 4.14: The amount of the different components of the system and their respectful installed capacity - non Local Generation 2030 scenario and Arabic Peninsula part of the system

| **Variables** | **Value** | **Installed Capacity** |
|---|---|---|
| Number of panels oriented south | 125033504 | 56.26 GW |
| Number of panels oriented east | 65000 | 0.029 GW |
| Number of panels oriented west | 56000 | 0.025 GW |
| Number of battery banks | 4125 | 11.385 GWh |
| Number of electrolyzer | 1400 | 0.35 GW |
| Volume of hydrogen storage tank | - | 132350 $m^3$ |
| Volume of hydrogen storage tank after adjustment | - | 105380 $m^3$ |

Table 4.15: The energy balance of the system which proves that the load equals the sum of the energy provided by the system, the batteries and the grid as well as the mass balance of hydrogen which proves that the load is equal to the sum of the hydrogen produced and purchased - non Local Generation 2030 scenario and Arabic Peninsula part of the system

| **Variables** | **Value** | **Units** |
|---|---|---|
| Electricity Load | 1092.11 | GWh |
| System to the electricity load | 547.36 | GWh |
| Batteries to the electricity load | 542.75 | GWh |
| Grid to the electricity load | 2 | GWh |
| Hydrogen load | 2.187 | billion $m^3$ |
| System to the hydrogen load | 2.177 | billion $m^3$ |
| Purchased hydrogen amount | 10 | million $m^3$ |

Table 4.16: The system performance variables that were optimized through the objective function chosen as described in 3.2.1 - non Local Generation 2030 scenario and Arabic Peninsula part of the system

| **Variables** | **Value** | **Units** |
|---|---|---|
| LCOE | 2.59 | €/kWh |
| $LCOE_{NET}$ | 0.0216 | €/kWh |
| SSR | 0.089 | % |
| Electricity Load Coverage | 99.911 | % |
| $SSR_{H_2}$ | 0467 | % |
| Hydrogen Load Coverage | 99.534 | % |

### 4.4.3 Discussion - non Local Generation Scenario 2030

#### Electricity generation part of the system

The constraint of the simulation referring to the battery banks was to match the initial and final state of charge to secure continuity for the total simulation of the system's lifetime. Thus, for the one year simulation time, the initial and final state of charge were matching equal to 0.8 as it can be observed in the following figure 4.24.

In the following figures 4.25 and 4.26, the wind and solar power generation is displayed. In the middle of the year the power generation for the solar energy is relatively higher than the rest of the year. For the wind energy, it is a fact that the 3% losses has been included and the maximum power generated is equal to 2.811 GW.

In the following summary graph, the power provided to the load from the system of solar panels and wind turbines are presented in 4.27.a. In 4.27.b the power provided by the batteries is displayed while in 4.27.c the power bought from the grid to fulfill the total load. It can be easily observed the symmetry between the power provided by the system of the solar panels and wind turbines as well as the really small amount bought from the grid, which is in accordance with the really high load coverage percentage.

Finally, the over - generation from the system, is indicated in the next figure 4.28. It can be observed that when the batteries are in their maximum allowed capacity of 80 %, the power is sent to the grid.

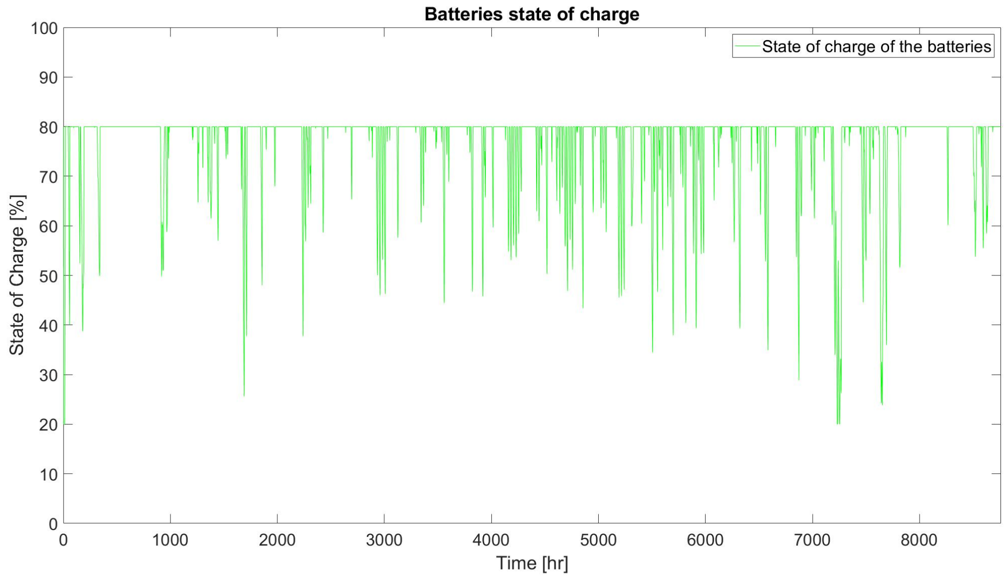


Figure 4.24: The graphic representation of the state of charge. The initial and the final state of charge for the one year simulation presented here is equal to 0.8 and they match with each other - non Local Generation 2030 scenario for the IJmuiden part of the system

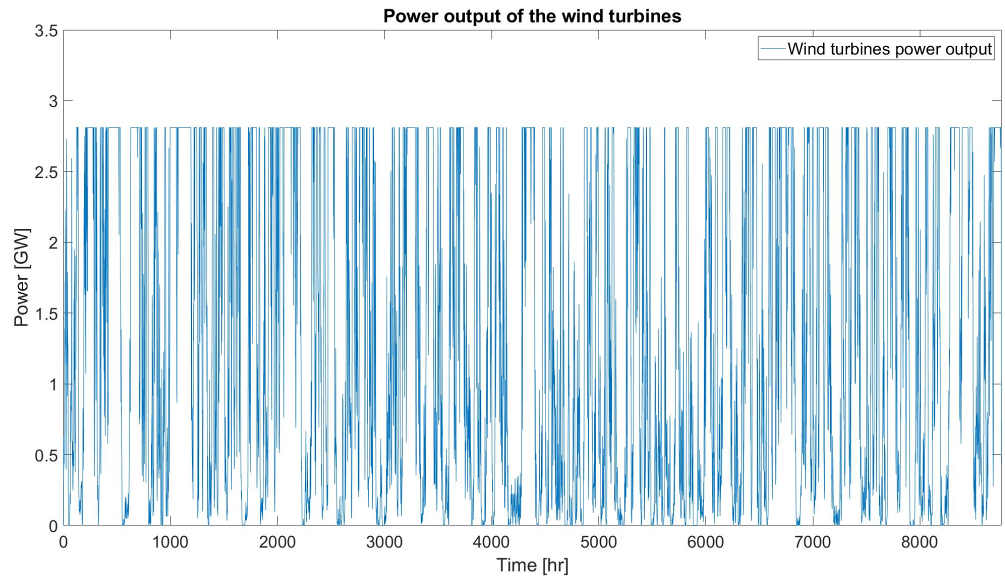


Figure 4.25: The graphic representation of the wind power output - non Local Generation 2030 scenario for the IJmuiden part of the system

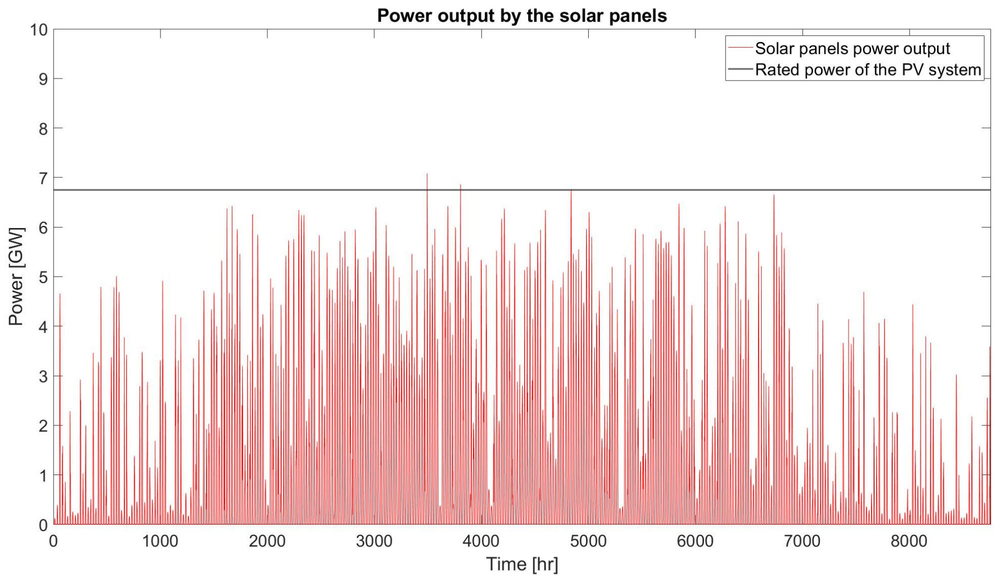


Figure 4.26: The graphic representation of the solar power output - non Local Generation 2030 scenario for the IJmuiden part of the system

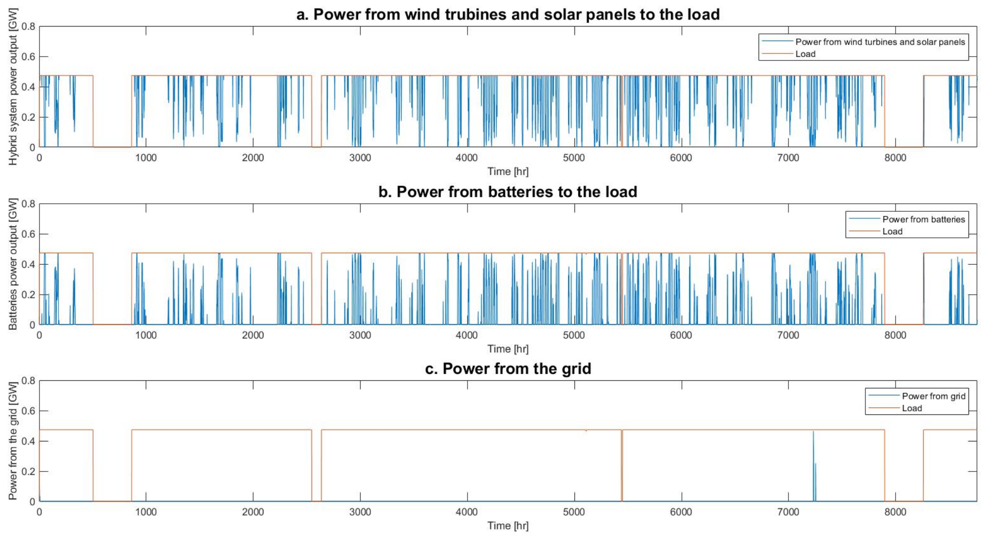


Figure 4.27: (a). The graphic representation of power provided by the hybrid system of the solar panels and the wind turbines to the load, (b). The graphic representation of the power provided from the batteries to the load, (c). The graphic representation of the power bought from the grid compared with the load. Non Local Generation 2030 scenario for the IJmuiden part of the system

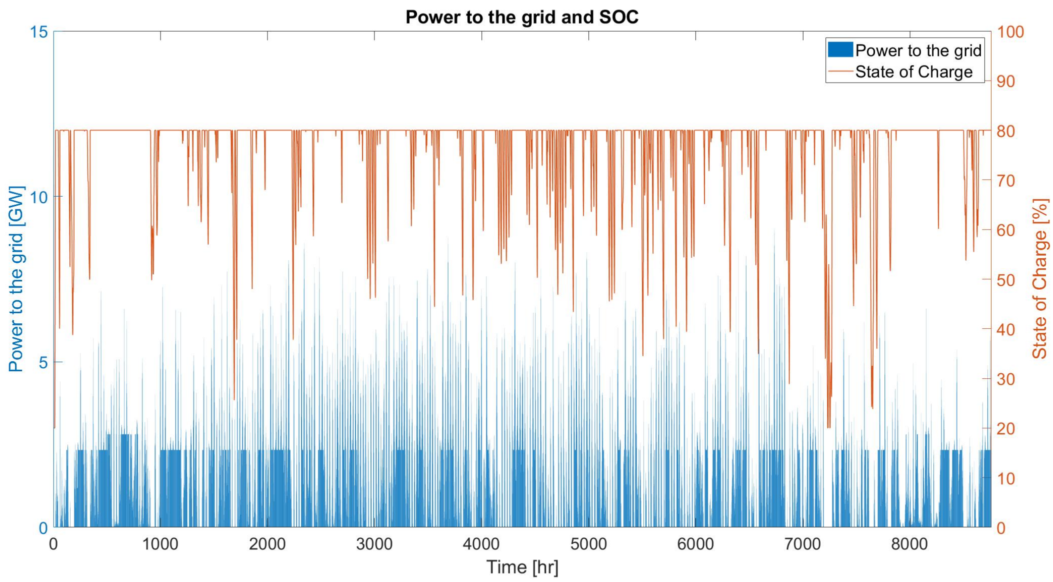


Figure 4.28: The over-generation of the system annually with the respective SOC - non Local Generation 2030 scenario for the IJmuiden part of the system

**Hydrogen part of the system**

For this part of the system the constraint for the batteries so the state of charge will match in the beginning and the end of the year should be fulfilled. The batteries state of charge are equal to 52.23% in the beginning and the end of the year. Thus, before the project starts, should be already charged to their 52.23%. The aforementioned can be seen in figure 4.29.

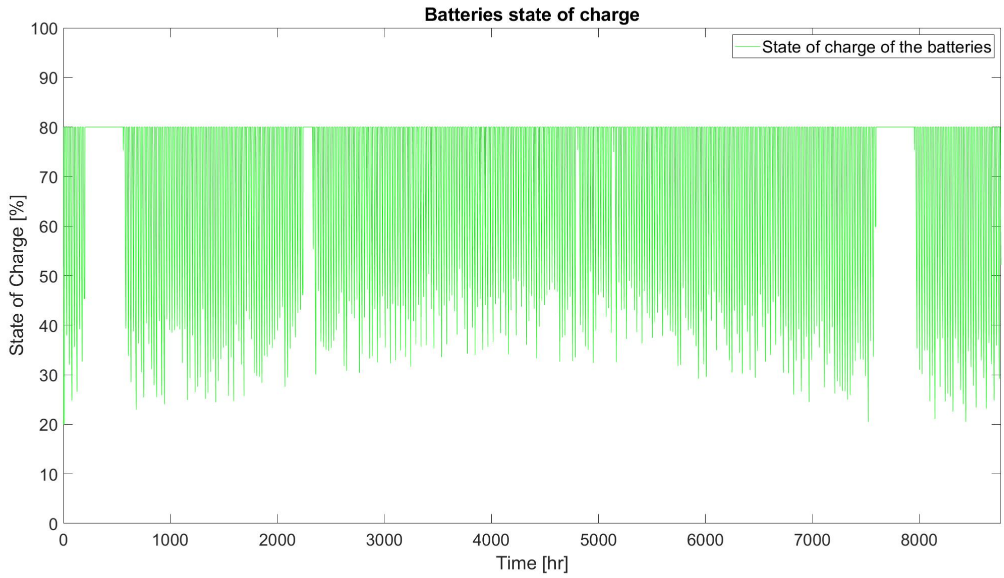


Figure 4.29: The graphic representation of the state of charge. The initial and the final state of charge for the one year simulation presented here is equal to 0.52 and they match with each other - non Local Generation 2030 scenario

For the power generation, this part of the system consists of solar panels. The power generated throughout a year can be seen in the following figure 4.30.

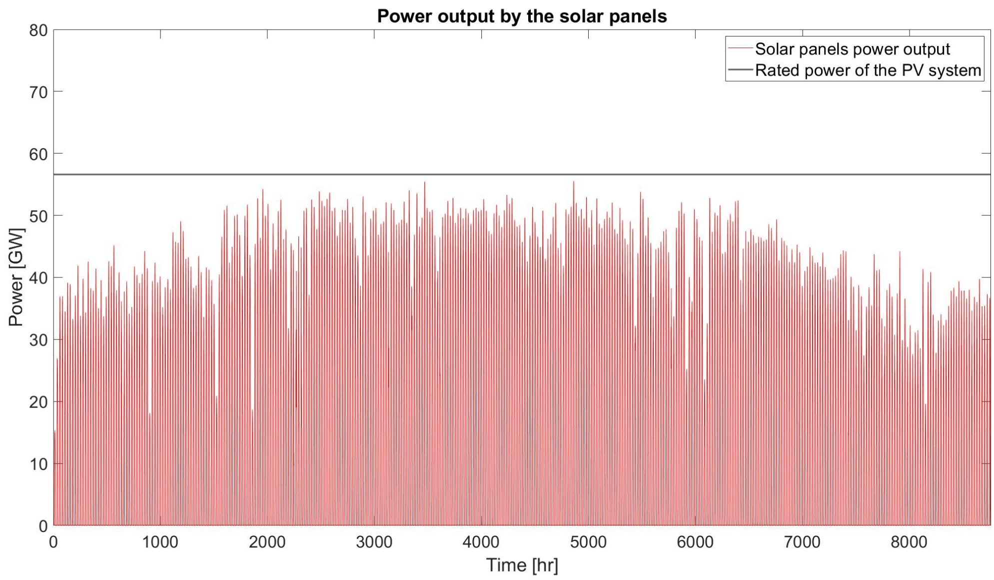


Figure 4.30: The graphic representation of the solar power output - non Local Generation 2030 scenario

The electricity load coverage can be seen in the following figure. In 4.31.a the power provided by the solar panels is displayed while in 4.31.b is the power provided from the batteries to the load. Finally, from 4.31.c, the power purchased from the grid is displayed. In this case it is visible that the batteries are charging and the solar panels are providing to the load while on the next step of the graph the opposite is happening. This is because batteries are providing at night while the solar panels during the day to the load. Further than that it is also visible the matching of the low SSR with the low amount of power that was purchased from the grid to fulfill such a load.

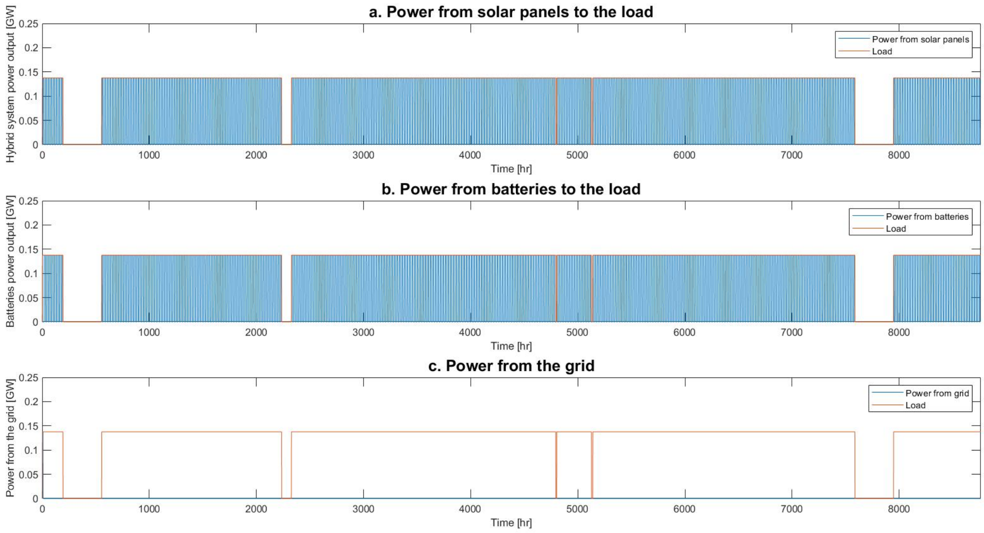


Figure 4.31: (a). The graphic representation of power provided by the hybrid system of the solar panels and the wind turbines to the load, (b). The graphic representation of the power provided from the batteries to the load, (c). The graphic representation of the power bought from the grid compared with the load - non Local Generation 2030 scenario

The next figure 4.32, shows the over - generation of the system with combination to the state of charge from the batteries. It is visible that when the batteries have reached their maximum capacity, the excess energy is sent directly to the grid.

For the hydrogen production side, at first the figure 4.33 shows the efficiency of the electrolyzer. It can be observed that in the beginning and in the end of the year the electrolyzer is turning on and off quite often. However, during the rest of the year it is operating in full capacity. This is happening due to the intermittency of the solar energy during the winter months when the irradiation is a bit lower while for the rest of the year, since the system is located in the Arabic peninsula and there the irradiation is relatively higher than the Netherlands, the generation seems to be stable and in rated capacity. This leads to replacing the electrolyzers system 3 times in total.

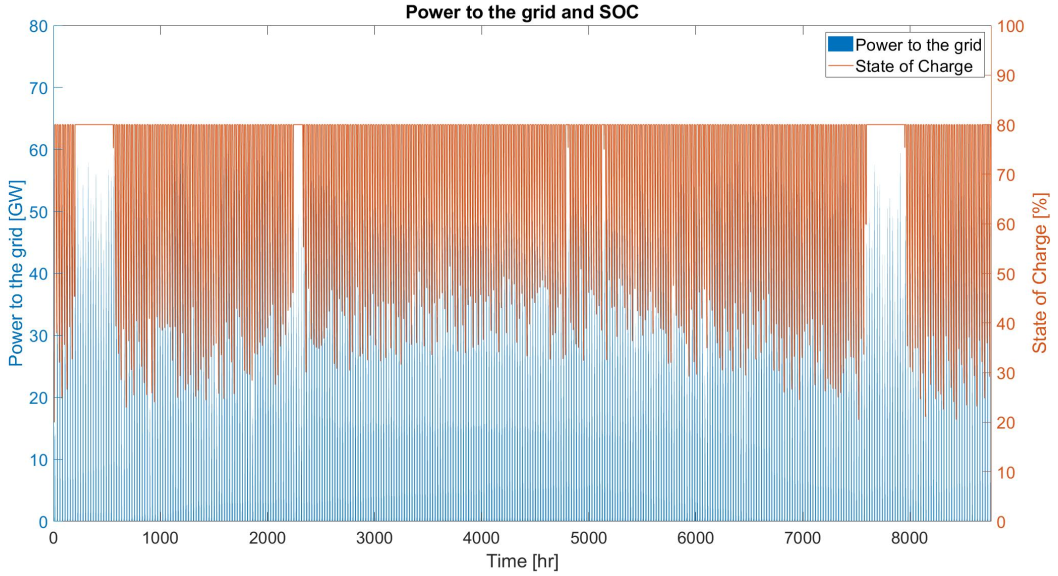


Figure 4.32: The over-generation of the system annually with the respective SOC - non Local Generation 2030 scenario

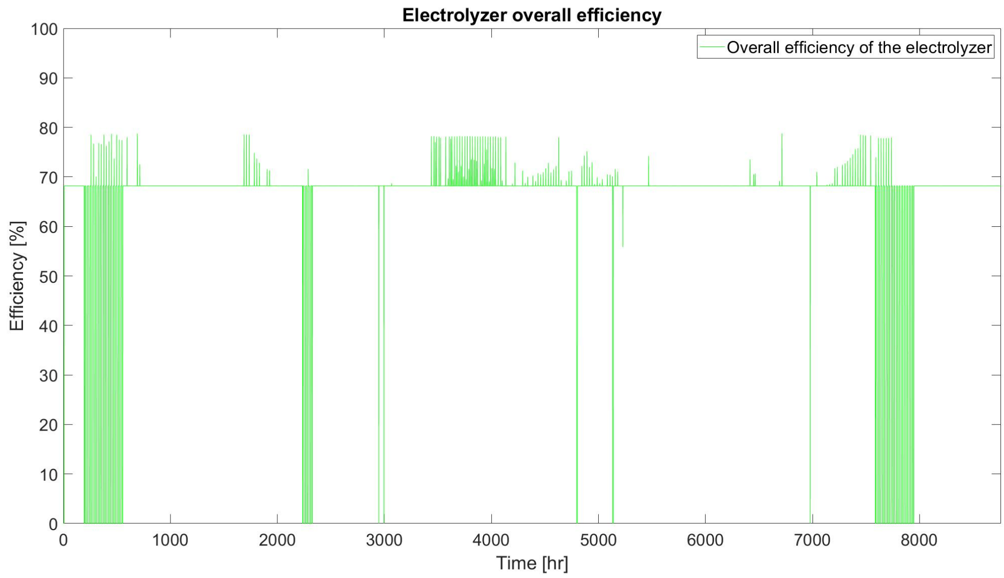


Figure 4.33: Efficiency of the electrolyzers - non Local Generation 2030 scenario

In figures 4.34.a and 4.34.b, the hydrogen produced and purchased are displayed respectively with comparison to the hydrogen load. It is visible that the one graph is the mirror of the other one. This symmetry is because when there is a deficit on the production side, the demand is covered through purchase from the hydrogen grid.

Finally, the figures 4.35 and 4.36, show the level of the tank before and after the adjustment due to the optimization complexity. Again the MATLAB was used to optimized the tank volume further and that way not only the LCOE was reduced but also the tank was used to its fullest. The state of charge was equal to 0.628 in the beginning and the end of the year. The amount of hydrogen needed to be released for safety reasons and for the constraint fulfilment was equal to 3.65% which leads to an amount of 3846.4 $m^3$ so the additional cost is equal to 1693 €.

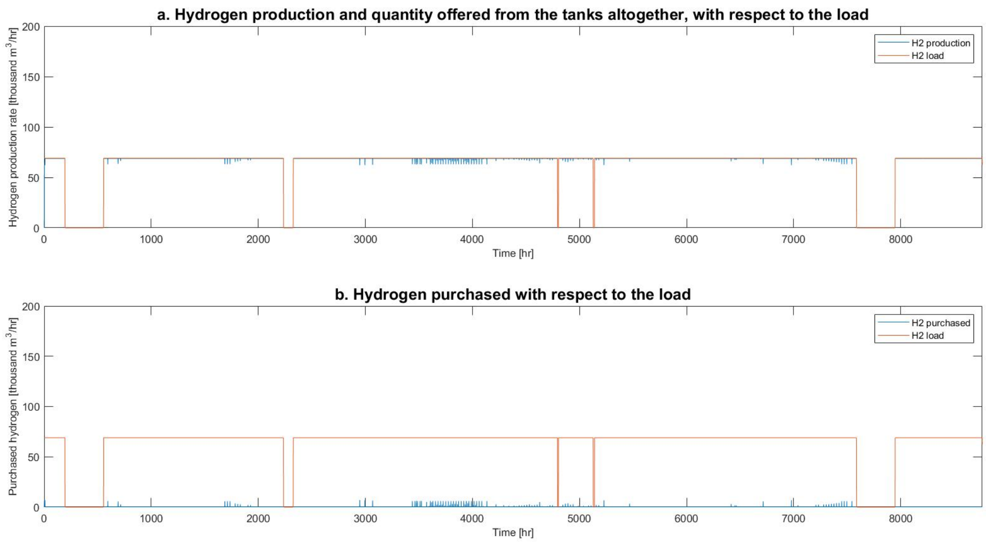


Figure 4.34: (a).Hydrogen production and amount offered from the tanks altogether with respect to the load, (b).Hydrogen amount being purchased with respect to the load - non Local Generation 2030 scenario

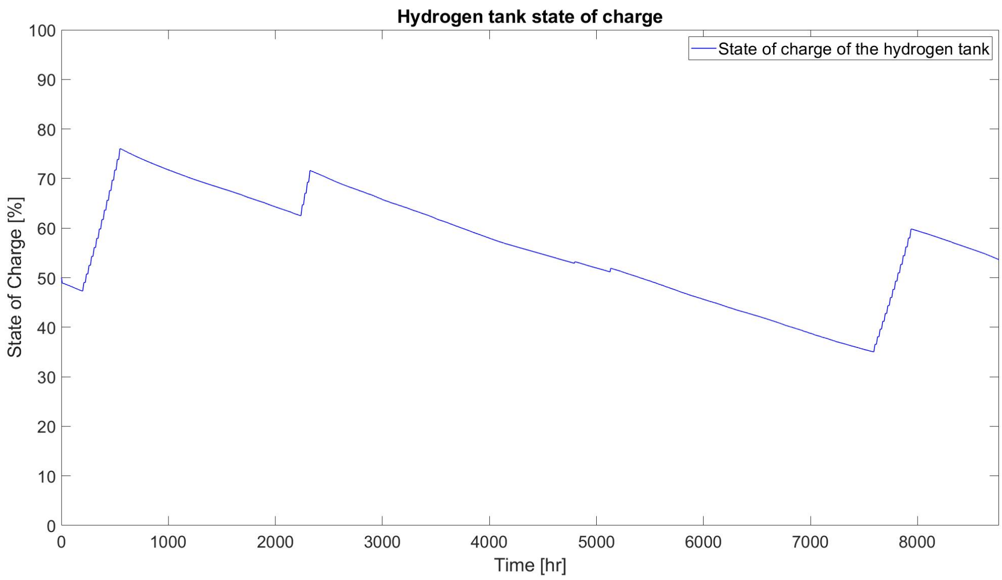


Figure 4.35: State of charge of the hydrogen tank from the initial optimization - non Local Generation 2030 scenario

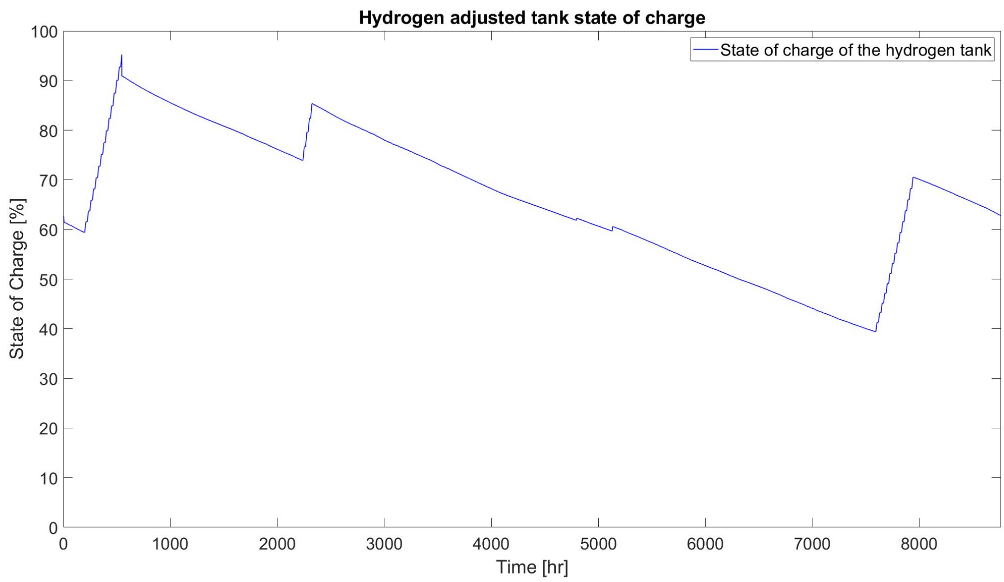


Figure 4.36: State of charge of the adjusted hydrogen tank after optimizing further the tank's size - non Local Generation 2030 scenario

**Results reflection**

At first the economics resulted from this scenario calculated an LCOE with the value of 0.764 €/kWh when no power is sold to the grid while the $LCOE_{NET}$ was 0.0279 €/kWh. A big difference between the two values has been occurred. This is because this system consists of two smaller systems that are autonomous in their operation and thus the over - generation has occurred after installing them is sensibly higher than any other case of the local generation scenarios.

The second part of the results reflection will be about the area specification of the system. The system consists of two parts. Starting with the part of the local electricity generation, a total of 2.898 GW of wind turbines will be installed and a total of 6.754 GW for the solar panels. Thus, by using the ratio of the capacity per area for the wind turbines equal to 10.61 MW/km$^2$, leads to an area calculation of 273.14 km$^2$, while for the solar panels, by using the ratio of 53.9 MW/km$^2$, an area of 125.3 km$^2$ is needed. For the battery banks of the system, a total amount of 4910 are needed and each one consumes an area of 29.72 m$^2$. Thus, the total area needed is equal to 0.146 km$^2$. The optimization output was for another case to install some solar panels in the east and west direction. The amount of these solar panels in comparison with the solar panels oriented south is relatively small and thus some other ideas could be other to use solar axis trackers to optimize the power generation or to compromise with only south oriented solar panels and a relatively higher LCOE and SSR. However, since the aforementioned cases were not studied in this project, there is no proof that they can lead to potentially better results.
The second part of the system is about the hydrogen production that is done in the Arabic Peninsula where also the liquefaction of hydrogen electricity load is produced in parallel by solar panels and then after being liquefied it is shipped back to the Netherlands. For this part of the system an installed capacity of solar panels equal to 56.314 GW. According to the analysis performed at the section 2.1.6, the capacity installed per area ratio is equal to 53.38 MW/km$^2$. Thus, the total area needed for the solar panels installation is equal to 1054.96 km$^2$. The battery banks are 4125 and with 29.72 m$^2$ for each one of them, the area needed is equal to 0.122 km$^2$. Finally, the electrolyzers that are output as a result from the optimization were 1400. Each one consumes a space of 2.53 m$^2$ and thus the total area needed is equal to 3542 m$^2$.
To bring into perspective again the total amount of the area needed a comparison again is done with the total area of the Netherlands. To have a fair comparison between the scenarios even the area that will be occupied in the Arabic Peninsula was added to this calculation to provide a percentage for the total system. To bring the areas calculated into perspective, the area of the Netherlands is equal to 41543 km$^2$ according to [61]. Thus, the area needed as a percentage of the total area of the Netherlands is equal to 2.85%. The initial motivation for performing this study was to investigate the reduction of emissions of Tata Steel as they are currently responsible for the 9% of the whole Netherlands. Thus, some calculations were performed to give an insight about the potential emissions reduction by realizing this project and also provide an index that will justify the huge are occupation that has been calculated above. For the total electricity load of the system needed to be generated, equal to 4848.26 GWh, the avoided emissions calculated to be equal to 3.79 million tons of $CO_2$. For the processes themselves, an amount of 0.95 ton $CO_2$ per ton of steel are produced without considering the electricity generation [64]. Tata Steel, produces annually 6.8 million tons of steel on average. Thus, only from the primary processes, 6.46 million tons of $CO_2$ are further emitted. The further avoided emissions will be equal to the 30% of this amount since a 30% of the fossil fuels used to perform the iron reduction were replaced by green hydrogen. Thus the emissions avoided were equal to 1.94 million tons of $CO_2$. This leads to a total amount of 5.73 million tons of avoided $CO_2$ emissions. For the shipping emissions of the hydrogen from the Arabic peninsula to the Netherlands, it is stated in DNV's Maritime Forecast for 2050 [65], that three alternative fuels which are ammonia, methanol and hydrogen will be commercially available to be used to the shipping industry. Thus, no calculation was performed about the potential emissions of the shipping process. Finally, to conclude the

results reflection section for this case, for the total system an electricity load coverage of 99.941% was achieved while for the hydrogen load 99.534% could be offered by the system itself. The LCOE value for the closed system was equal to 0.764 €/kWh. According to [63], to operate a closed cycle gas turbines plant in the year of 2030, the cost range will be between 0.08 and 0.12 €/kWh. It is a fact that the occurring LCOE value is almost 8 times higher than operating such a plant. Economically, the investment will be considered either attractive on not in dependence with the prices that will be set for the carbon tax credits in the future. If the system becomes really strict, then it can potentially be a feasible solution to tackle both the environmental harm of Tata Steel's emissions as well as an investment opportunity. However, no further reflection on this aspect is being done as the research question refers to the techno - economic feasibility of such a project and not to the potential of such a business case.

## 4.5 Non - Local Generation Scenario - 2050

The final results for this scenario will be presented into two parts as the parts of the system. The first part of the system covers the electricity loads for the processes of Tata Steel in the Netherlands as well as the regasification of the liquid hydrogen. The second part of the system is the hydrogen production in the Arabic Peninsula and the load fulfillment for the liquefaction of hydrogen to ship it back to the Netherlands. For the combined system an LCOE of 0.758 €/kWh occurred with a total system cost of 89 billion €. A $LCOE_{NET}$ value, when the electricity selling is enabled to the grid, was calculated equal to 0.0314 €/kWh. The SSR value for the total electricity loads of the system was found equal to 0.045% while for the hydrogen loads was found equal to 0.099%. Thus a load coverage of 99.955% was achieved for the electricity loads, while for the hydrogen loads it was calculated equal to 99.901%. In the following table 4.17, the aforementioned values for the combined system's variables are presented.

Table 4.17: The system performance variables that were optimized through the objective function chosen as described in 3.2.1 for the combined system of the electricity and hydrogen parts - non Local Generation 2050 scenario

| **Variables** | **Value** | **Units** |
|---|---|---|
| LCOE | 0.758 | €/kWh |
| $LCOE_{NET}$ | 0.0314 | €/kWh |
| SSR | 0.045 | % |
| Electricity Load Coverage | 99.955 | % |
| $SSR_{H_2}$ | 0.099 | % |
| Hydrogen Load Coverage | 99.901 | % |

### 4.5.1 Electricity part of the system - Non local generation scenario for 2050

The system that occurred after the optimization, consists of 500 wind turbines, with a capacity of 3.5 GW. The solar panels need to be installed only in the south orientation and they are equal to 59112500, which means an installed capacity of 26.6 GW. For the battery banks that will be tackling the intermittency of the renewable energy sources of the system, an amount of 5800 was outputted, which is an energy capacity of 16 GWh. The total load needed to be covered by the system was equal to 5407.5 GWh and covered by 4763.14 GWh from the system of wind turbines and the solar panels and by 643.36 GWh from the batteries. The rest 1 GWh was purchased by the grid. For this part of the system, the LCOE value was equal to 0.312 €/kWh while the $LCOE_{NET}$ value was calculated equal to 0.035 €/kWh. Finally, the SSR of the system was found equal to 0.018% and this leads to a load coverage of 99.982%. The results that are described above are presented in the following tables 4.18, 4.19 and 4.20 that respectively show the components of the system, the energy balance of the system and the optimization variables results.

Table 4.18: The amount of the different components of the system and their respectful installed capacity - non Local Generation 2050 scenario

| Variables | Value | Installed Capacity |
|---|---|---|
| Number of wind turbines | 500 | 3.5 GW |
| Number of panels oriented south | 59112500 | 26.6 GW |
| Number of panels oriented east | - | - |
| Number of panels oriented west | - | - |
| Number of battery banks | 5800 | 16 GWh |

Table 4.19: The energy balance of the system which proves that the load equals the sum of the energy provided by the system, the batteries and the grid - non Local Generation 2050 scenario

| Variables | Value | Units |
|---|---|---|
| Electricity Load | 5407.5 | GWh |
| System to the electricity load | 4763.14 | GWh |
| Batteries to the electricity load | 643.36 | GWh |
| Grid to the electricity load | 1 | GWh |

Table 4.20: The system performance variables that were optimized through the objective function chosen as described in 3.2.1 - non Local Generation 2050 scenario

| Variables | Value | Units |
|---|---|---|
| LCOE | 0.312 | €/kWh |
| $\mathrm{LCOE_{NET}}$ | 0.035 | €/kWh |
| SSR | 0.018 | % |
| Electricity Load Coverage | 99.982 | % |

### 4.5.2 Hydrogen part of the system - Non local generation for 2050

The hydrogen part of the system consists of solar panels, battery banks and the electrolyzer - hydrogen tank system. The amount for the installed solar panels is 175129456 in the south orientation, 213000 for the east and 215500 for the west one. The respective installed capacity is equal to 78.8 GW, 0.096 GW and 0.097 GW. Thus the total installed capacity of the solar panels is equal to 78.99 The battery banks are 11525 with an energy capacity of 31.809 GWh. Finally, the electrolyzer system consists of 4000 electrolyzers, and a tank that initially was found equal to 224250 $m^3$, but after the adjustment the final size is equal to 235450 $m^3$. For the energy balance of the system, the total electricity load for the liquefaction of hydrogen is equal to 2918.96 GWh. This load was covered by 1465.8 GWh through the batteries while 1450 GWh were directly covering the load from the solar panels. This leads to a purchased amount of 3.16 GWh from the grid. For the hydrogen mass balance, the system needed to cover an amount of 6.217 billion $m^3$, including also the additional amount that is predicted to escape as boil - off gas. This load was covered by producing 6.188 billion $m^3$ and purchasing 29.02 million $m^3$. The system described above comes with an LCOE of 0.954 €/kWh and a $\mathrm{LCOE_{NET}}$ of 0.014 €/kWh, an SSR for the electricity loads of 0.095% that leads to a load coverage of 99.905%, while for the hydrogen SSR a value of 0.099% occurred that leads to a hydrogen load coverage of 99.901%. In the following tables 4.21, 4.22 and 4.23, the components of the system, the mass and energy balance as well as the optimization variables values are presented respectfully.

Table 4.21: The amount of the different components of the system and their respectful installed capacity - non Local Generation 2050 scenario and Arabic Peninsula part of the system

| Variables | Value | Installed Capacity |
|---|---|---|
| Number of panels oriented south | 175129456 | 78.8 GW |
| Number of panels oriented east | 213000 | 0.096 GW |
| Number of panels oriented west | 215500 | 0.097 GW |
| Number of battery banks | 11525 | 31.809 GWh |
| Number of electrolyzer | 4000 | 1 GW |
| Volume of hydrogen storage tank | - | 224250 $m^3$ |
| Volume of hydrogen storage tank after adjustment | - | 235450 $m^3$ |

Table 4.22: The energy balance of the system which proves that the load equals the sum of the energy provided by the system, the batteries and the grid as well as the mass balance of hydrogen which proves that the load is equal to the sum of the hydrogen produced and purchased - non Local Generation 2050 scenario and Arabic Peninsula part of the system

| Variables | Value | Units |
|---|---|---|
| Electricity Load | 2918.96 | GWh |
| System to the electricity load | 1450 | GWh |
| Batteries to the electricity load | 1465.8 | GWh |
| Grid to the electricity load | 3.16 | GWh |
| Hydrogen load | 6.217 | billion $m^3$ |
| System to the hydrogen load | 6.188 | billion $m^3$ |
| Purchased hydrogen amount | 29.02 | million $m^3$ |

Table 4.23: The system performance variables that were optimized through the objective function chosen as described in 3.2.1 - non Local Generation 2050 scenario and Arabic Peninsula part of the system

| Variables | Value | Units |
|---|---|---|
| LCOE | 0.954 | €/kWh |
| $LCOE_{NET}$ | 0.014 | €/kWh |
| SSR | 0.095 | % |
| Electricity Load Coverage | 99.905 | % |
| $SSR_{H_2}$ | 0.099 | % |
| Hydrogen Load Coverage | 99.901 | % |

### 4.5.3 Discussion - non Local Generation Scenario 2050

#### Electricity generation part of the system

The constraint of the simulation referring to the battery banks was to match the initial and final state of charge to secure continuity for the total simulation of the system's lifetime. Thus, for the one year simulation time, the initial and final state of charge were matching equal to 0.8 as it can be observed in the following figure 4.37.

In the following figures 4.38 and 4.39, the wind and solar power generation is displayed. In the middle of the year the power generation for the solar energy is relatively higher than the rest of the year. For the wind energy, it is a fact that the 3% losses has been included and the maximum power generated is equal to 3.395 GW.

In the following summary graph, the power provided to the load from the system of solar panels and wind turbines are presented in 4.40.a. In 4.40.b the power provided by the batteries is displayed while in 4.40.c the power bought from the grid to fulfill the total load. It can be

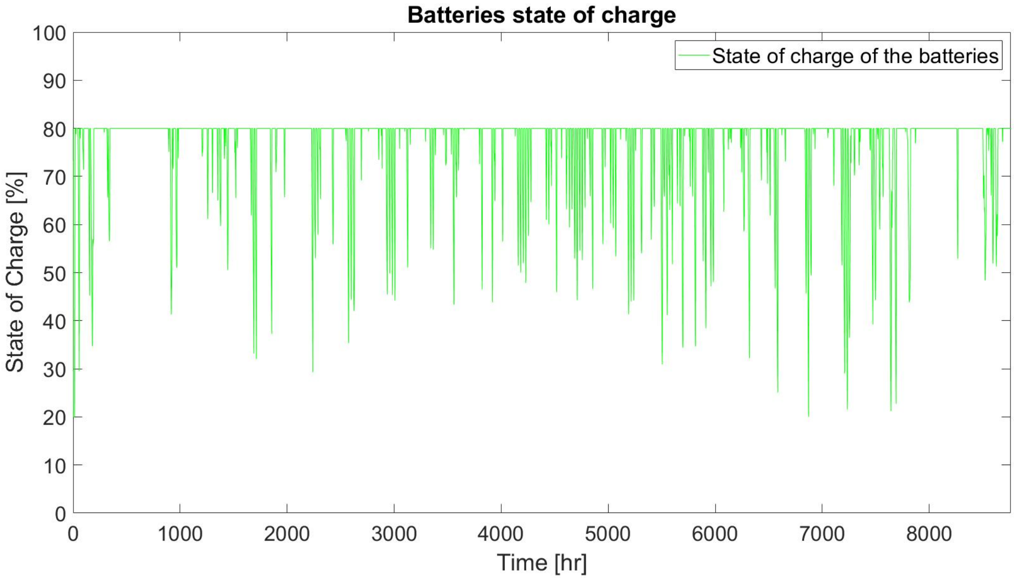


Figure 4.37: The graphic representation of the state of charge. The initial and the final state of charge for the one year simulation presented here is equal to 0.8 and they match with each other - non Local Generation 2050 scenario for the IJmuiden part of the system

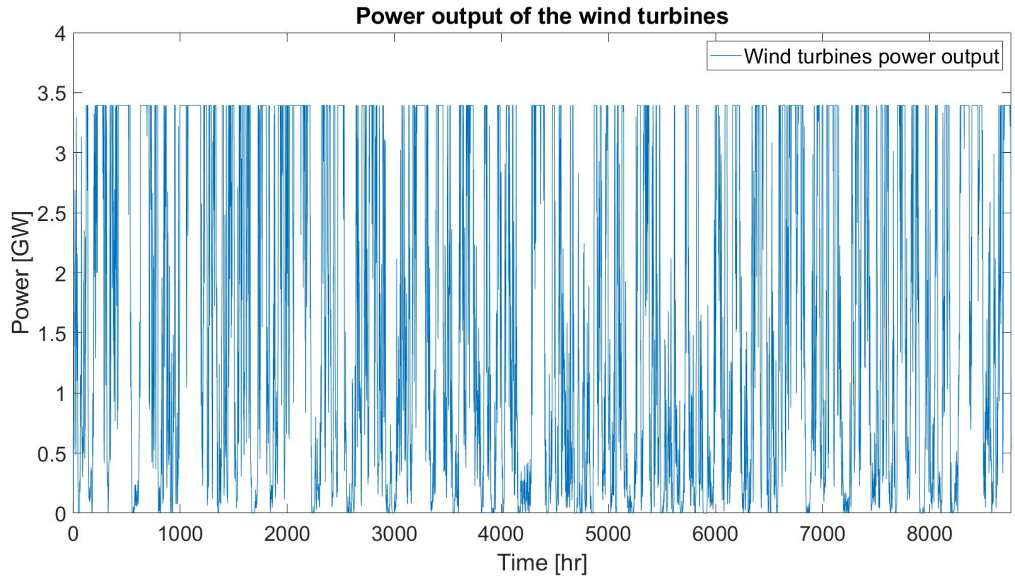


Figure 4.38: The graphic representation of the wind power output - non Local Generation 2050 scenario for the IJmuiden part of the system

easily observed the symmetry between the power provided by the system of the solar panels and wind turbines as well as the really small amount bought from the grid, which is in accordance with the really high load coverage percentage.

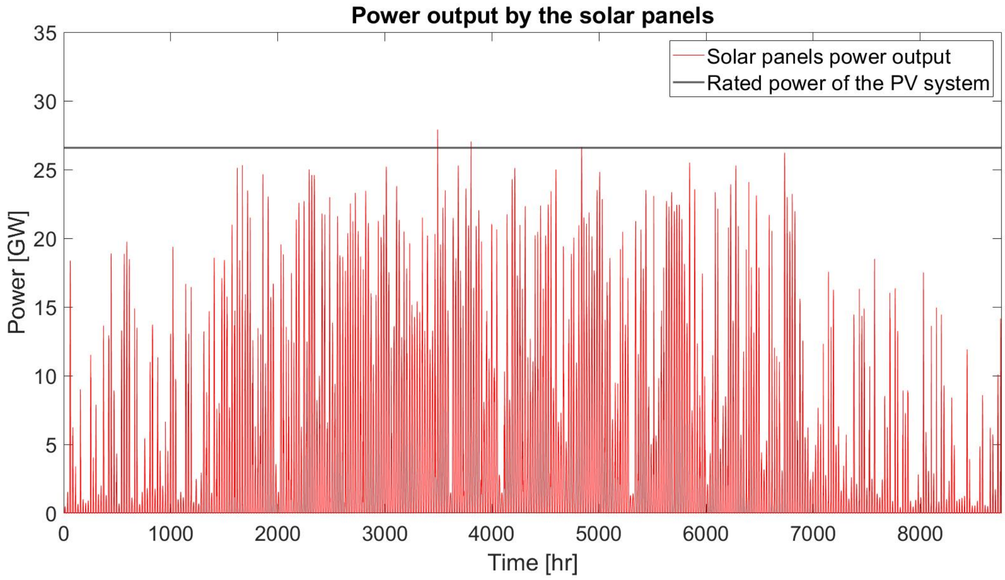


Figure 4.39: The graphic representation of the solar power output - non Local Generation 2050 scenario for the IJmuiden part of the system

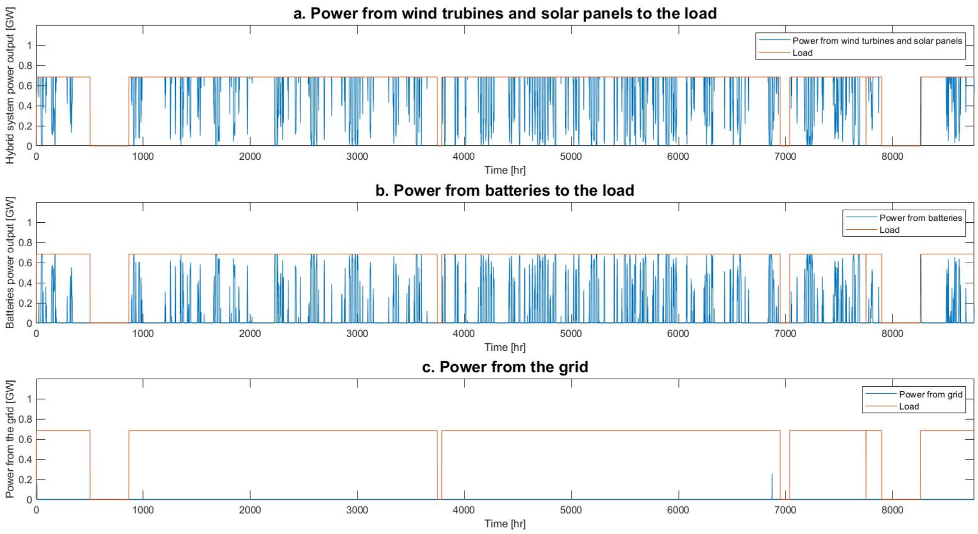


Figure 4.40: (a). The graphic representation of power provided by the hybrid system of the solar panels and the wind turbines to the load, (b). The graphic representation of the power provided from the batteries to the load, (c). The graphic representation of the power bought from the grid compared with the load. Non Local Generation 2050 scenario for the IJmuiden part of the system

Finally, the over - generation from the system, is indicated in the next figure 4.41. It can be observed that when the batteries are in their maximum allowed capacity of 80 %, the power is sent to the grid, while the rest of the times the power is directly sent to the batteries.

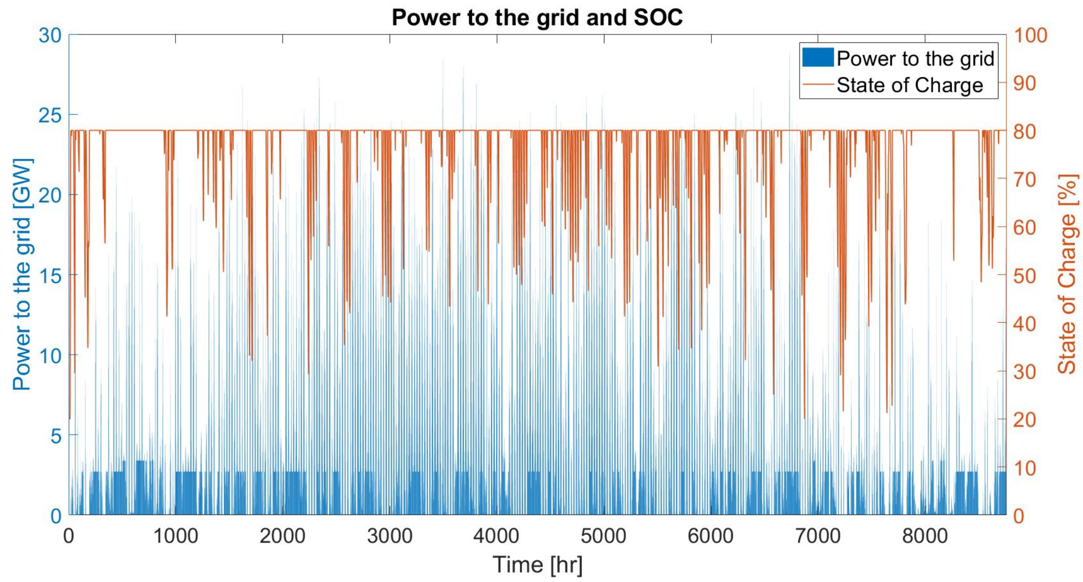


Figure 4.41: The over-generation of the system annually with the respective SOC - non Local Generation 2050 scenario for the IJmuiden part of the system

**Hydrogen part of the system**

For this part of the system the constraint for the batteries so the state of charge will match in the beginning and the end of the year should be fulfilled. The state of charge should be equal to 0.7 in the beginning of the year to match the final one, thus the batteries are assumed to be charged to their 70% before the project starts for this scenario's realization. The aforementioned can be seen in figure 4.42.

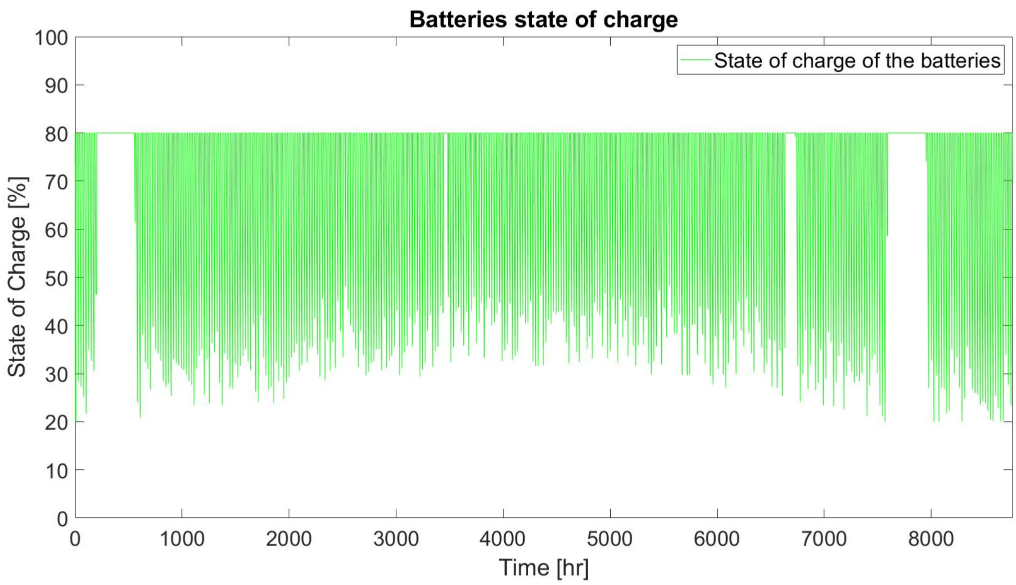


Figure 4.42: The graphic representation of the state of charge. The initial and the final state of charge for the one year simulation presented here is equal to 0.7 and they match with each other - non Local Generation 2050 scenario

For the power generation, this part of the system consists of solar panels. The power generated throughout a year can be seen in the following figure 4.43.

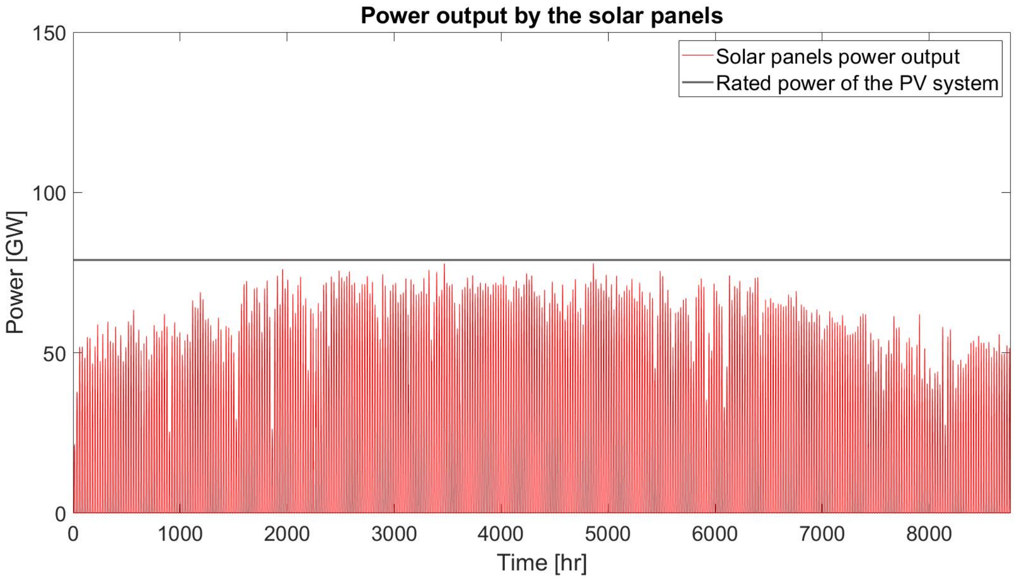


Figure 4.43: The graphic representation of the solar power output - non Local Generation 2050 scenario

The electricity load coverage can be seen in the following figure. In 4.44.a the power provided by the solar panels is displayed while in 4.44.b is the power provided from the batteries to the load. Finally, from 4.44.c, the power purchased from the grid is displayed. In this case it is visible that the batteries are charging and the solar panels are providing to the load while on the next step of the graph the opposite is happening. This is because batteries are providing at night while the solar panels during the day to the load. Further than that it is also visible the matching of the low SSR with the low amount of power that was purchased from the grid to fulfill such a load.

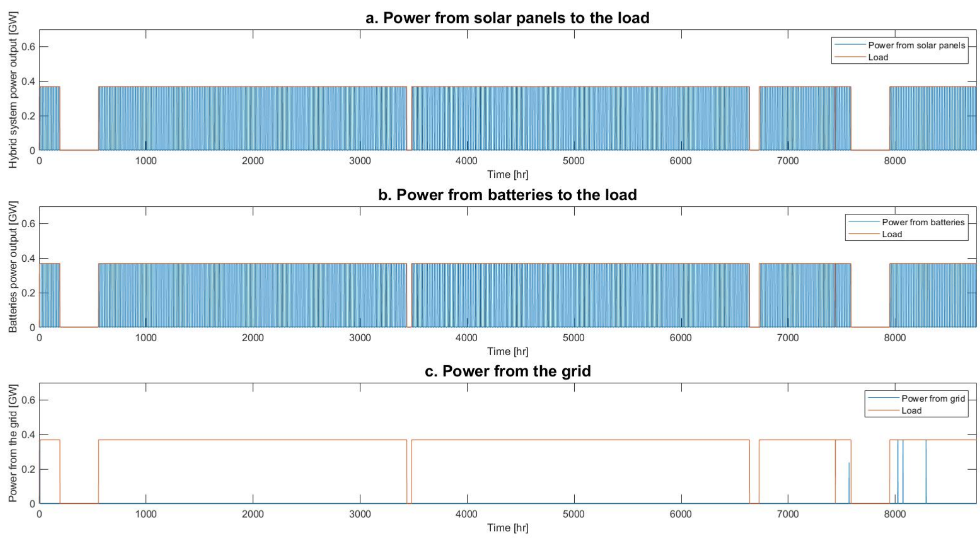


Figure 4.44: (a). The graphic representation of power provided by the hybrid system of the solar panels and the wind turbines to the load, (b). The graphic representation of the power provided from the batteries to the load, (c). The graphic representation of the power bought from the grid compared with the load - non Local Generation 2050 scenario

The next figure 4.45, shows the over - generation of the system with combination to the state of charge from the batteries. It is visible that when the batteries have reached their maximum capacity, the excess energy is sent directly to the grid.

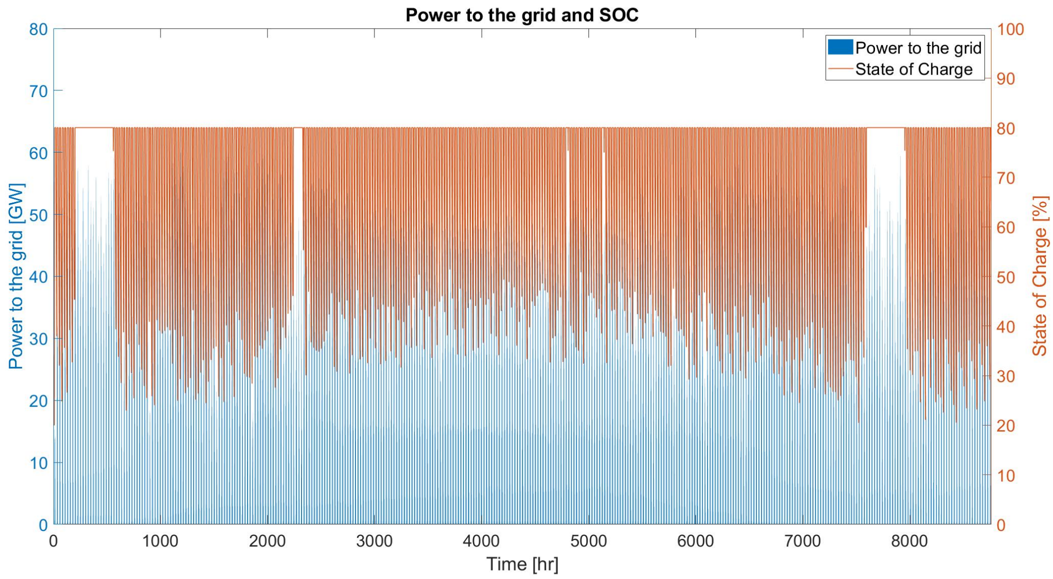


Figure 4.45: The over-generation of the system annually with the respective SOC - non Local Generation 2050 scenario

For the hydrogen production side, at first the figure 4.46 shows the efficiency of the electrolyzer. It can be observed that in the beginning and in the end of the year the electrolyzer is turning on and off quite often. However, during the rest of the year it is operating in full capacity. This is happening due to the intermittency of the solar energy during the winter months when the irradiation is a bit lower while for the rest of the year, since the system is located in the Arabic peninsula and there the irradiation is relatively higher than the Netherlands, the generation seems to be stable and in rated capacity. This leads to replacing the electrolyzers system 3 times in total. A further trade - off can be that an alkaline electrolyzer is not ramping up and down as quickly as a PEM one however for this project the motivation for the lifetime and the cost was already given in section 2.1.4.

In figures 4.47.a and 4.47.b, the hydrogen produced and purchased are displayed respectively with comparison to the hydrogen load. It is visible that the one graph is the mirror of the other one. This symmetry is because when there is a deficit on the production side, the demand is covered through purchasing from the hydrogen grid.

Finally, the figures 4.48 and 4.49, show the level of the tank before and after the adjustment due to the optimization complexity. Again the MATLAB was used to optimized the tank volume further and that way not only the LCOE was reduced but also the tank was used to its fullest. The state of charge was equal to 0.5 in the beginning and the end of the year. The amount of hydrogen needed to be released for safety reasons and for the constraint fulfilment was equal to 8.73% which leads to an amount of 19577 $m^3$ so the additional cost is equal to 7596 €.

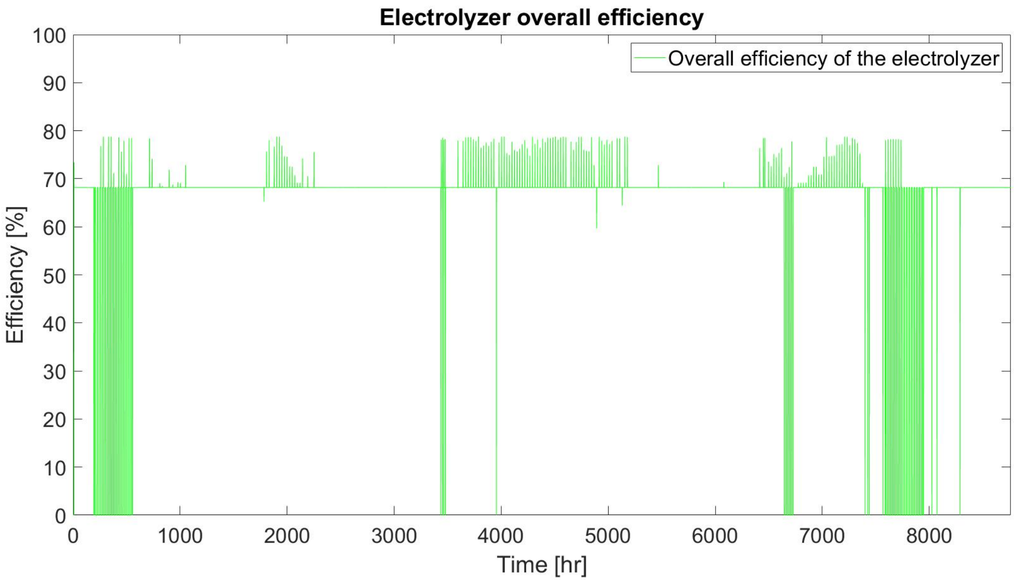


Figure 4.46: Efficiency of the electrolyzers - non Local Generation 2050 scenario

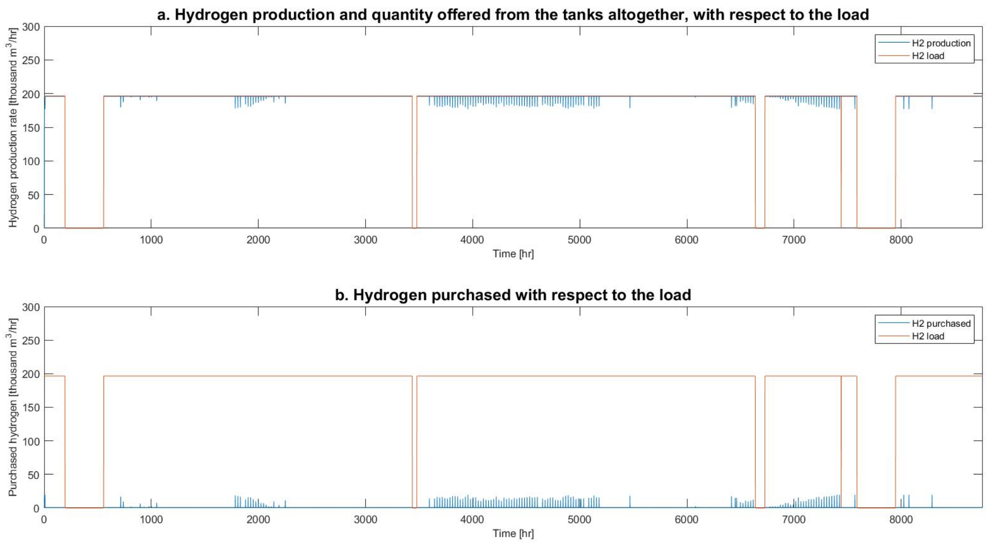


Figure 4.47: (a).Hydrogen production and amount offered from the tanks altogether with respect to the load, (b).Hydrogen amount being purchased with respect to the load - non Local Generation 2050 scenario

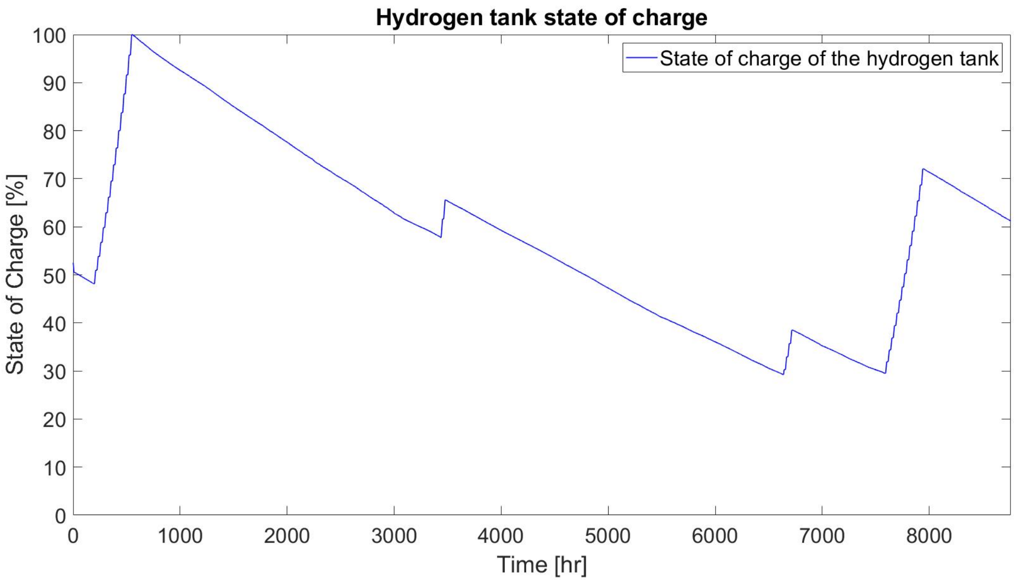


Figure 4.48: State of charge of the hydrogen tank from the initial optimization - non Local Generation 2050 scenario

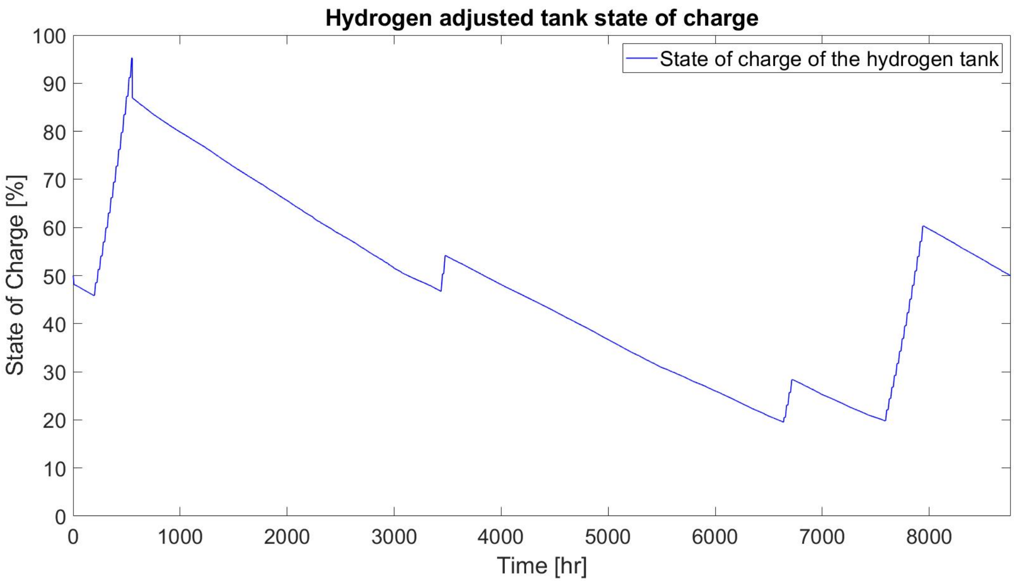


Figure 4.49: State of charge of the adjusted hydrogen tank after optimizing further the tank's size - non Local Generation 2050 scenario

**Results reflection**

The economics reflection will be done with the LCOE calculated for the combined system equal to 0.758 €/kWh. The $LCOE_{NET}$ occurred equal to 0.0314 €/kWh. The difference between the two values is high and it is because the over - generation for both the two systems in the IJmuiden and Arabic Peninsula has been considered to the final calculations.

The second part of the results reflection will be about the area specification to realize such a system. Starting with the electricity part of the system for the IJmuiden area, where 500 wind turbines of 3.5 GW installed capacity are considered. With 10.61 MW/km$^2$ capacity to area ratio leads to a total area of 329.88 km$^2$. For the solar panels, a total capacity of 26.6 GW is needed to be installed and thus with a ratio of 53.9 MW/km$^2$, leads to an area of 493.5 km$^2$. Finally for the battery banks of the system equal to 5800, and with 29.72 m$^2$ per battery bank, leads to an area of 0.172 km$^2$. The other part of the system refers to the production of hydrogen in the Arabic Peninsula and a capacity of 78.99 GW leads to an area occupation of 1479.77 km$^2$. For the battery banks of the system an amount of 11525 is needed and with 29.72 m$^2$ per battery bank leads to an area occupation of 0.34 km$^2$. Finally, the amount of electrolyzers is equal to 4000 and per electrolyzer an area of 2.53 m$^2$ is needed which leads to an area occupation of 10120 m$^2$. To bring into perspective again the total amount of the area needed a comparison again is done with the total area of the Netherlands. To have a fair comparison between the scenarios even the area that will be occupied in the Arabic Peninsula was added to this calculation to provide a percentage for the total system. To bring the areas calculated into perspective, the area of the Netherlands is equal to 41543 km2 according to [61]. Thus, the area needed as a percentage of the total area of the Netherlands is equal to 4.37%. The first motivation for studying Tata Steel as the industry of this project was the fact that they emit the 9% of the total Netherlands emissions. The total load to be covered for the combined system was equal to 8326.45 GWh and the avoided emissions calculated to produce that amount with green energy sources were equal to 5.9 million tons of $CO_2$. As already analyzed, only for the primary processes, Tata Steel were emitting 6.46 million tons of $CO_2$. Thus, since the whole process chain has become fully renewable by 100% addition of hydrogen to the fuel mix for this processes and the electricity generation is only happening with renewable energy sources, the total avoided emissions are equal to 12.36 million tons of $CO_2$. For the shipping of hydrogen again no calculations performed as the shipping sector is considered to be fully renewable as well by 2050.

Finally to conclude the results reflection, the electricity load coverage for the combined system is equal to 99.955% and the hydrogen load coverage equal to 99.901%. According to [63], to operate a closed cycle gas turbines plant in the year of 2050, the operation cost is in the range of 0.09 and 0.15 €/kWh. This leads to the conclusion that financially it is not economically viable to be attracted for such an investment due to the high difference between the LCOE occurred and the operation costs of closed cycle gas turbines plant. However, in the aforementioned values the carbon taxes are not yet added and thus this would potentially lead to an economically viable solution if the add too much to the operation costs throughout the years. Since, this conclusion to be analyzed further needs the data and assumptions for a business case is out of the scope of the research question and it will not be analyzed further in this results reflection section.

## 4.6 Overall reflection of the results

In this section, the overall reflection to the results will be done after presenting in the following table 4.25 a summary of all the different results occurred through the optimization of all the five different scenarios. In the following table 4.25, it can be seen a complete summary that represents the system.

To be able to compare the results with each other and construct the following table 4.25, some disclaimers need to be made:

At first the BAU scenario's loads corresponds to the electricity loads which are 11.42% of the total energy intensity of such an industry as analyzed in section 2.2. On the other hand for the scenarios of 2030, the processes implicated refer to the electric arc furnace, the direct reduction of iron furnace, the hot rolling and the continuous casting. Also in comparison with the BAU scenario, the loads are lower because of more efficient waste heat recovery added to the processes. Finally, for the 2050 scenarios the loads are for the same processes as for 2030 but also including a further heating, a higher amount of electricity for the auxiliary equipment like valves and pumps and of course 100% hydrogen in the fuel mix for the reduction process.

As far as the LCOE calculation is concerned, it is not including for the BAU scenario and for the 2030 steel making route scenarios, that also include in the fuel mix a fossil fuel percentage, the purchasing of this fuel amount nor the carbon taxes. In all the LCOE calculations done in this project, the total cost for the investment of the system, the replacement of some components and the maintenance of the system are considered.

Then, it's important to mention that the total cost refers to prices adjustments for the future years of 2030 and 2050 as analyzed already in sections 3.3.1 and 3.3.2. To compare these values with each other they have to be discounted to a specific year's money. To be able to compare all the costs, the amounts are converted to their present value according to the following equation 4.6.1.

$$PV = \frac{FV}{(1+r)^n} \tag{4.6.1}$$

Where,

PV: Present value

FV: Future value

r: The interest rate

n: the number of years ahead from the present that the future value refers to

Thus, the adjusted values of the total cost of the present year of 2022 are as showed in the following table 4.24.

Table 4.24: The total cost of each system converted to its present value with an interest rate of 5%.

| **Scenario** | BAU | Local Generation 2030 | Local Generation 2050 | Non Local Generation 2030 | Non Local Generation 2050 |
|---|---|---|---|---|---|
| Total Cost PV [billion € ] | 16.22 | 8.79 | 15.96 | 21.69 | 22.7 |

Furthermore, the total avoided emissions values refer to the emissions that would have been avoided by generating this load with green electricity instead of fossil fuels. Thus, since the load in every scenario is changing, the ratio of avoided tons of $CO_2$ per MWh is calculated for a fair comparison between the different scenarios.

Finally, to bring into perspective the land use for this project's realization two different metrics were calculated. At first the ratio of offshore and onshore space occupied to the total space of the Netherlands is given and also the ratio of the avoided emissions to the offshore and onshore space used.

Table 4.25: Summary table presenting the metrics for each scenario studied to provide an overview for the overall reflection to the results

| ***Summary of the results*** | | | | | |
|---|---|---|---|---|---|
| **Scenario** / **Metrics** | **BAU** | **Local Generation 2030** | **Local Generation 2050** | **Non local Generation 2030** | **Non local Generation 2050** |
| Total Electricity Load [GWh] | 4701.34 | 3682.42 | 5262.5 | 4847.15 | 8326.45 |
| Liquefaction [GWh] / Regasification [GWh] | - | - | - | 1091 / 73.73 | 2920 / 143.95 |
| Hydrogen load [billion $m^3$] | - | 1.855 | 4.491 | 2.187 | 6.217 |
| LCOE [€/kWh] | 0.245 | 0.383 | 0.421 | 0.764 | 0.758 |
| LCOEnet [€/kWh] | 0.065 | 0.066 | 0.042 | 0.028 | 0.0314 |
| SSR [%] | 0.44 | 0.993 | 0.125 | 0.042 | 0.045 |
| SSR H2 [%] | - | 0.865 | 0.793 | 0.456 | 0.099 |
| Total Cost [billion €] | 16.22 | 21.16 | 62.55 | 52.2 | 89 |
| Total Cost PV [billion €] | 16.22 | 8.79 | 15.96 | 21.69 | 22.7 |
| Installed PV Capacity [GW] | 6.75 | 7.882 | 33.94 | Local: 6.745<br>Non local: 56.314 | Local: 26.6<br>Non local: 78.8 |
| Installed Wind Capacity [GW] | 2.45 | 2.905 | 3.038 | Local: 2.898<br>Non local: - | Local: 3.5<br>Non local: - |
| Installed Battery Capacity [GWh] | 13.81 | 13.786 | 46.66 | Local: 13.511<br>Non local: 11.385 | Local: 16<br>Non local: 31.809 |
| Installed Electrolyzer Capacity [GW] | - | 0.298 | 0.73 | Local: -<br>Non local: 0.35 | Local: -<br>Non local: 1 |
| Total onshore space use [$km^2$] | 125.38 | 146.38 | 630.18 | Local: 125.45<br>Non local: 1055.08 | Local: 493.67<br>Non local: 1480.11 |
| Total offshore space use [$km^2$] | 230.91 | 273.8 | 286.33 | Local: 273.14<br>Non local: - | Local: 329.88<br>Non local: - |
| Total avoided emissions [million tons $CO_2$] | 3.67 | 4.79 | 10.564 | 5.73 | 12.36 |
| Avoided emissions per MWh [tons $CO_2$/MWh] | 0.78 | 1.3 | 2.01 | 1.18 | 1.48 |
| Space used to the NL total area [ % ] | 0.3 | 0.35 | 1.5 | 2.85 | 4.37 |
| Avoided emissions per area [ktons $CO_2/km^2$] | 10.3 | 11.4 | 11.53 | 3.94 | 5.37 |

# 5| Sensitivity Analysis

In this chapter, a sensitivity analysis was conducted in a range near the optimal points for each scenario. The method used was the Sobol Sensitivity analysis which is proper for multi variable problems. In the first section 5.1 of this chapter, the theory behind the sensitivity analysis with the Sobol method is presented. After the first section, in each further section of this chapter the results of the sensitivity analysis for each scenario are presented. Thus, in section 5.2 are the results for the BAU scenario, in section 5.3 for the local generation of 2030, in section 5.4 for the local generation of 2050, in section 5.5 for the non local generation of 2030 and in section 5.6 for the non local generation of 2050. The results presented here are the effect that each input variable, which are different per scenario, has to the levelized cost of electricity. Further than that, also the interactions between the different variables were outputted from the sensitivity analysis and are presented as well.

## 5.1 Sobol sensitivity analysis

Sobol sensitivity analysis is a global sensitivity analysis method which is aiming to the quantification of which input parameters or combinations of them are explaining the best the variability of the quantity of interest, in this case LCOE [66]. The sensitivity of the LCOE, is given by three indices calculated with the Sobol method. Before the three indices are explained, some statistic terms definition is presented. At first according to [67], the variance is a measure of dispersion, which means that is a measure of how far a set of number is spread over its average value. Further than that, another term used in this analysis is the conditional expected value which is defined as the value that a variable would take on average over a large number of occurrences given that this certain set of conditions is known to occur. Thus, the variance of the conditional expected value can be calculated. Having presented the above, the first order index of the Sobol analysis can be calculated as shown in the equation 5.1.1. The first order Sobol index represents the direct effect one input variable has in the output variable [68].

$$S_{\mathrm{i}} = \frac{V(E(y|x_{\mathrm{i}}))}{V(y)} \tag{5.1.1}$$

Where,

$S_i$: the first order sobol index

$V(E(y|x_i))$: The variance of the conditional expected value, meaning the value y will take given the value of $x_i$

$V_i$: the variance of the input variable $x_i$

$V_j$: the variance of the input variable $x_j$

y: the output variable, in this case LCOE

$x_i$: the input variable, in this case the input variables optimized for each scenario

The second order Sobol index, according to [66], expresses the effect of the interaction of two input variables to the output variable's variance. Thus, the variance between an input variable $x_i$ and $x_j$, is calculated as it can be seen from the equation 5.1.2 and the effect to the output variable is given through the ratio that defines the second order Sobol index as it can be seen in the equation 5.1.3, below.

$$V_{ij} = V(E(y|x_i, x_j) - V_i - V_j \tag{5.1.2}$$

Where,

$V_{ij}$: the amount of the variance of the output variable due to the interaction of the variables $x_i$ and $x_j$

$V(E(y|x_i,\ x_j))$: The variance of the conditional expected value, meaning the value y will take given the value of $x_i$ and $x_j$

V(y): the variance of the output value

y: the output variable, in this case LCOE

$x_{i \text{ or } j}$: the input variable i or j

$$S_{ij} = \frac{V_{ij}}{V(y)} \tag{5.1.3}$$

Where,

$S_{ij}$: the second order sobol index

$V_{ij}$: the amount of the variance of the output variable due to the interaction of the variables $x_i$ and $x_j$

V(y): the variance of the output value

y: the output variable, in this case LCOE

$x_{i \text{ or } j}$: the input variable i or j

Finally, the total Sobol index is calculated, which represents both the effect of an input variable directly to the output variable as well as the effect of the interaction of two input variables to the output variable. Is defined as the sum of all the different indices calculated as it can be seen in equation 5.1.4.

$$S_i{}^{T} = \sum_{i \epsilon u} S_u \tag{5.1.4}$$

Where,

$S_i{}^{T}$: the second order sobol index

u: Represents all the single subscripts and the pairs where it can be in u = {i} and u = {i,j}

So, summarizing all the above in the following list, the following conclusions can be extracted from the Sobol indices values:

1. If the first order Sobol index is high, means that this variable influences a lot the LCOE, while if it is low it does not.
2. If the second order Sobol index is high, means that the interaction of the two variables this index represents have a high effect on the LCOE, while if it is relatively low they do not.
3. If the total order Sobol index is high, means that this variable has a high influence on LCOE including also the interactions with the other variables, while if it is low it does not.
4. If the first order Sobol index is low but the total order Sobol index is high, means that the interactions of this variable with the others are responsible for the high influence this variable has on the LCOE.
5. A disclaimer also is that sometimes in the results there is a zero value for the Sobol total index, while the second order Sobol index is non zero. This is because the total effect that this variable has in the output variable is not important. This occurs either when the value is less than 1% or when the higher order indexes that are calculated for the total order index but are not presented in the following results are decreasing the total order index value.

### 5.1.1 Method used for the Sobol sensitivity analysis

To perform the sensitivity analysis a combination between the TRNSYS software and the open source programming environment python [69], was used by using a library specifically made for the Sobol Sensitivity analysis. This library is called SALib [[70], [71]] and through it, as a first step, a sample of data pairs of the input variables were generated. Then, this sample was added to the TRNSYS parametric analysis and for each pair of the input variables the LCOE value was calculated. Having the input variables x and the output variable y, the SALib was used again to perform the calculations of the Sobol indices. Finally, the values occurred are plotted and presented.

## 5.2 BAU Scenario - Sensitivity Analysis

In this section the results from the sensitivity analysis are presented for the BAU scenario. The input variables used for this analysis were the number of wind turbines (Nwt), the number of solar panels (Npv) and the number of batteries (Nbat). A sample of 256 pairs of these three variables was created and the parametric analysis extracted the respectful LCOE values. As it can be seen from the figure 5.1, the wind turbines have the highest influence in the LCOE as the first order Sobol index is relatively high. Batteries, as it can be seen from figure 5.2 are influencing LCOE much through the interaction they have with the wind turbines amount. This is because the total order Sobol index is high but the first order Sobol index is low on the batteries amount variable. Thus, this explains why a relatively high total order Sobol index was calculated for the batteries as they indirectly, through their interaction with the wind turbines amount, are affecting the LCOE value. As far as the solar panels are concerned, they do not affect the LCOE value. This is because they are cheap in comparison with the batteries and the wind turbines and the final value of the second order Sobol index was occurred equal to less than 1% which is considered to be zero as the influence is really low.

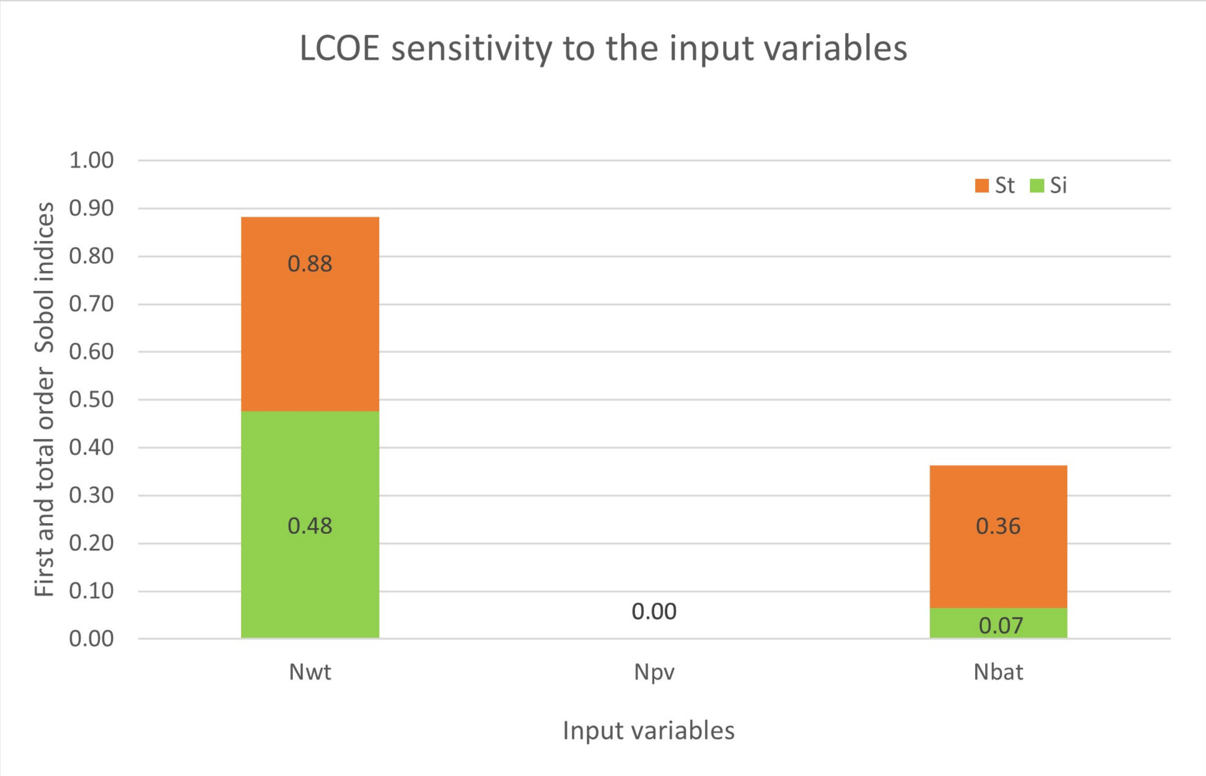


Figure 5.1: Sobol first order index and total order index are presented, which are showing the direct effect of the input variable to the LCOE and the total effect including the interactions of one input variable with the others to the LCOE respectively.

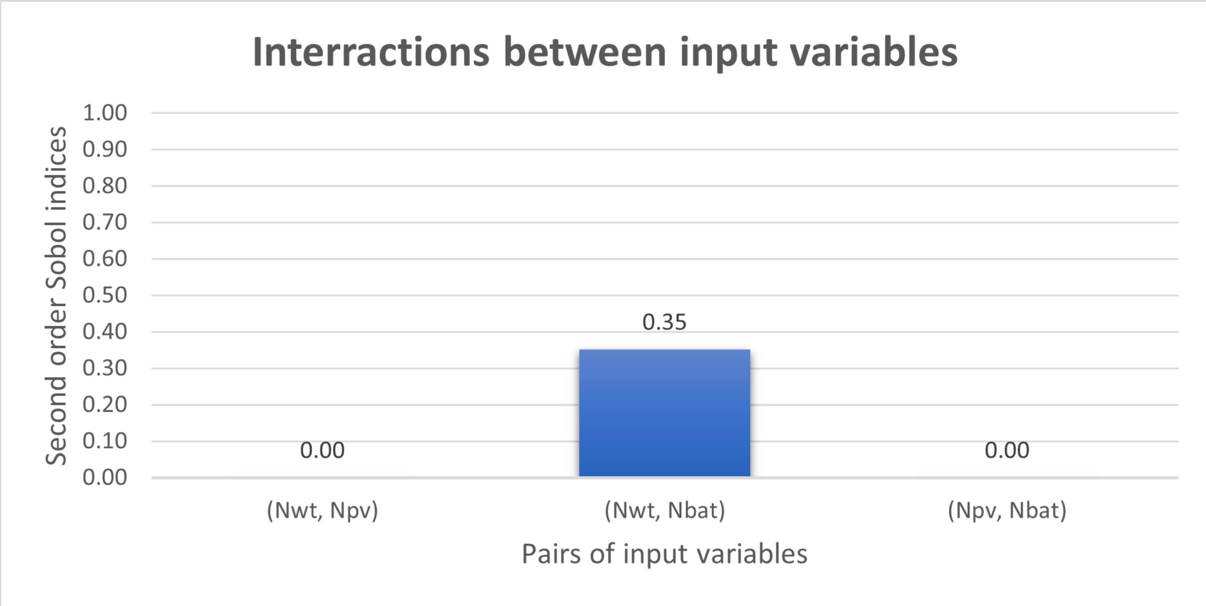


Figure 5.2: Sobol second order index is presented, which is showing the effect of the interaction of the input variables to the LCOE.

## 5.3 Local generation 2030 - Sensitivity Analysis

In this section the results from the sensitivity analysis are presented for the local generation of 2030 scenario. The input variables used for this analysis were the number of wind turbines (Nwt), the number of solar panels (Npv), the number of batteries (Nbat) and the number of electrolyzers (Nely). A sample of 320 pairs of these four variables was created and the parametric analysis extracted the respectful LCOE values. As it can be seen from the figure 5.3, the wind turbines have the highest influence in the LCOE as the first order Sobol index is relatively high. Batteries, as it can be seen from figure 5.4 are influencing LCOE much through the interaction they have with the wind turbines amount. This is because the total order Sobol index is high but the first order Sobol index is lower than 1% on the batteries amount variable and thus it was considered equal to 0. Thus, this explains why a relatively high total order Sobol index was calculated for the batteries as they indirectly, through their interaction with the wind turbines amount and then with the electrolyzers amount, are affecting the LCOE value. As far as the solar panels and the electrolyzers are concerned, they do not affect the LCOE value. This is because they are cheap in comparison with the batteries and the wind turbines and the final value of the second order Sobol index was occurred equal to less than 1% for both, which is considered to be zero as the influence is really low. Thus, if one wants to reduce the LCOE of the system can either add more solar panels to replace the wind turbines or even use more electrolyzers and utilize the hydrogen produced as fuel. However further analysis should be conducted because the utilization of hydrogen as fuel will need further equipment as for example hydrogen boilers or fuel cells that may influence the LCOE more in the end.

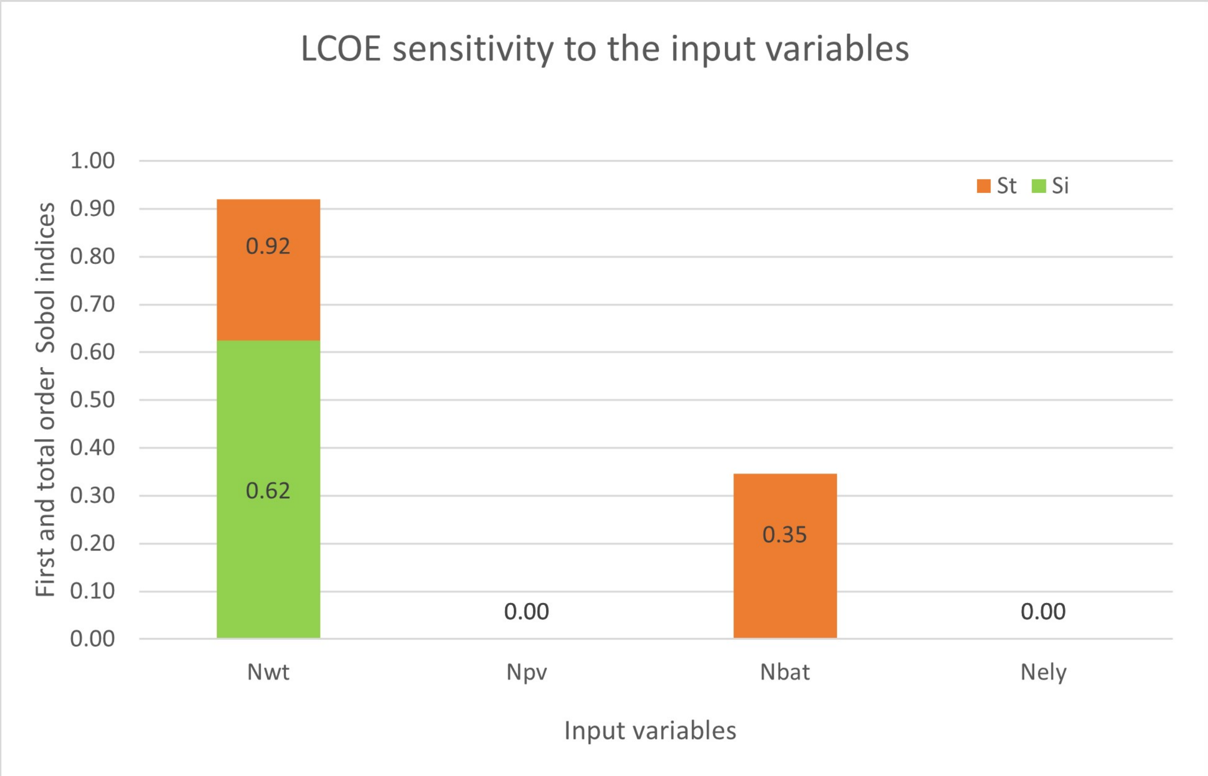


Figure 5.3: Sobol first order index and total order index are presented, which are showing the direct effect of the input variable to the LCOE and the total effect including the interactions of one input variable with the others to the LCOE respectively.

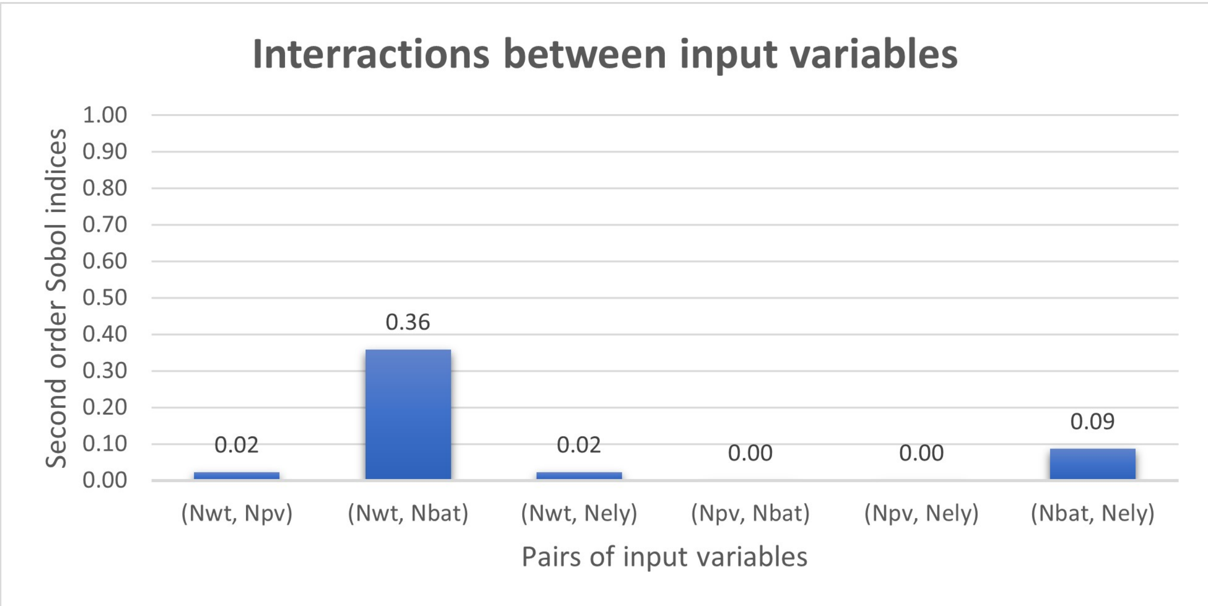


Figure 5.4: Sobol second order index is presented, which is showing the effect of the interaction of the input variables to the LCOE.

## 5.4 Local generation 2050 - Sensitivity Analysis

In this section the results from the sensitivity analysis are presented for the local generation of 2050 scenario. The input variables used for this analysis were the number of wind turbines (Nwt), the number of solar panels (Npv), the number of batteries (Nbat) and the number of electrolyzers (Nely). A sample of 320 pairs of these four variables was created and the parametric analysis extracted the respectful LCOE values. As it can be seen from the figure 5.5, the wind turbines have the highest influence in the LCOE as the first order Sobol index is relatively high. Batteries, as it can be seen from figure 5.6 are influencing LCOE much through the interaction they have with the wind turbines amount. This is because the total order Sobol index is high but the first order Sobol index is low for the batteries amount variable. Thus, this explains why a relatively high total order Sobol index was calculated for the batteries as they indirectly, through their interaction with the wind turbines amount and then with the electrolyzers amount, are affecting the LCOE value. As far as the solar panels and the electrolyzers are concerned, they do not affect the LCOE value. This is because they are cheap in comparison with the batteries and the wind turbines and the final value of the second order Sobol index was occurred equal to less than 1% for both, which is considered to be zero as the influence is really low. Thus, if one wants to reduce the LCOE of the system can either add more solar panels to replace the wind turbines or even use more electrolyzers and utilize the hydrogen produced as fuel. However, further analysis should be conducted because the utilization of hydrogen as fuel will need further equipment as for example hydrogen boilers or fuel cells that may influence the LCOE more in the end.

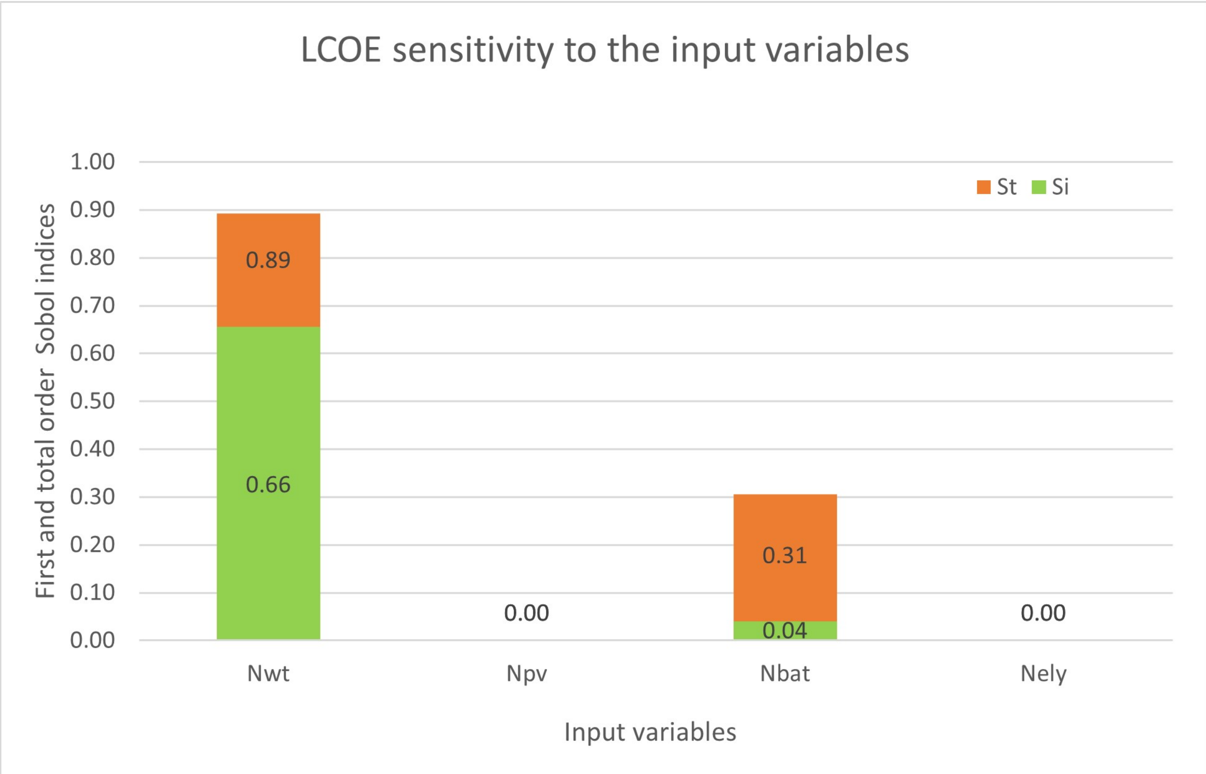


Figure 5.5: Sobol first order index and total order index are presented, which are showing the direct effect of the input variable to the LCOE and the total effect including the interactions of one input variable with the others to the LCOE respectively.

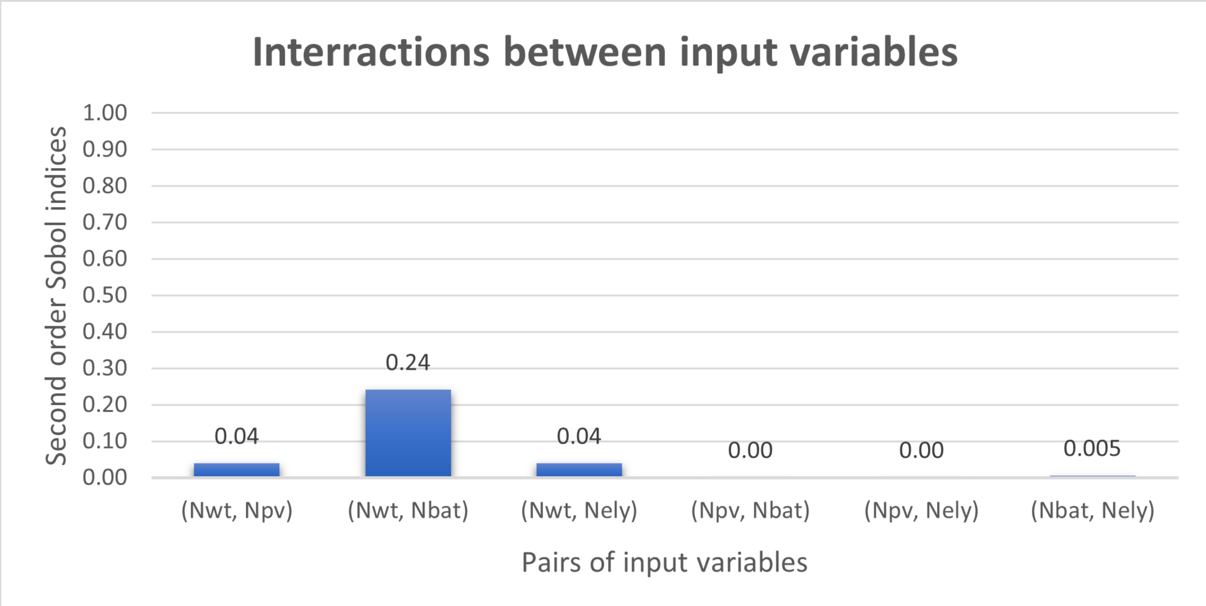


Figure 5.6: Sobol second order index is presented, which is showing the effect of the interaction of the input variables to the LCOE.

## 5.5 Non-local generation 2030 - Sensitivity Analysis

In this section the results from the sensitivity analysis are presented for the non local generation of 2030 scenario. This scenario as it was described in section 3.2.3, it was studied as two separate systems combined in one in the end for providing the results. Thus, the sensitivity analysis was conducted for the two subsystems which are the electricity part and the hydrogen part of the system.

### 5.5.1 Electricity part of the system - Sensitivity analysis

In the electricity part of the non local generation system for the 2030 the input variables that were under the sensitivity analysis to estimate the effect they have on LCOE were the number of wind turbines (Nwt), the number of solar panels (Npv) and the number of batteries (Nbat). The results that occurred are matching with the conclusions of the BAU scenario as described in section 5.2 while the system consisted of the same components. It can be seen from figure 5.7, that the wind turbines have the highest influence to the LCOE, while the batteries are following. In this scenario, the total order Sobol indices have close values for the wind turbines amount and the batteries amount. Further than that, a lower interaction between the two is resulted as it can be seen from figure 5.8. While the interaction of the wind turbines with the solar panels are in the magnitude of 10% to the LCOE value, it is concluded that the solar panels are not directly influence the LCOE semantically and thus the total order index of this variable is zero.

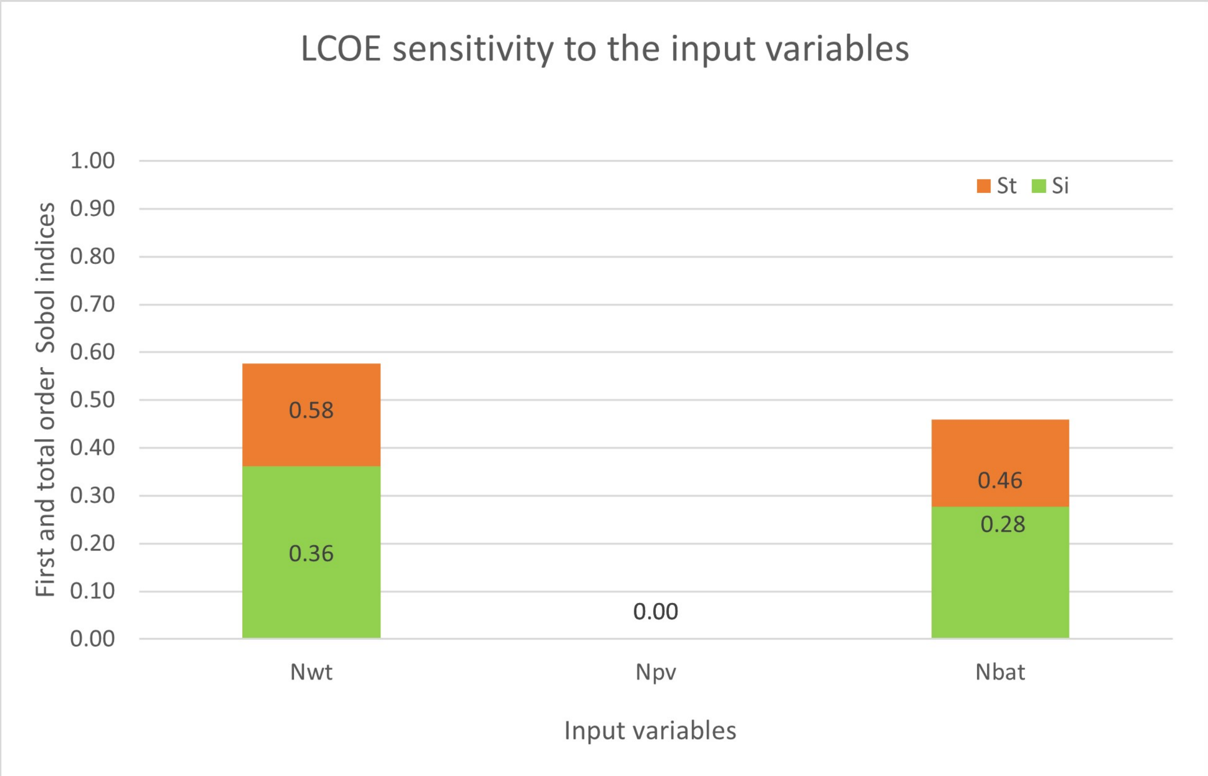


Figure 5.7: Sobol first order index and total order index are presented, which are showing the direct effect of the input variable to the LCOE and the total effect including the interactions of one input variable with the others to the LCOE respectively.

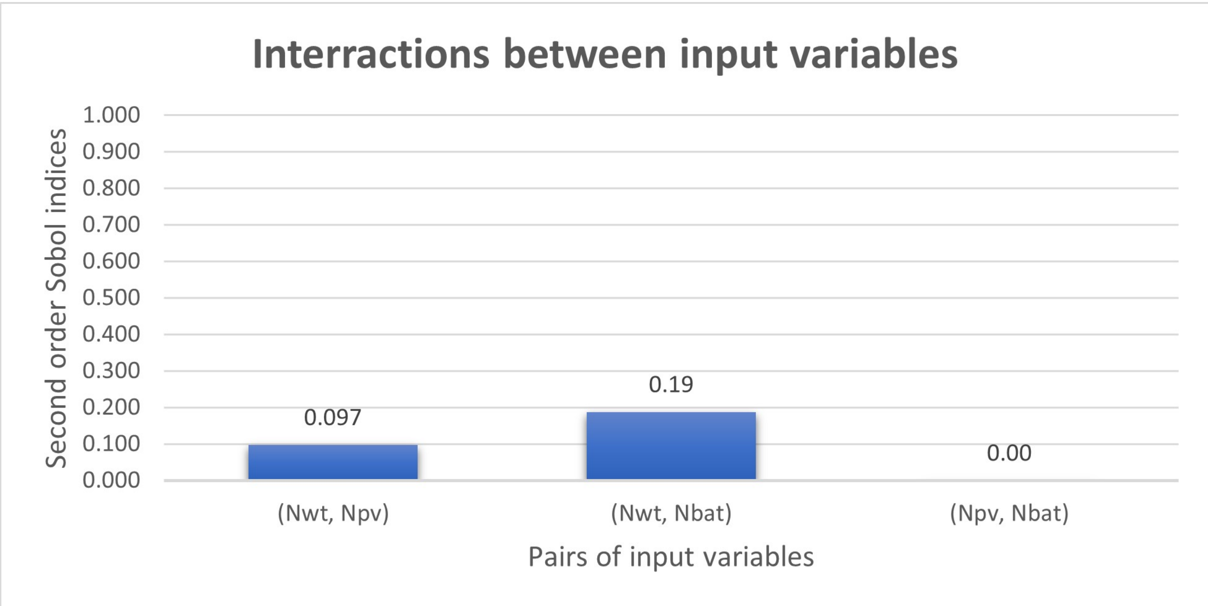


Figure 5.8: Sobol second order index is presented, which is showing the effect of the interaction of the input variables to the LCOE.

### 5.5.2 Hydrogen part of the system - Sensitivity analysis

On the other part of the system, the input variables that were investigated were the number of solar panels (Npv), the number of batteries (Nbat) and the number of electrolyzers (Nely). In this part of the system, it can be seen in figure 5.9 that the most influential variable are the electrolyzers since the solar panels remain the cheaper component of the system with respect to the energy generation added. It can be seen an interaction of the solar panels mostly with the electrolyzers in figure 5.10 as the higher second order index is in this pair of variables while relatively high is also for the interaction of the solar panels with the batteries. This is because of the power logic chosen to be followed and the relation that this finally acquires with the LCOE value. Since solar panels directly send the electricity generated to the electrolyzers and then the rest is stored on the batteries, this relationship is also interpreted with the Sobol indices as well.

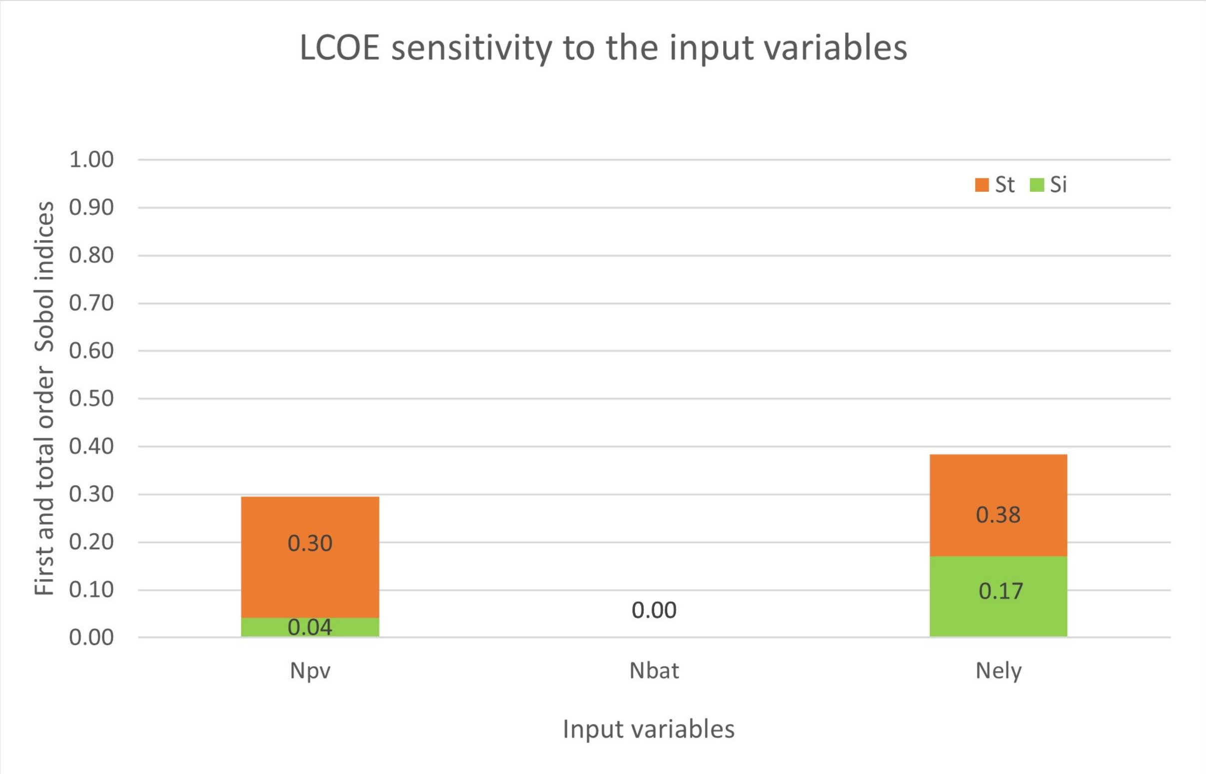


Figure 5.9: Sobol first order index and total order index are presented, which are showing the direct effect of the input variable to the LCOE and the total effect including the interactions of one input variable with the others to the LCOE respectively.

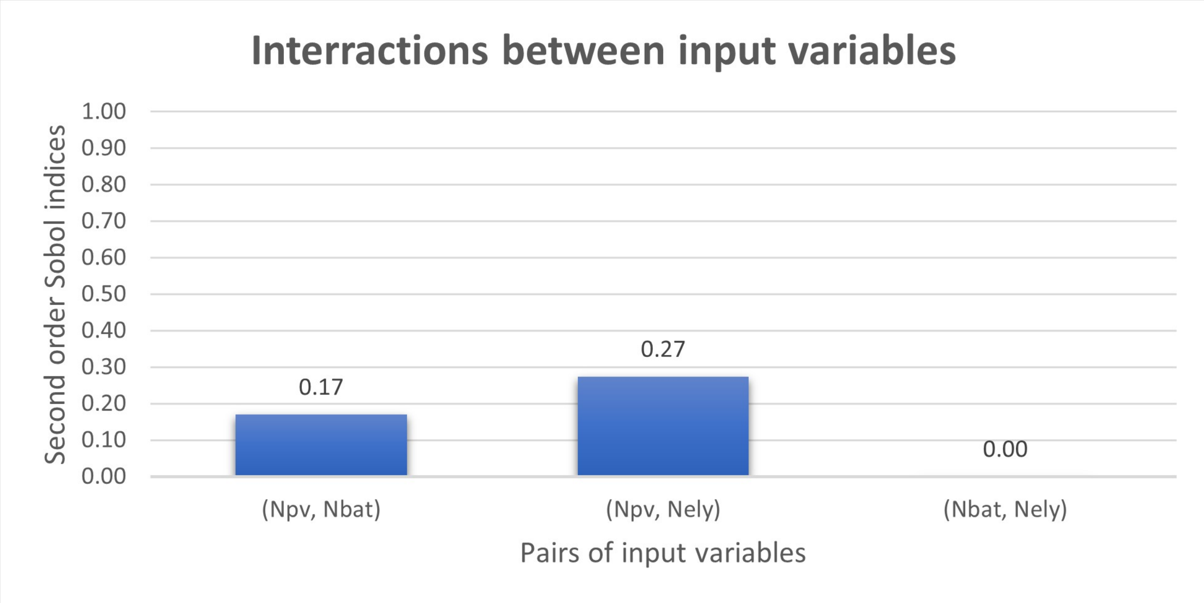


Figure 5.10: Sobol second order index is presented, which is showing the effect of the interaction of the input variables to the LCOE.

## 5.6 Non-local generation 2050 - Sensitivity Analysis

In this section the results from the sensitivity analysis are presented for the non local generation of 2050 scenario. This scenario as it was described in section 3.2.3, it was studied as two separate systems combined in one in the end for providing the results. Thus, the sensitivity analysis was conducted for the two subsystems which are the electricity part and the hydrogen part of the system.

### 5.6.1 Electricity part of the system - Sensitivity analysis

In the electricity part of the non local generation system for the 2050 the input variables that were under the sensitivity analysis to estimate the effect they have on LCOE were the number of wind turbines (Nwt), the number of solar panels (Npv) and the number of batteries (Nbat). The results that occurred are matching with the conclusions of the BAU scenario as described in section 5.2 while the system consisted of the same components. It can be seen from figure 5.11, that the wind turbines have the highest influence to the LCOE, while the batteries are following. In this scenario, the total order Sobol indices have close values for the wind turbines amount and the batteries amount. Further than that, a lower interaction between the two is resulted as it can be seen from figure 5.12. While the interaction of the wind turbines with the solar panels are in the magnitude of 10% to the LCOE value, it is concluded that the solar panels are not directly influence the LCOE semantically and thus the total order index of this variable is zero.

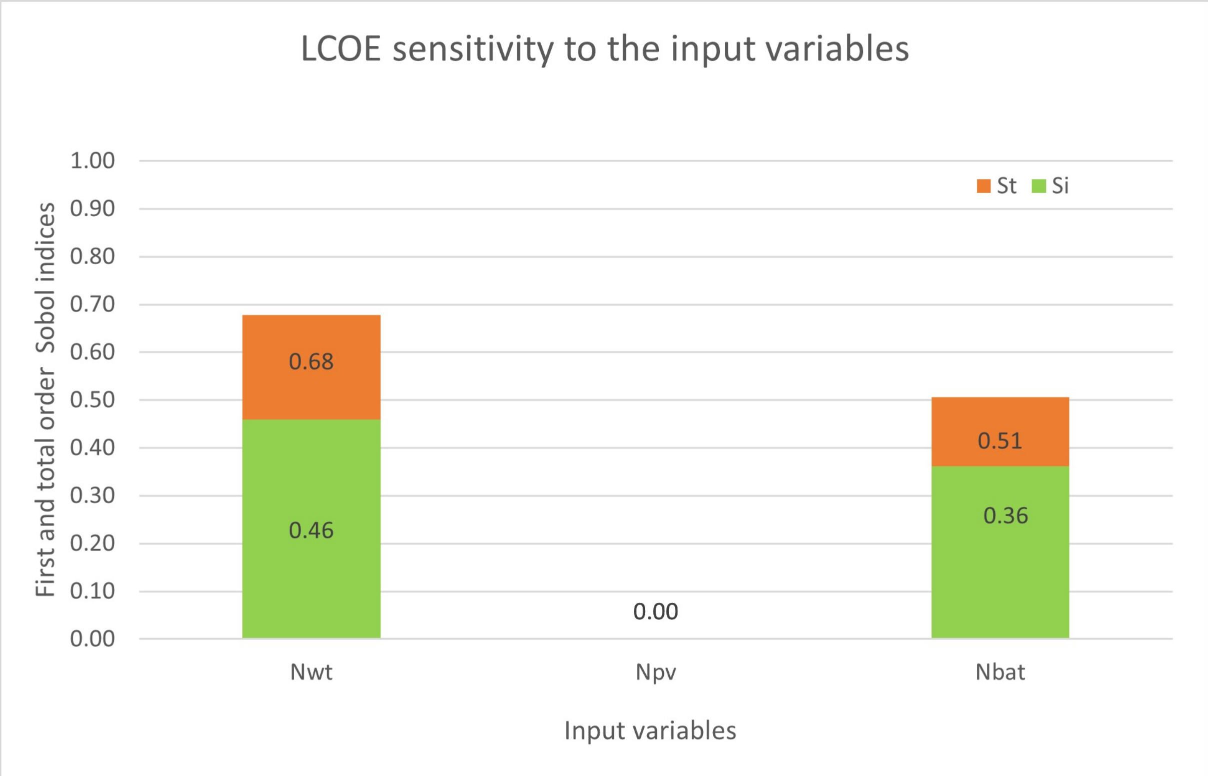


Figure 5.11: Sobol first order index and total order index are presented, which are showing the direct effect of the input variable to the LCOE and the total effect including the interactions of one input variable with the others to the LCOE respectively.

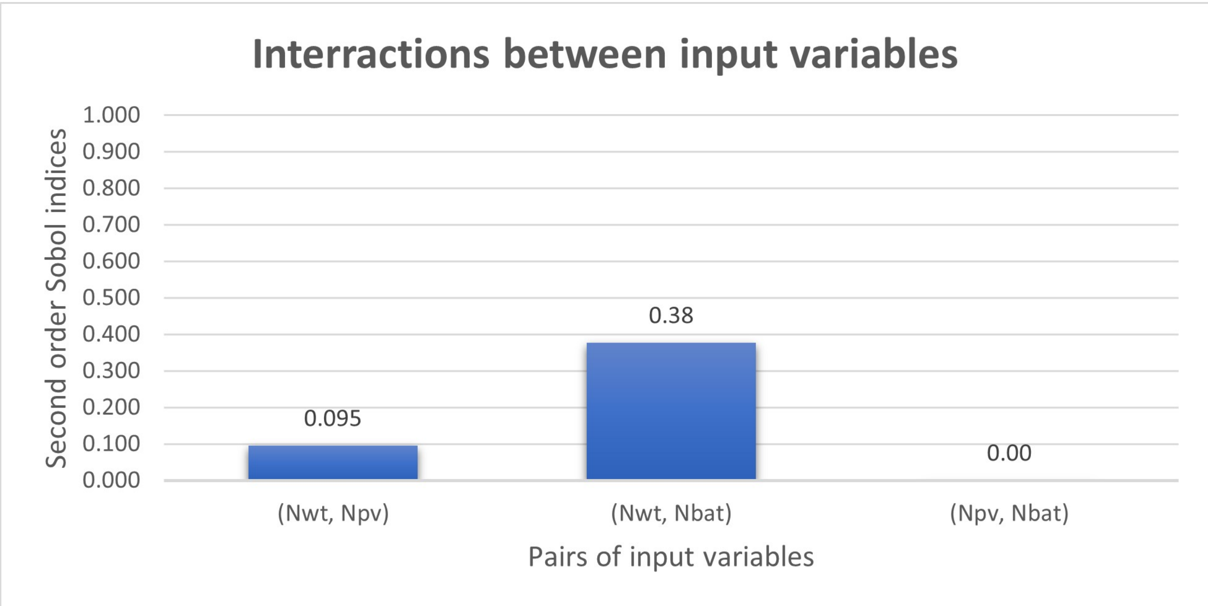


Figure 5.12: Sobol second order index is presented, which is showing the effect of the interaction of the input variables to the LCOE.

### 5.6.2 Hydrogen part of the system - Sensitivity analysis

On the other part of the system, the input variables that were investigated were the number of solar panels (Npv), the number of batteries (Nbat) and the number of electrolyzers (Nely). In this part of the system, it can be seen in figure 5.13 that the most influential variable are the solar panels in this case. This can be explained because of the high increase of the load to be generated for the liquefaction of the hydrogen through the solar panels and on the same time the providence to the electrolyzers for the production of hydrogen. It can be seen an interaction of the solar panels mostly with the electrolyzers in figure 5.14 as the higher second order index is in this pair of variables while around the same effect is also observed for the interaction of the solar panels with the batteries. This is because of the power logic chosen to be followed and the relation that this finally acquires with the LCOE value. Since solar panels directly send the electricity generated to the electrolyzers and then the rest is stored on the batteries. Meanwhile, in this scenario the electricity load of the liquefaction is high enough and the conclusions drew is that the priority on coverage is to serve the load at first for the liquefaction and then for the hydrogen. However, since the power logic flow remains the same then the capacity is increased further to be able to cover both. Thus, the effect that both the pairs (Npv,Nbat) and (Npv,Nely) have are in the same order of magnitude of 5-6 % influence to the LCOE.

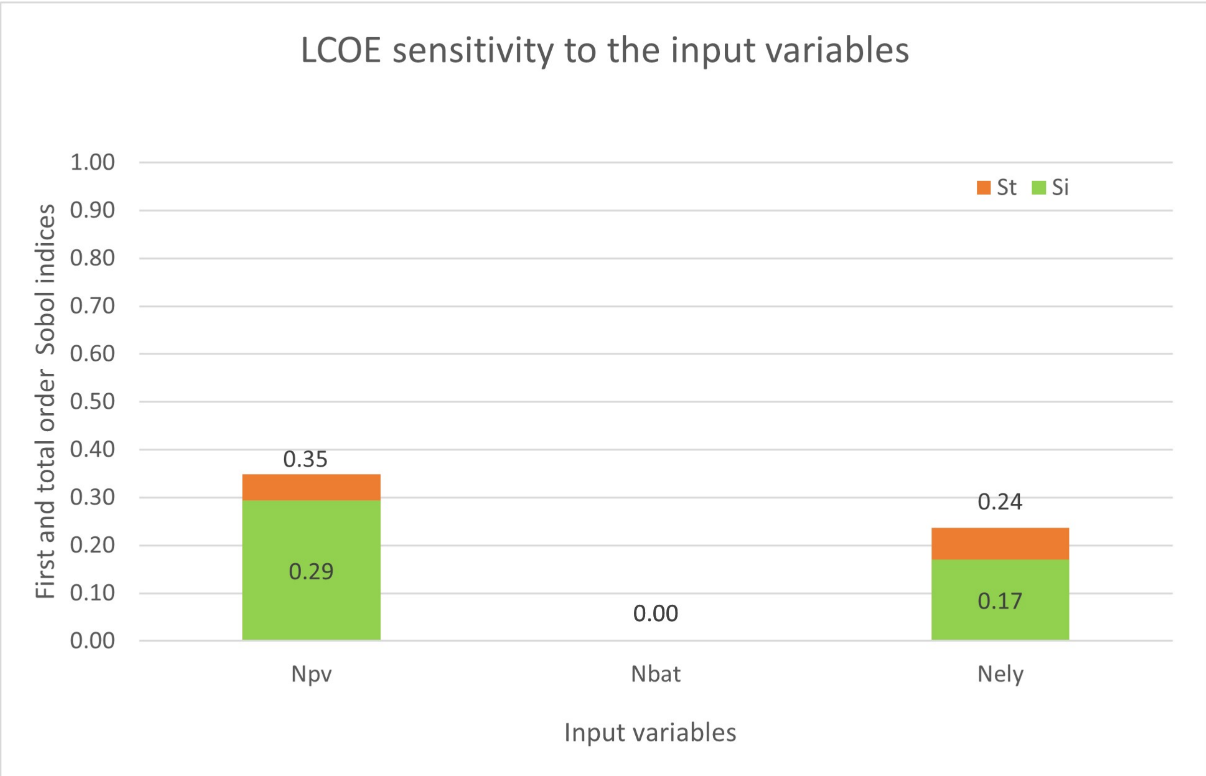


Figure 5.13: Sobol first order index and total order index are presented, which are showing the direct effect of the input variable to the LCOE and the total effect including the interactions of one input variable with the others to the LCOE respectively.

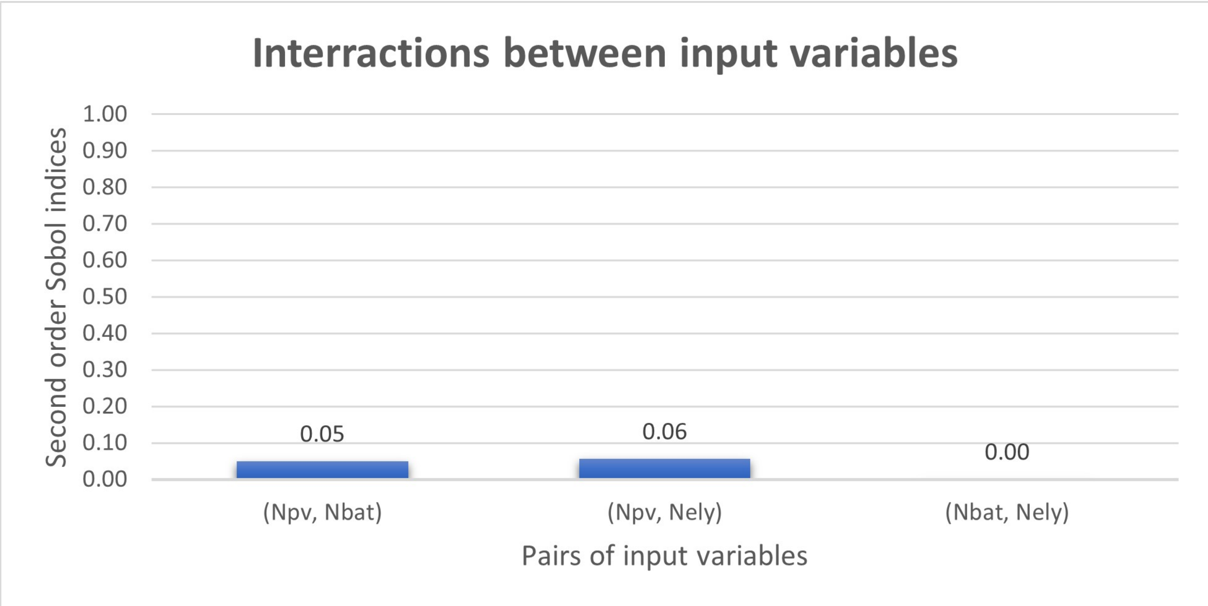


Figure 5.14: Sobol second order index is presented, which is showing the effect of the interaction of the input variables to the LCOE.

# 6| Conclusions and Recommendations

In this chapter the main conclusions extracted from the study of this project will be presented at first. Then, the recommendations for future work will be discussed. At first, the most important metrics outputted from each scenario studied to answer the research question: "*What is the feasibility to cover with a solar - wind - hydrogen system, the loads of the different steel making routes of Tata Steel*", are presented. Further than that, a discussion will also be presented about what is the best scenario throughout the different metrics and what can potentially improve the results or the output of this project by presenting a list of recommendations for future work.

## 6.1 Conclusion of the project

In this thesis project, the loads for the different steel making routes of Tata Steel from the present with the intermediate step of 2030 and a net zero process of 2050 were modeled through the software TRNSYS. The different loads for electricity and hydrogen, were calculated and added to the simulation as well, depending on the scenario studied. In the loads construction, a maintenance time for the industry was also included by adding a planned maintenance in the less efficient times of energy production and also added randomly unplanned maintenance periods.
By using GenOpt, the TRNSYS optimization tool, and applying a combination of the PSO and Hooke - Jeeves algorithms, the system was optimized while aiming for the lowest cost of electricity possible and the self sufficiency ratio of the system both for hydrogen and electricity to be less than 1%.
After the optimization, some further assumptions were made to approach further a more realistic study. These were that the batteries should be charged before the project's initiation to a specific percentage to match the initial and final state of charge on the simulation. Also, the hydrogen tank had to be optimized further so the most of its volume was used and also to charge the tanks up to a percentage as done in the batteries case, so the initial and final state of charge of the tank match in this case as well.
Further than that, by using the library SALib in python and the parametric analysis of TRNSYS, a sensitivity analysis was conducted to evaluate the influence that each variable and the pairs of variables have in the levelized cost of electricity. The results of the cases are considered to answer the main part of the research question which refers to the feasibility to cover such loads with renewable energy sources. All the scenarios were feasible to cover the loads demanded as all the self sufficiency ratio values were lower than 1% both for electricity and hydrogen. Thus, since all the scenarios ended up to be technical feasible, the two scenario that have the better metrics will be compared for the final suggestion of this project. The two best scenarios were the Local Generation of 2050 one and the Local Generation of 2030. The metrics used to compare the different scenarios so the aforementioned two end up to be the best ones were the LCOE, SSR, $SSR_{H_2}$, total cost, avoided emissions per MWh, the area ratio and the avoided emissions per area as it can be seen in the following table 6.1. With green color are highlighted the best metric values and with orange color the second best to conclude that the two best scenarios of this study are the local generation of 2030 and 2050.

Table 6.1: The metrics used to compare the different scenarios with each other and the respective values.

| **Scenario** | **Local Generation 2030** | **Local Generation 2050** | **Non Local Generation 2030** | **Non Local Generation 2050** |
|---|---|---|---|---|
| Total Cost PV [billion €] | 8.79 | 15.96 | 21.69 | 22.7 |
| LCOE [€/kWh] | 0.383 | 0.421 | 0.764 | 0.758 |
| SSR | 0.993 | 0.125 | 0.042 | 0.045 |
| $SSR_{H_2}$ | 0.865 | 0.793 | 0.456 | 0.099 |
| Avoided emissions per MWh [tons $CO_2$/MWh] | 1.3 | 2.01 | 1.18 | 1.48 |
| Area to NL area ratio [ % ] | 0.35 | 1.5 | 2.85 | 4.37 |
| Avoided emissions per area [ktons $CO_2$/km$^2$] | 11.4 | 11.53 | 3.94 | 5.37 |

From the table 6.1, it is visible that the two scenarios for the non local generation are covering the loads both for electricity and hydrogen in the most efficient way, while having the lowest SSR values. On the other hand, in all the other metrics they seem to be the worst cases of the four. The reason for that is the high irradiation in the Arabic Peninsula keeping the electricity generation relatively high during the year from the solar panels. Furthermore, the total energy generation in the local part of the system is directed to the loads of the primary processes of the industry without providing energy for hydrogen production. Thus, the system can really provide both to the hydrogen and the electricity load. The drawback for both the non local generation scenario systems is that two separate systems need to be installed and thus the cost and the LCOE are high.

Comparing the two scenarios that seems to be the most feasible with the metric values occurred, it is visible that the local generation for 2050 scenario is the best one. This is because in the LCOE comparison, the costs per kWh are really similar even if the total cost itself seems to be twice as much as the one of the 2030 scenario. Both the self sufficiency ratio for the electricity and the hydrogen were lower for this scenario with the electricity one being around 8 times lower than the one of 2030 scenario. The local generation scenario for 2050 was the best also for the ratio of the avoided emissions per MWh offered to the loads and also for the ratio of the avoided emissions per area required. For the ratio of the area required to the total Netherlands area is again the second best option and all the aforementioned leads to the final suggestion from this project to be the local generation for 2050 scenario case.

## 6.2 Recommendations for future work

After extracting the final conclusion for this project, some further points could be investigated to offer a more complete picture of what can be the ideal next steps for making such an industry more sustainable in the future:

1. After concluding that the two best scenarios were the two intermediate steps of Tata Steel's sustainability road map for the years of 2030 and 2050, a more complete suggestion would be to start with an investment for a local generation scenario with following the route of 2030 as an intermediate step with a final goal to realize the 100% hydrogen process in the year of 2050. This conclusion is also supported from the metrics comparison which showed

that the two best scenarios are these two. Thus, a study of combining the scenarios with each other could be a start.

2. Adding limitations to the area requirement for the solar panels park or investigate new trends like offshore solar panels, could also be a further work to be done, relevant to this project, as it will also characterize it either technical feasible or not. On this suggestion, an investigation also for solar axis trackers addition in the solar parks could be possible to tackle the technical feasibility of installing many solar panels in different orientations as occurred in some of the scenarios results.

3. A further suggestions would be to change the plant's location in an area that is more efficient in the electricity generation due to higher availability for the renewable energy sources. A further investigation could be done with potential locations around the world to offer the same loads. Further than that, the liquefaction and regasification loads can be excluded if in the new potential location is possible to transport the hydrogen to the plant in another way which would potentially be more energy efficient.

4. Perform a more complete economic analysis with including also the fuel costs of the processes used and also study the projections for the carbon taxes in the coming years so a more accurate LCOE estimation can be made.

5. Increase the sample size for each scenario and run again the parametric analysis so higher order Sobol indices can be calculated as well and investigate that way the interaction of more than two variables each time that was done in this project.

6. Investigate the addition of further technologies like fuel cells or hydrogen boilers in such a system as the sensitivity analysis showed that more electrolyzers and solar panels can be usually added in the system for further hydrogen generation without affecting importantly the LCOE

# Bibliography


[1] *Tata Steel IJmuiden steel plant.* 2022. URL: https://www.gem.wiki/Tata_Steel_IJmuiden_steel_plant.

[2] *IEA - the Netherlands.* URL: https://www.iea.org/countries/the-netherlands.

[3] *Tata Steel Europe - Sustainability Performance.* URL: https://www.tatasteeleurope.com/construction/sustainability/performance-at-our-sites/ijmuiden.

[4] Tata Steel Europe. "Tata Steel in Europe Sustainability report 2019/2020". In: (2020).

[5] Wenqiang Sun et al. "Material and energy flows of the iron and steel industry: Status quo, challenges and perspectives". In: *Applied Energy* 268.April (2020). ISSN: 03062619. DOI: 10.1016/j.apenergy.2020.114946.

[6] José S. Moya, Carmen Baudín, and Pilar Miranzo. "Sintering". In: *Encyclopedia of Physical Science and Technology* (2003), pp. 865–878. DOI: 10.1016/B0-12-227410-5/00694-3. URL: https://linkinghub.elsevier.com/retrieve/pii/B0122274105006943.

[7] D. Zhu et al. "Iron ore pelletization". In: *Iron Ore: Mineralogy, Processing and Environmental Sustainability* (Aug. 2015), pp. 435–473. DOI: 10.1016/B978-1-78242-156-6.00015-0.

[8] *Pig Iron.* 0. URL: https://en.wikipedia.org/wiki/Pig_iron.

[9] *TRNSYS Software 18.* URL: https://sel.me.wisc.edu/trnsys/features/trnsys18_0_updates.pdf.

[10] Government of the Netherlands. *Dutch Offshore Wind Farm Zones.* URL: https://www.government.nl/topics/renewable-energy/offshore-wind-energy.

[11] Francesco Benetti. "Green hydrogen supply potential on the Arabian Peninsula". In: ().

[12] Government of the Netherlands. *Offshore wind energy.* URL: https://www.government.nl/topics/renewable-energy/offshore-wind-energy.

[13] Neeraj Gupta. "A review on the inclusion of wind generation in power system studies". In: *Renewable and Sustainable Energy Reviews* 59.June 2016 (2016), pp. 530–543. ISSN: 18790690. DOI: 10.1016/j.rser.2016.01.009.

[14] Bajric Mersudin and Bente Vestergaard. *Siemens SWT - 7.0 - 154 Datasheet and IECRE certification.*

[15] *Reglobal Technology roadmap.* URL: https://reglobal.co/technology-roadmap-anticipated-trends-in-the-c-si-pv-industry/.

[16] Adeel Saleem et al. "The effect of environmental changes on the efficiency of the PV system". In: *Indonesian Journal of Electrical Engineering and Computer Science* 18.1 (2019), pp. 558–564. ISSN: 25024760. DOI: 10.11591/ijeecs.v18.i1.pp558-564.

[17] aurorasolar. *Solar Panel Types guide.* 2022. URL: https://aurorasolar.com/blog/solar-panel-types-guide/.

[18] Panasonic. *Panasonic 435 - 450 Wp PERC technology solar module datasheet.*

[19] Daniel Lugo-laguna, Angel Arcos-Vargas, and Fernando Nuñez-hernandez. "A european assessment of the solar energy cost: Key factors and optimal technology". In: *Sustainability (Switzerland)* 13.6 (2021), pp. 1–25. ISSN: 20711050. DOI: 10.3390/su13063238.

[20] CubeEnergy. "PowerCombo-C40 battery bank". In: ().

[21] Kushan Jayasinghe. "POWER LOSS EVALUATION OF SUBMARINE CABLES IN 500MW OFFSHORE WIND FARM". Doctoral dissertation. 2017. DOI: 10.32964/tj16.11.

[22] Arnold Sagonda and Komla Folly. "Review on the Modeling and Electrical Output Power Assessment of a Solar PV System". In: *25th Southern African Universities Power and Engineering Conference (SAUPEC 2017)* 3 (2017), pp. 1–5.

[23] Brian Cory. "Pricing in electricity transmission and distribution". In: *Proceedings of the Mediterranean Electrotechnical Conference - MELECON* 1.April (1996), pp. 19–25. DOI: 10.1109/melcon.1996.550955.

[24] Mohd Fadhzir Ahmad Kamaroddin et al. "Membrane-based electrolysis for hydrogen production: A review". In: *Membranes* 11.11 (2021), pp. 1–27. ISSN: 20770375. DOI: 10.3390/membranes11110810.

[25] Yujing Guo et al. "Comparison between hydrogen production by alkaline water electrolysis and hydrogen production by PEM electrolysis". In: *IOP Conference Series: Earth and Environmental Science* 371.4 (2019). ISSN: 17551315. DOI: 10.1088/1755-1315/371/4/042022.

[26] GreenHydrogen.dk et al. "HyProvide Large-Scale Alkaline Electrolyser (MW )". In: *Eudp 11-Ii, 64011-0105* (2016).

[27] M. Conte and M. Ronchetti. *ENERGY | Hydrogen Economy*. August. Elsevier Inc., 2013, pp. 1–23. ISBN: 9780124095472. DOI: 10.1016/b978-0-12-409547-2.01196-3. URL: http://dx.doi.org/10.1016/B978-0-12-409547-2.01196-3.

[28] *Sea route & distance between ports*. URL: http://ports.com/sea-route/.

[29] *Average speed of different ship types at the sea*. URL: https://www.marineinsight.com/guidelines/speed-of-a-ship-at-sea/.

[30] Reneke Kolff. "Converting the LNG-Peakshaver to be fit for processing LH 2". Doctoral dissertation. 2021.

[31] Hendrie Derking, Luuk van der Togt, and Marcel Keezer. "Liquid Hydrogen Storage: Status and Future Persectives". In: *Cryoworld advanced cryogenics* (2019), p. 18.

[32] International Energy Agency. "The Future of Hydrogen: Seizing today's opportunities". In: *IEA Publications* June (2019), p. 203. URL: https://www.iea.org/reports/the-future-of-hydrogen.

[33] *Meteonorm Website*. URL: https://meteonorm.com/en/.

[34] Olindo Isabela Arno Smets. "Solar Energy Book". Doctoral dissertation. TU Delft, 2016, p. 488.

[35] *Global Wind Atlas*. URL: https://globalwindatlas.info/.

[36] Neeraj Gupta. "A review on the inclusion of wind generation in power system studies". In: *Renewable and Sustainable Energy Reviews* 59.October (2016), pp. 530–543. ISSN: 18790690. DOI: 10.1016/j.rser.2016.01.009.

[37] *IJmuiden - Global Solar Atlas*. URL: https://globalsolaratlas.info/detail?c=52.465214,4.599838,11&s=52.464879,4.573059&m=site&pv=ground,180,37,1000.

[38] *Al Madinah optimal tilt angle*. URL: https://globalsolaratlas.info/detail?c=26.465656,40.056152,7&s=25.502785,38.880615&m=site.

[39] Martin McBrien, André Cabrera Serrenho, and Julian M. Allwood. “Potential for energy savings by heat recovery in an integrated steel supply chain”. In: *Applied Thermal Engineering* 103 (2016), pp. 592–606. ISSN: 13594311. DOI: 10.1016/j.applthermaleng.2016.04.099. URL: http://dx.doi.org/10.1016/j.applthermaleng.2016.04.099.

[40] Britannica. *Basic oxygen steel making*. URL: https://www.britannica.com/technology/steel/Forming-of-steel.

[41] Fabrice Patisson et al. “Hydrogen Ironmaking : How It Works”. In: *Metals 2020* 10.7 (2020). URL: www.mdpi.com/journal/metals.

[42] Sujay Kumar Dutta and Rameshwar Sah. “Direct Reduced Iron: Production”. In: *Encyclopedia of Iron, Steel, and Their Alloys* March (2016), pp. 1082–1108. DOI: 10.1081/e-eisa-120050996.

[43] Jayson; Kopfle John Ripke. “MIDREX H2: Ultimate Low CO2 Ironmaking and its place in the new Hydrogen Economy”. In: *Direct from midrex*. Oxford University Press, Jan. 2017, pp. 7–13.

[44] Katharina Rechberger et al. “Green Hydrogen-Based Direct Reduction for Low-Carbon Steelmaking”. In: *Steel Research International* 91.11 (2020), pp. 1–10. ISSN: 16113683. DOI: 10.1002/srin.202000110.

[45] Jean-pierre Birat. “Society , Materials , and the Environment : The Case”. In: (2020).

[46] Marc Hölling. “Direct Reduction: Transition from Natural Gas to Hydrogen?” In: September (2018). URL: https://www.researchgate.net/publication/327962750.

[47] P. E. Duarte et al. “Energiron direct reduction ironmaking - Economical, flexible, environmentally friendly”. In: *Steel Times International* 34.3 (2010), pp. 25–30. ISSN: 01437798.

[48] Can Yilmaz and Thomas Turek. “Modeling and simulation of the use of direct reduced iron in a blast furnace to reduce carbon dioxide emissions”. In: *Journal of Cleaner Production* 164 (2017), pp. 1519–1530. ISSN: 09596526. DOI: 10.1016/j.jclepro.2017.07.043. URL: http://dx.doi.org/10.1016/j.jclepro.2017.07.043.

[49] *High-performance open rack LNG vaporizer SUPERORV*. URL: https://www.osakagas.co.jp/en/rd/technical/1198901_6995.html.

[50] Debjyoti Bose and Devesh Shrivastava. “Total Productive Maintenance Parameters Analysis of a Small Medium Indian Manufacturing Industry – A Case Study”. In: 8.103 (2018), pp. 103–117.

[51] Michael Wetter. “Generic Optimization Program User Manual”. In: *Energy* c (2011), pp. 1998–2011.

[52] Yuhui Shi James Kennedy C. Russell Eberhard. *Swarm Intelligence*. 2001.

[53] Robert Hooke and T. A. Jeeves. ““Direct Search” Solution of Numerical and Statistical Problems”. In: *Journal of the ACM (JACM)* 8.2 (1961), pp. 212–229. ISSN: 1557735X. DOI: 10.1145/321062.321069.

[54] *Solar panel price watch 2022*. URL: http://www.pv4.eu/solar-panel-price-watch_2022.html.

[55] S.A. Vis. “A new look for residential hybrid systems - A PV-battery-electrolyser-fuel cell power system for a neighbourhood in the Netherlands”. Doctoral dissertation. 2021.

[56] Sander Lensink and Iulia Pisca. *Costs of Offshore Wind Energy*. Tech. rep. February. PBL Netherlands Environmental Assessment Agency, 2019.

[57] Eero Vartiainen et al. “Impact of weighted average cost of capital, capital expenditure, and other parameters on future utility-scale PV levelised cost of electricity”. In: *Progress in Photovoltaics: Research and Applications* 28.6 (2020), pp. 439–453. ISSN: 1099159X. DOI: 10.1002/pip.3189.

[58] International Renewable Energy Agency (IRENA). "Future of Wind - Executive Summary". In: (2019).

[59] DNV. "Hydrogen Forecast To 2050". In: (2022), pp. -114.

[60] Said El-Asha, Lu Zhan, and Giacomo Valerio Iungo. "Quantification of power losses due to wind turbine wake interactions through SCADA, meteorological and wind LiDAR data". In: *Wind Energy* 20.11 (2017), pp. 1823–1839. ISSN: 10991824. DOI: 10.1002/we.2123.

[61] *The Netherlands area.* URL: https://en.wikipedia.org/wiki/Netherlands.

[62] *Environmental Protection Agency of USA - GHG calculator.* URL: https://www.epa.gov/energy/greenhouse-gas-equivalencies-calculator#results.

[63] Christoph Kost et al. "Levelized Cost of Electricity- Renewable Energy Technologies June 2021". In: June (2021), pp. 1–45. DOI: 10.13140/RG.2.2.22457.08800. URL: www.ise.fraunhofer.de%0ADirectors.

[64] Johannes Morfeldt, Wouter Nijs, and Semida Silveira. "The impact of climate targets on future steel production - An analysis based on a global energy system model". In: *Journal of Cleaner Production* 103 (2015), pp. 469–482. ISSN: 09596526. DOI: 10.1016/j.jclepro.2014.04.045. URL: http://dx.doi.org/10.1016/j.jclepro.2014.04.045.

[65] DNV. "Maritime Forecast To 2050 - Energy Transition Outlook 2021". In: *Dnv* (2021), p. 118. URL: https://www.naucher.com/wp-content/uploads/2021/09/DNV_Maritime_Forecast_2050_2021-Web.pdf.

[66] Daniel Harenberg et al. "Uncertainty quantification and global sensitivity analysis for economic models". In: *Quantitative Economics* 10.1 (2019), pp. 1–41. ISSN: 1759-7323. DOI: 10.3982/qe866.

[67] *Variance - Wikipedia.* URL: https://en.wikipedia.org/wiki/Variance.

[68] Abdelhadi Serbouti et al. "Application of sensitivity analysis and genopt to optimize the energy performance of a building in Morocco". In: *International Journal of Engineering and Technology(UAE)* 7.4 (2018), pp. 2068–2074. ISSN: 2227524X. DOI: 10.14419/ijet.v7i4.13280.

[69] *python: Home page.* URL: https://www.python.org/.

[70] Herman Jonathan Iwanaga Takuya Usher William. "Toward SALib 2.0: Advancing the accessibility and interpretability of global sensitivity analyses". In: *Socio - environmental systems Modelling* 4 (2022), p. 18155. DOI: 10.18174/sesmo.18155. URL: https://sesmo.org/article/view/18155.

[71] Usher William Herman Jon. "An open-source Python library for sensitivity analysis". In: *The Journal of Open Source Software* 2 (2017). DOI: 10.21105/joss.00097. URL: https://doi.org/10.21105/joss.00097.

# Appendix

## A.1 MATLAB Code for the unplanned maintenance randomization

The code for the 2030 scenario for local generation is given so it includes also the H2 load maintenance addition to the load data series. For all the scenarios the main logic of the MATLAB Code that was followed was the same and only the variables used as inputs were different.

### Matlab Code

```
clc
clear

LGen2030 = xlsread('LGen2030_w_Maintenance.xlsx');
LGen2030H2 = xlsread('LocalGen2030_H2.xlsx');
%Select the hours of the year randomly for the 5.5 days of unplanned maintenance time
k = 528; %5.5 days in quarters
m = randi(4,1); %Maximum 3 unplanned maintenances in 5.5 days - Assumption

qs_maint = zeros(4,1);


if m == 1
qs_maint(1) = k; %Random number from 1 to 528/m

A=ones(qs_maint(1),m); %First number is the amount of consecutive numbers, second number is the amount of different ranges of consecutive numbers
A(1,:)=ceil(35039*rand(1,size(A,2))+1);
R=reshape(cumsum(A(:)'),size(A));
R=R(:,randperm(end));
R=R(:);

Rf = R;
Rf = sort(Rf);
end

if m == 2
    qs_maint(1) = randi(k/m,1);
```

```
A=ones(qs_maint(1),1); %First number is the amount of consecutive numbers, second number is the amount of different ranges of consecutive numbers
A(1,:)=ceil(35039*rand(1,size(A,2))+1);
R=reshape(cumsum(A(:)'),size(A));
R=R(:,randperm(end));
R1=R(:);

    qs_maint(2) = k - qs_maint(1);
A=ones(qs_maint(2),1); %First number is the amount of consecutive numbers, second number is the amount of different ranges of consecutive numbers
A(1,:)=ceil(35039*rand(1,size(A,2))+1);
R=reshape(cumsum(A(:)'),size(A));
R=R(:,randperm(end));
R2=R(:);

Rf = [R1; R2];
Rf = sort(Rf);
end


if m == 3
    qs_maint(1) = randi(k/m,1);
A=ones(qs_maint(1),1); %First number is the amount of consecutive numbers, second number is the amount of different ranges of consecutive numbers
A(1,:)=ceil(35039*rand(1,size(A,2))+1);
R=reshape(cumsum(A(:)'),size(A));
R=R(:,randperm(end));
R1=R(:);
    qs_maint(2) = randi(k - qs_maint(1),1);
A=ones(qs_maint(2),1); %First number is the amount of consecutive numbers, second number is the amount of different ranges of consecutive numbers
A(1,:)=ceil(35039*rand(1,size(A,2))+1);
R=reshape(cumsum(A(:)'),size(A));
R=R(:,randperm(end));
R2=R(:);
    qs_maint(3) = k - qs_maint(2)-qs_maint(1);
A=ones(qs_maint(3),1); %First number is the amount of consecutive numbers, second number is the amount of different ranges of consecutive numbers
A(1,:)=ceil(35039*rand(1,size(A,2))+1);
R=reshape(cumsum(A(:)'),size(A));
R=R(:,randperm(end));
R3=R(:);

Rf = [R1; R2; R3];
Rf = sort(Rf);
end
```

```
if m == 4
    qs_maint(1) = randi(k/m,1);
A=ones(qs_maint(1),1); %First number is the amount of consecutive
   numbers, second number is the amount of different ranges of
   consecutive numbers
A(1,:)=ceil(35039*rand(1,size(A,2))+1);
R=reshape(cumsum(A(:)'),size(A));
R=R(:,randperm(end));
R1=R(:);
    qs_maint(2) = randi(k - qs_maint(1),1);
A=ones(qs_maint(2),1); %First number is the amount of consecutive
   numbers, second number is the amount of different ranges of
   consecutive numbers
A(1,:)=ceil(35039*rand(1,size(A,2))+1);
R=reshape(cumsum(A(:)'),size(A));
R=R(:,randperm(end));
R2=R(:);
    qs_maint(3) = randi(k - qs_maint(2)-qs_maint(1),1);
A=ones(qs_maint(3),1); %First number is the amount of consecutive
   numbers, second number is the amount of different ranges of
   consecutive numbers
A(1,:)=ceil(35039*rand(1,size(A,2))+1);
R=reshape(cumsum(A(:)'),size(A));
R=R(:,randperm(end));
R3=R(:);

    qs_maint(4) = k - qs_maint(3)-qs_maint(2)-qs_maint(1);
A=ones(qs_maint(4),1); %First number is the amount of consecutive
   numbers, second number is the amount of different ranges of
   consecutive numbers
A(1,:)=ceil(35039*rand(1,size(A,2))+1);
R=reshape(cumsum(A(:)'),size(A));
R=R(:,randperm(end));
R4=R(:);

Rf = [R1; R2; R3; R4];
Rf = sort(Rf);
end


Unplanned_qs = Rf;

LGen2030(Unplanned_qs,1) = 0;
LGen2030H2(Unplanned_qs,1) = 0;

writematrix(LGen2030, 'LGen2030_maintenance.txt')
writematrix(LGen2030H2, 'LocalGen2030_H2_maintenance.txt')
```